RELEASE DATE OCT 22 1947 CLASSIFICATION CANCELLED CONFIDENTIAL CANCELLED RM No. L7J09

Copy No. 5 1104

CLASSIFICATION CANCELLED

Authority J. W. Crowley Date 3-11-55
Ch., Aeron. Research
NACA
By OES See NACA change # 2958

Status: INACTIVE

Vought F7U-1

PERMANENT FILE COPY

RESEARCH MEMORANDUM

for the

Bureau of Aeronautics, Navy Department

AN INVESTIGATION OF THE AERODYNAMIC CHARACTERISTICS OF AN 0.08-SCALE MODEL OF THE CHANCE VOUGHT XF7U-1 AIRPLANE IN THE LANGLEY HIGH-SPEED 7- BY 10-FOOT TUNNEL

PART V - WING-ALONE TESTS AND EFFECT OF MODIFICATIONS TO THE VERTICAL FINS, SPEED BRAKES, AND FUSELAGE

TED NO. NACA DE308

By

Richard E. Kuhn and Boyd C. Myers, II

Langley Memorial Aeronautical Laboratory
Langley Field, Va.

CLASSIFICATION CANCELLED

NATIONAL ADVISORY COMMITTEE FOR AERONAUTICS

WASHINGTON

OCT 10 1947

CONFIDENTIAL CLASSIFICATION CANCELLED

  CONFIDENTIAL

NATIONAL ADVISORY COMMITTEE FOR AERONAUTICS

RESEARCH MEMORANDUM

for the

Bureau of Aeronautics, Navy Department

AN INVESTIGATION OF THE AERODYNAMIC CHARACTERISTICS OF AN 0.08-SCALE MODEL OF THE CHANCE VOUGHT XF7U-1 AIRPLANE IN THE LANGLEY HIGH-SPEED 7- BY 10-FOOT TUNNEL

PART V - WING-ALONE TESTS AND EFFECT OF MODIFICATIONS TO THE VERTICAL FINS, SPEED BRAKES, AND FUSELAGE

TED NO. NACA DE308

By Richard E. Kuhn and Boyd C. Myers, II

SUMMARY

Tests have been conducted in the Langley high-speed 7- by 10-foot tunnel over a Mach number range from 0.40 to 0.91 to determine the stability and control characteristics of an 0.08-scale model of the Chance Vought XF7U-1 airplane. The wing-alone tests and the effect of the various vertical-fin modifications, speed-brake modifications, and fuselage modifications on the aerodynamic characteristics in pitch and yaw are presented in the present paper with a limited analysis of the results. Also included are tuft studies of the flow for some of the modifications tested.

INTRODUCTION

At the request of the Bureau of Aeronautics, Navy Department, an investigation of the stability and control characteristics of an 0.08-scale model of the Chance Vought XF7U-1 airplane was conducted in the Langley high-speed 7- by 10-foot tunnel.

This paper presents the results of wing-alone tests and the effect of the various modifications to the vertical fins, speed brakes, and fuselage on the aerodynamic characteristics of the model in pitch and yaw.

The results include lift, drag, and pitching-moment data over an angle-of-attack range for the various configurations at 0° and -4.4° control deflection and include yawing-moment, side force, and rolling-moment data over a yaw range of $\pm 4^\circ$ for the various configurations at static angles of attack of 0° and 6°. The results are presented for a range of Mach numbers varying from 0.40 to 0.91. Tuft studies of the flow for some configurations are also presented.

This paper is issued with the purpose of presenting the data available at present from high-speed tests of the 0.08-scale model of the XF7U-1 airplane. Accordingly, no detailed analysis of the data has been made. The basic longitudinal and lateral stability characteristics are presented in references 1 and 2, respectively. The longitudinal control characteristics are presented in reference 3 and the aileron characteristics are presented in reference 4.

COEFFICIENTS AND SYMBOLS

The system of axes used for the presentation of the data, together with an indication of the positive forces, moments, and angles, is presented in figure 1. Pertinent symbols are defined as follows:

C_L lift coefficient $\left(\frac{\text{Lift}}{qS}\right)$

C_D drag coefficient $\left(\frac{\text{Drag}}{qS}\right)$

C_m pitching-moment coefficient measured about the 17 percent M.G.C. position $\left(\frac{\text{Pitching moment}}{qSc'}\right)$

C_Y lateral-force coefficient $\left(\frac{Y}{qS}\right)$

C_n yawing-moment coefficient $\left(\frac{N}{qSb}\right)$

C_l rolling-moment coefficient $\left(\frac{L}{qSb}\right)$

Y lateral force measured along Y-axis

L rolling moment about X-axis

N yawing moment about Z-axis

q	free-stream dynamic pressure, pounds per square foot $\left(\frac{\rho V^2}{2}\right)$
S	wing area (3.174 sq ft on model)
c'	wing mean geometric chord (M.G.C.)(1.046 ft on model)
c	chord, parallel to plane of symmetry
c_1	chord, perpendicular to 0.25c line
b	wing span (3.093 ft on model)
V	air velocity, feet per second
a	speed of sound, feet per second
M	Mach number $\left(\frac{V}{a}\right)$
R	Reynolds number $\left(\frac{\rho V c'}{\mu}\right)$
μ	absolute viscosity, pound-seconds per square foot
ρ	mass density of air, slugs per cubic foot
α	angle of attack, measured from X-axis to the fuselage center line, degrees
ψ	angle of yaw, degrees
α_{static}	angle of attack under no-load conditions, degrees
δ	control-surface deflection with reference to wing chord line parallel to plane of symmetry, degrees (c)

$$C_{n_\psi} = \frac{\partial C_n}{\partial \psi}$$

$$C_{l_\psi} = \frac{\partial C_l}{\partial \psi}$$

$$C_{Y_\psi} = \frac{\partial C_Y}{\partial \psi}$$

$$C_{L_\alpha} = \frac{\partial C_L}{\partial \alpha}$$

Subscripts:

a_l left ailavator

a_r right ailavator

S speed brakes

M Mach number

APPARATUS AND METHODS

Model

The 0.08-scale steel model of the XF7U-1 airplane used in this investigation was constructed by the Chance Vought Division of the United Aircraft Corporation. Pertinent dimensions of the model are presented in figure 2. The control surfaces (ailavators) were constant-chord, true-contour flaps with sealed gaps.

Tests

The various configurations were tested through the Mach number range at various angles of attack and yaw with 0° and -4.4° ailavator deflection. The model was tested on a sting support as shown in figure 3. In order to evaluate the tares, the model was also tested on wing-tip stings (fig. 4) with and without the center sting. A more complete description of the testing technique employed is given in reference 1.

The variation of test Reynolds number with Mach number for average test conditions is presented in figure 5. The size of the model used in the present investigation resulted in a corrected tunnel choking Mach number of about 0.94. Experience has indicated that with this value of choking Mach number the data should be reliable up to a corrected Mach number of about 0.91.

Corrections

The test results have been corrected for the tare forces and moments produced by the support system except for a small constant

pitching-moment and rolling-moment coefficient which appear to be inherent in the support system but which were not accounted for in the tare determination. The origin of these moments has not been determined as yet but the data in this paper can be corrected by subtracting 0.003 from the pitching-moment coefficients presented and 0.0008 from the rolling-moment coefficients presented. Similar corrections are applicable to the data presented in references 1 to 4.

The jet-boundary corrections were computed from the following equations which were determined by the method of reference 5.

$$\alpha = \alpha_M + 0.331C_{L_M}$$

$$C_D = C_{D_M} + 0.0058{C_{L_M}}^2$$

where the subscript M indicates measured value. The jet-boundary correction to the pitching moment was considered negligible.

The drag has been corrected for the buoyancy produced by the small longitudinal static-pressure gradient in the tunnel and all coefficients and Mach numbers were corrected for blocking by the model and its wake.

RESULTS AND DISCUSSION

Effect of Basic Components

Longitudinal stability and control.- The aerodynamic characteristics in pitch of the wing alone, the complete model with the speed brakes open, the complete model with the vertical fins removed, and the complete model with the fuselage canopy removed are presented in figures 6 and 7. Inasmuch as the various configurations were not all tested at identically the same Mach number, it was necessary to cross-plot the original test results at constant Mach number to obtain the data of figures 6 and 7. The pitching-moment coefficients are presented about a center of gravity located at 17 percent of the mean geometric chord.

The effect of the various configurations on $\left(\frac{\partial C_m}{\partial C_L}\right)_M$ is presented in figure 8, and their effect on the lift-curve slope in the low lift range is presented in figure 9. The variation of lift-curve slope with

Mach number for the complete model presented in figure 9 does not agree exactly with that presented in reference 1. The lift-curve slopes of reference 1 were obtained from the basic data at zero control deflection. Subsequent lift data obtained with deflected controls (reference 3) has led to a more judicious fairing of the original lift data for zero control deflection and the lift-curve slopes obtained from the refaired data are presented in figure 9.

The effectiveness of the ailavators in producing changes in pitching-moment coefficient and lift coefficient at zero angle of attack is presented in figures 10 and 11, respectively. The effectiveness parameters $\left(\frac{\Delta C_m}{\Delta \delta}\right)_{0^\circ \text{ to } -4.4^\circ}$ and $\left(\frac{\Delta C_L}{\Delta \delta}\right)_{0^\circ \text{ to } -4.4^\circ}$ are based on data obtained at ailavator deflections of 0° and -4.4° only.

Tuft studies of the flow over the wing of the complete model for several angles of attack and Mach numbers are presented in figure 12.

Lateral stability.- The variation of lateral stability characteristics with Mach number $\left(\alpha_{static} = 0^\circ \text{ and } 6^\circ\right)$ for several configurations of the model are presented in figures 13 and 14. During the test runs in which these data were obtained, the lift coefficient varied as indicated by the curves in figure 15. The angle-of-attack change from the wind-off static values $\left(\alpha_{static} = 0^\circ \text{ and } 6^\circ\right)$ was caused by the deflection of the support system under aerodynamic load and is indicated by the values of the actual angle of attack shown in figure 15. The lateral stability derivatives C_{n_ψ}, C_{Y_ψ}, and C_{l_ψ} for static angles of attack of 0° and 6° are presented in figure 16. It will be noted that at a static angle of attack of 0°, the speed brakes produced a small amount of negative effective dihedral at the higher Mach numbers.

Speed-Brake Modifications

Force tests and tuft studies were conducted with the complete model using the four different arrangements of speed brakes shown in figure 17. Tuft studies of the flow over the model with the original speed brakes (fig. 18(a)) indicated bad separation of the flow over the vertical fins, particularly the inboard surface, over most of the Mach number range. In an effort to improve this condition the other speed-brake configurations were tested and the results of the tuft studies with these configurations are presented in figures 18(b) to 18(d). On the basis of those tuft observations, it appears that all the modifications tested eliminated the poor flow conditions evident at the vertical fin with the original configuration.

The effect of these speed-brake configurations on the aerodynamic characteristics in pitch is presented in figure 19 for a static angle of attack of 1.8°. The variation of the drag increments (ΔC_D), produced by the various speed brakes, with Mach number is presented in figure 20. It is evident from these data that the modified wing brakes produced considerably larger drag increments than the fuselage brakes.

Vertical-Fin Modifications

Tuft studies of the flow over the original vertical fins (fig. 21(a)) indicated that the flow over the part below the wing chord line from the maximum thickness rearward is very rough and has a tendency to separate at high Mach numbers. Several modifications of this part of the vertical fin were tested in an attempt to improve this flow condition. A sketch of the original fin and the three modifications tested is shown in figure 22. Modifications 1 and 2 effected no improvement in the flow conditions but tuft studies of the flow with modification number 3 did indicate some improvement (fig. 21(b)), in that the flow did not show any tendency to separate at any point in the Mach number range covered by these tests.

Langley Memorial Aeronautical Laboratory
National Advisory Committee for Aeronautics
Langley Field, Va.

Richard E. Kuhn

Richard E. Kuhn
Aeronautical Engineer

Boyd C. Myers, II

Boyd C. Myers, II
Aeronautical Engineer

Approved: Thomas A. Harris

Thomas A. Harris
Chief of Stability Research Division

MLE

REFERENCES

1. Kemp, William B., Jr., Kuhn, Richard E., and Goodson, Kenneth W.: An Investigation of the Aerodynamic Characteristics of an 0.08-Scale Model of the Chance Vought XF7U-1 Airplane in the Langley High-Speed 7- by 10-Foot Tunnel. Part I - Basic Longitudinal Stability Characteristics. TED No. NACA DE308. NACA RM No. L7G08, Bur. Aero., 1947.

2. Kemp, William B., Jr., Goodson, Kenneth W., and Kuhn, Richard E.: An Investigation of the Aerodynamic Characteristics of an 0.08-Scale Model of the Chance Vought XF7U-1 Airplane in the Langley High-Speed 7- by 10-Foot Tunnel. Part II - Basic Lateral Stability Characteristics. TED No. NACA DE308. NACA RM No. L7G10, Bur. Aero., 1947.

3. Kuhn, Richard E., and King, Thomas J., Jr.: An Investigation of the Aerodynamic Characteristics of an 0.08-Scale Model of the Chance Vought XF7U-1 Airplane in the Langley High-Speed 7- by 10-Foot Tunnel. Part III - Longitudinal Control Characteristics. TED No. NACA DE308. NACA RM No. L7H01, Bur. Aero., 1947.

4. Goodson, Kenneth W., and Myers, Boyd C., II: An Investigation of the Aerodynamic Characteristics of an 0.08-Scale Model of the Chance Vought XF7U-1 Airplane in the Langley High-Speed 7- by 10-Foot Tunnel. Part IV - Aileron Characteristics. TED No. NACA DE308. NACA RM No. L7H22, Bur. Aero., 1947.

5. Gillis, Clarence L., Polhamus, Edward C., and Gray, Joseph L., Jr.: Charts for Determining Jet-Boundary Corrections for Complete Models in 7- by 10-Foot Closed Rectangular Wind Tunnels. NACA ARR No. L5G31, 1945.

CONFIDENTIAL

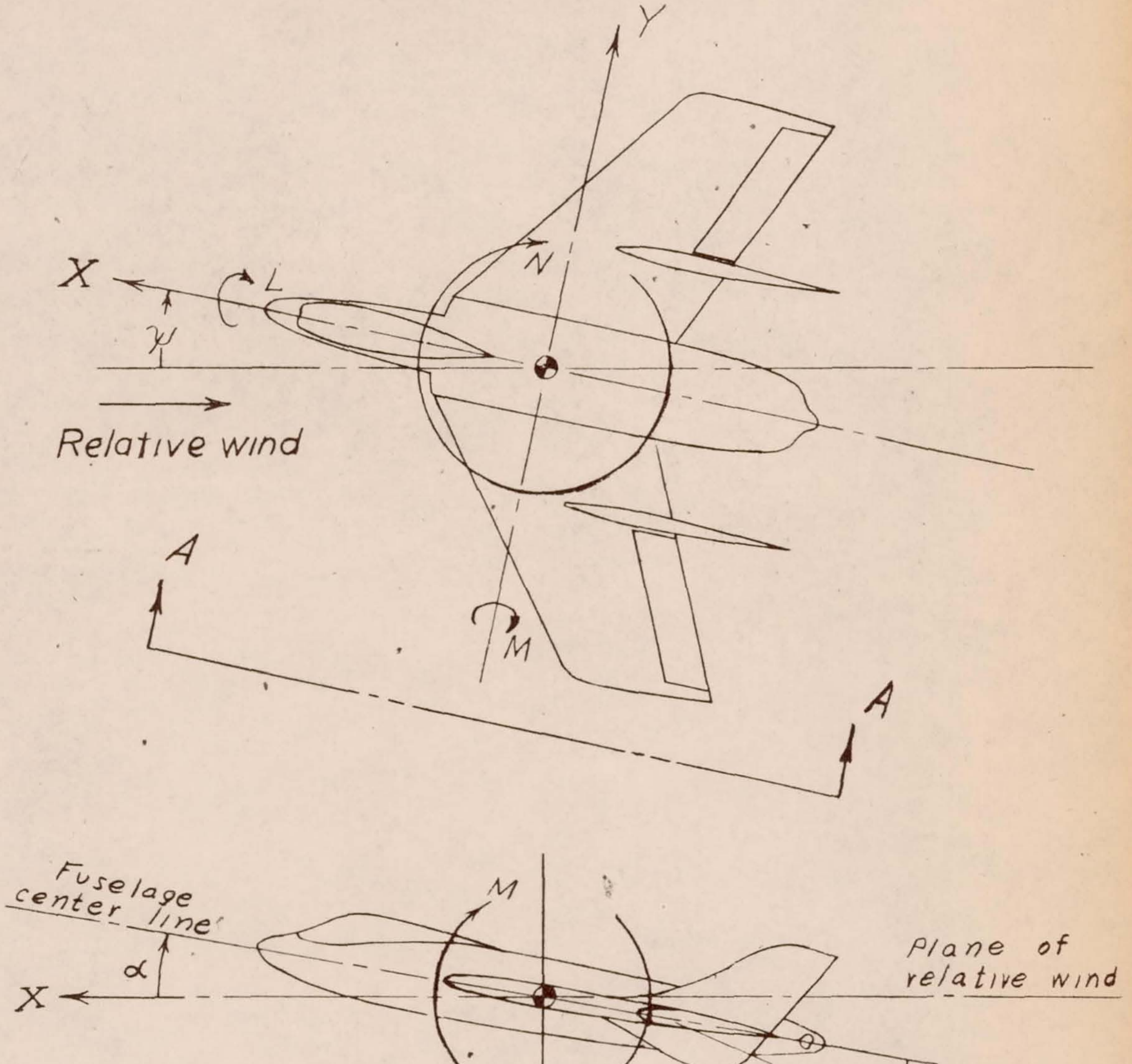

Figure 1.- System of axes and control-surface deflections. Positive values of forces, moments, and angles are indicated by arrows.

CONFIDENTIAL

CONFIDENTIAL

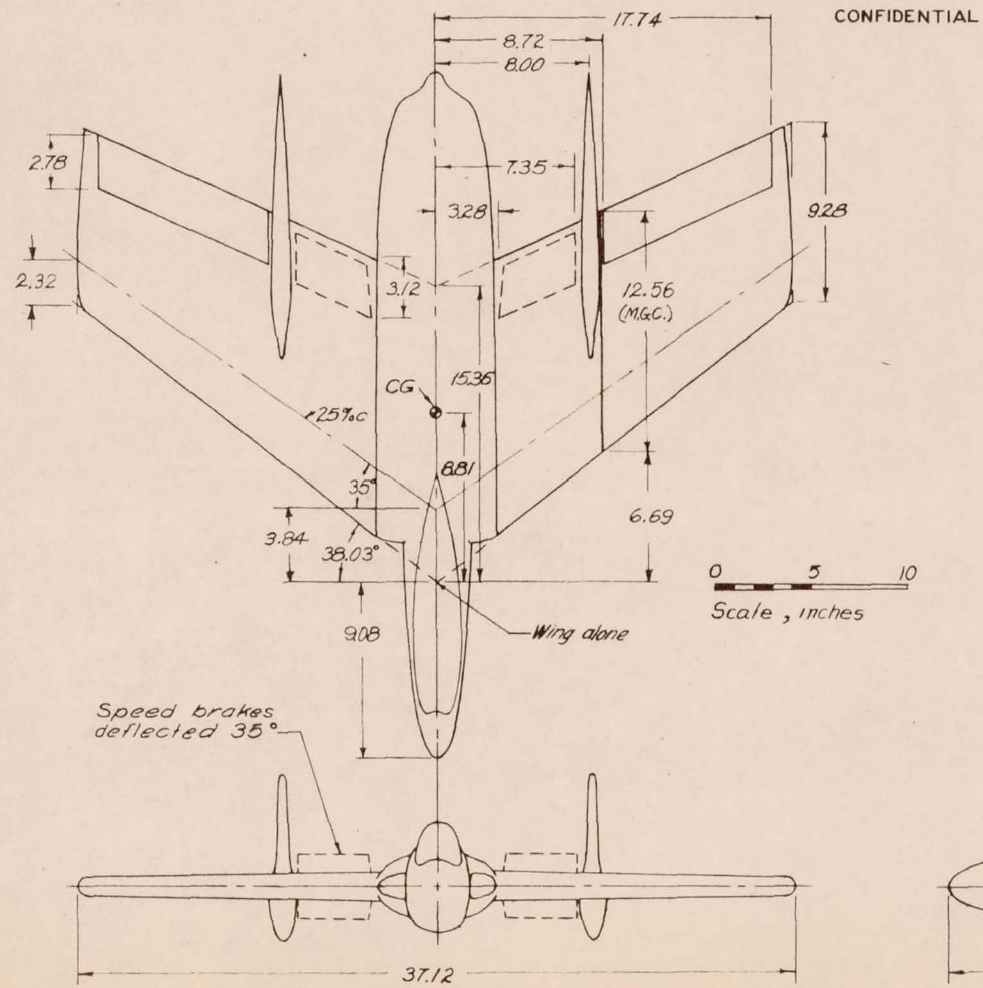

TABULATED DATA

Wing	
Area	3.174 sq ft
Aspect ratio	3.014
Mean geometric chord	1.046 ft
Incidence	0°
Dihedral	0°
Airfoil (perpendicular to 0.25c)	Symmetrical
Max. thickness	$0.12c_1$
Location of max. thickness	$0.40c_1$
Vertical tail	
Area (two)	0.82 sq ft
Aspect ratio	1.75
CG location	0.17 M.G.C.

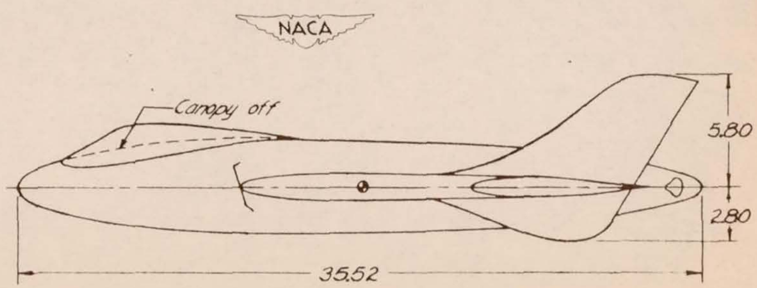

CONFIDENTIAL

Figure 2.- General arrangement of 0.08-scale model of Chance Vought XF7U-1 airplane.

CONFIDENTIAL

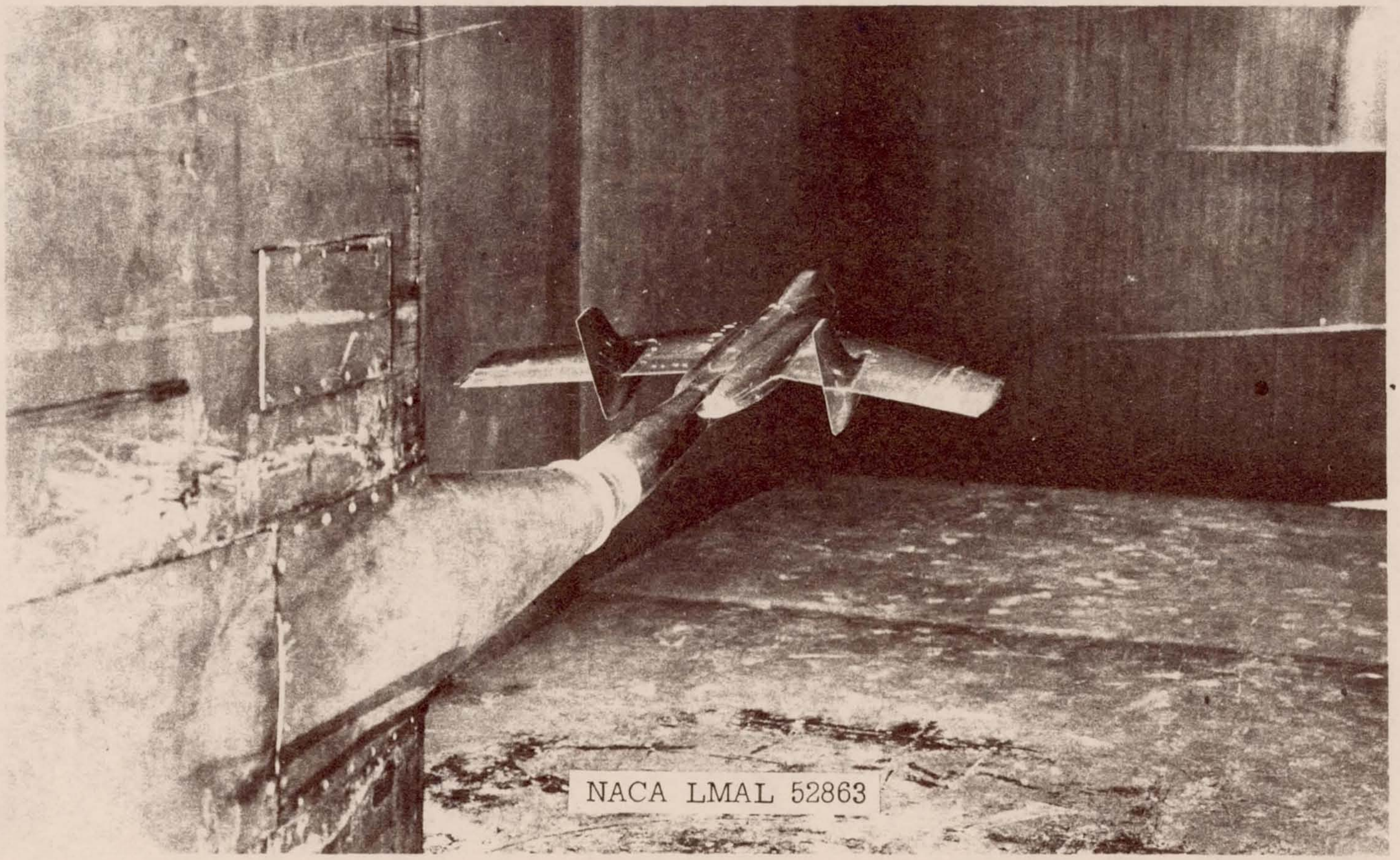

Figure 3.- Photograph of the 0.08-scale model of the XF7U-1 airplane mounted on the center sting at a positive angle of attack.

CONFIDENTIAL

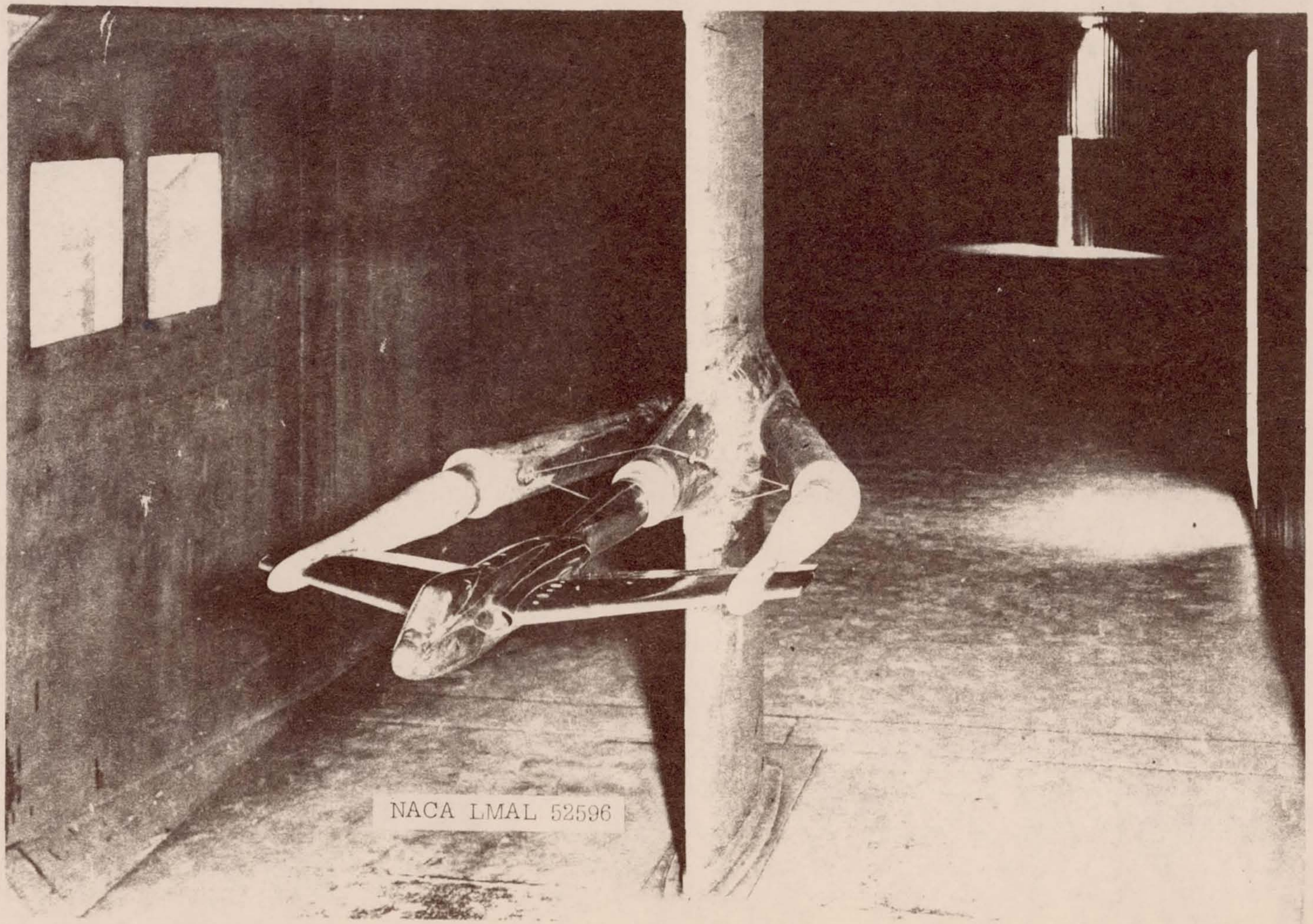

Figure 4.- Photograph of the 0.08-scale model of the XF7U-1 airplane with vertical tails removed mounted on the wing supports with center sting in place.

NATIONAL ADVISORY COMMITTEE FOR AERONAUTICS
LANGLEY MEMORIAL AERONAUTICAL LABORATORY - LANGLEY FIELD, VA.

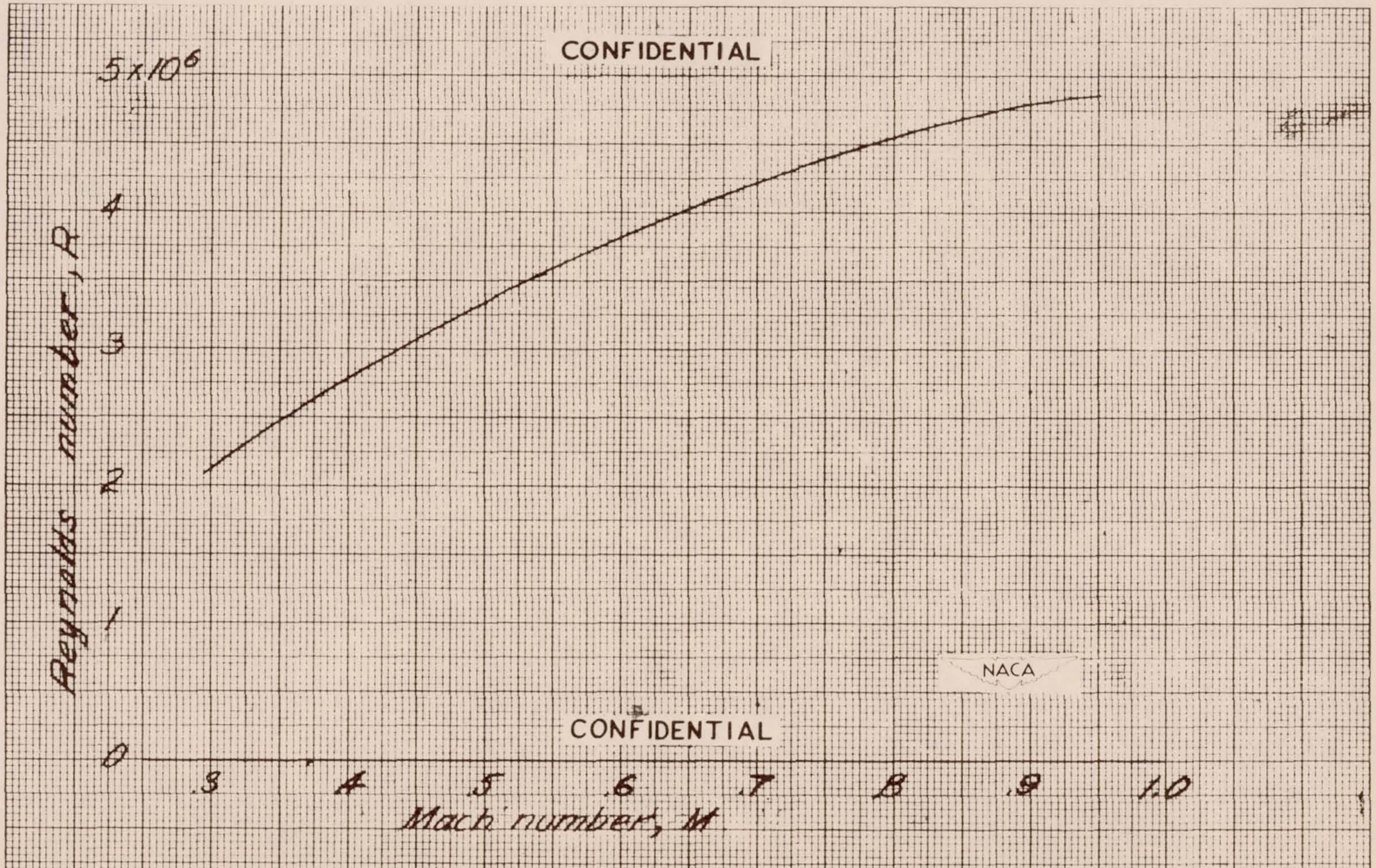

Figure 5.— Variation of test Reynolds number with Mach number for 0.08-scale model of the Chance Vought XF7U-1 in the high-speed 7- by 10-foot tunnel.

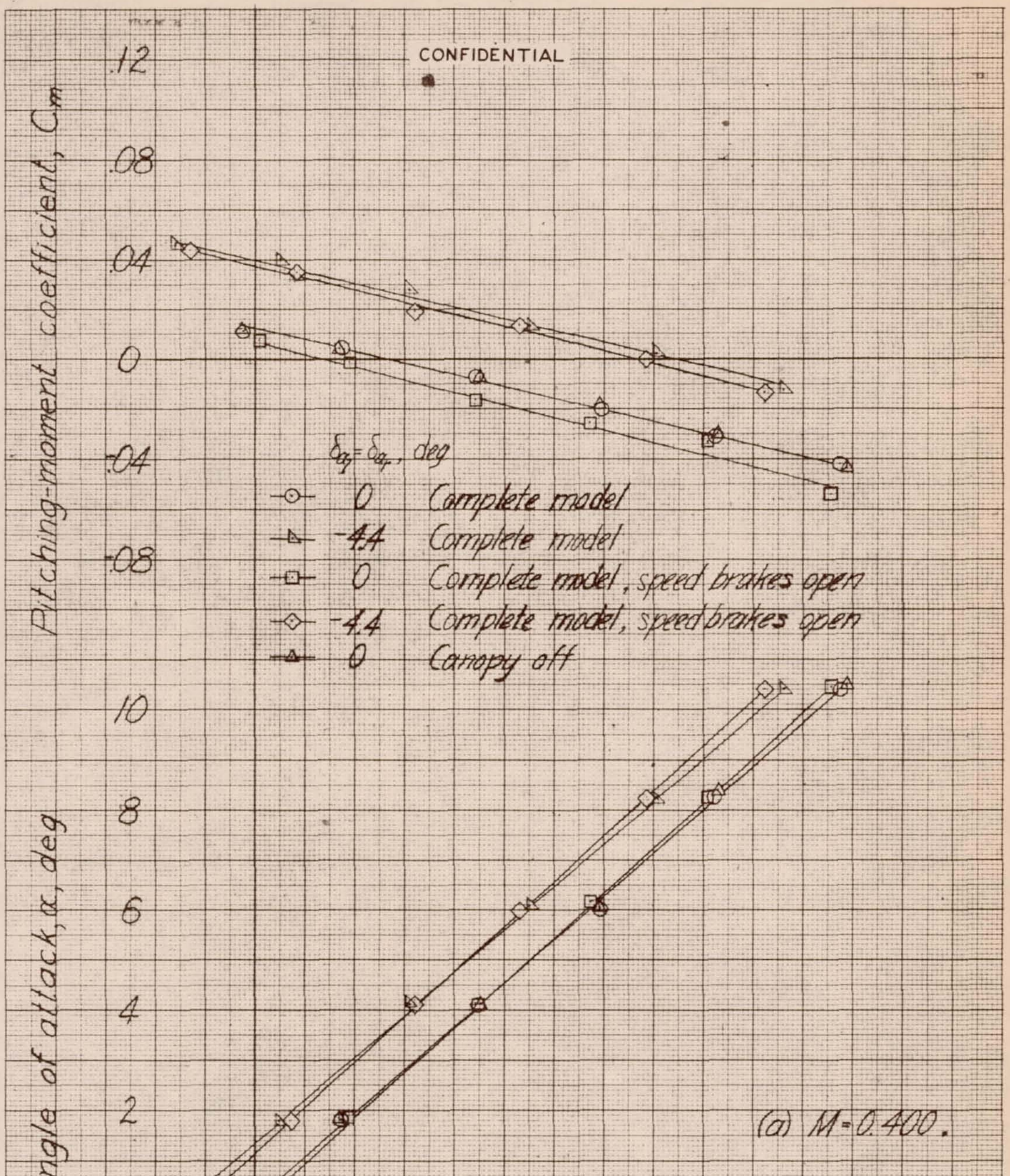

Figure 6.- Effect of speed brakes and canopy on the aerodynamic characteristics of the 0.08-scale model of the Chance Vought XF7U-1 airplane.

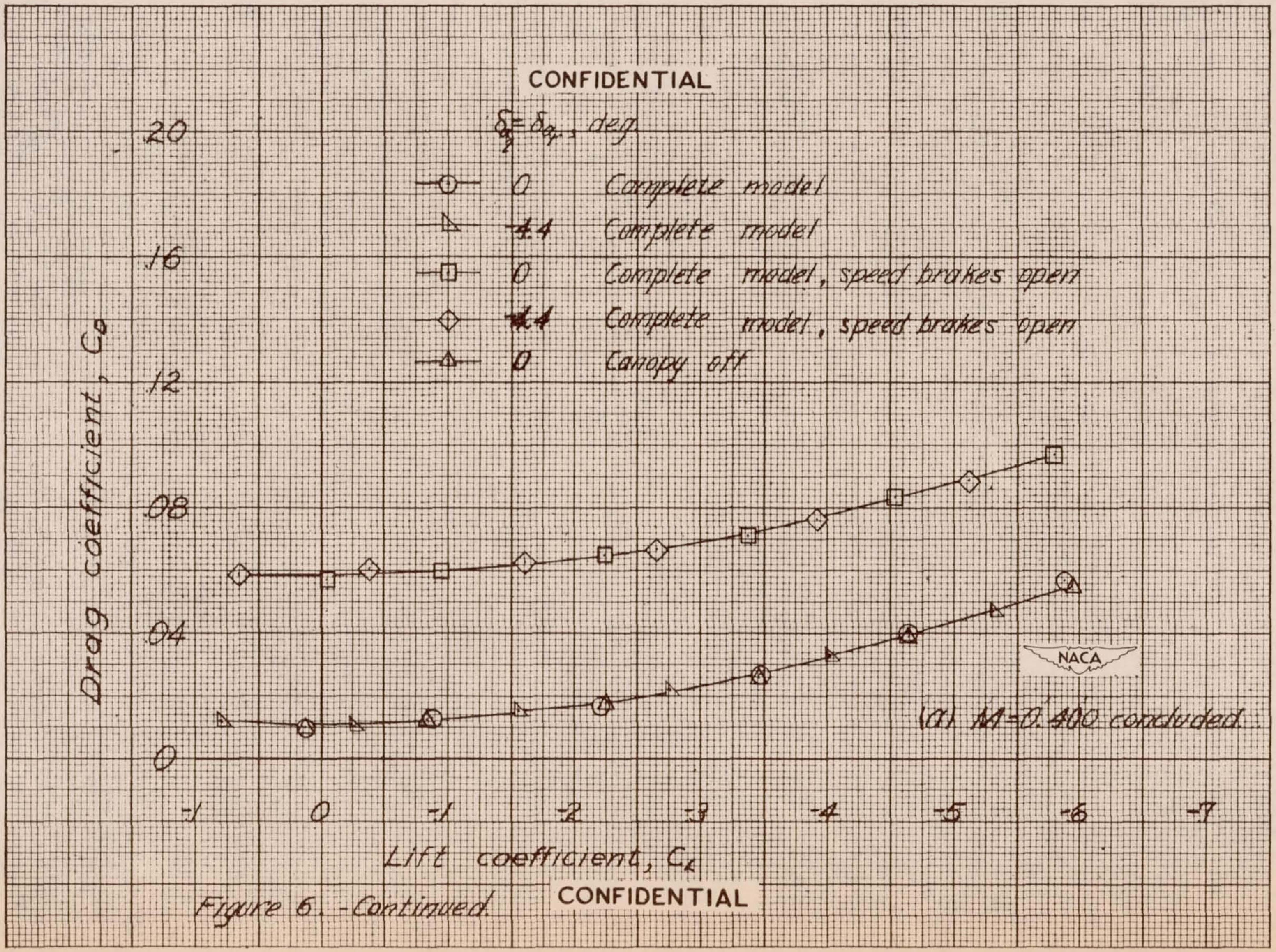

Figure 6. - Continued.

CONFIDENTIAL

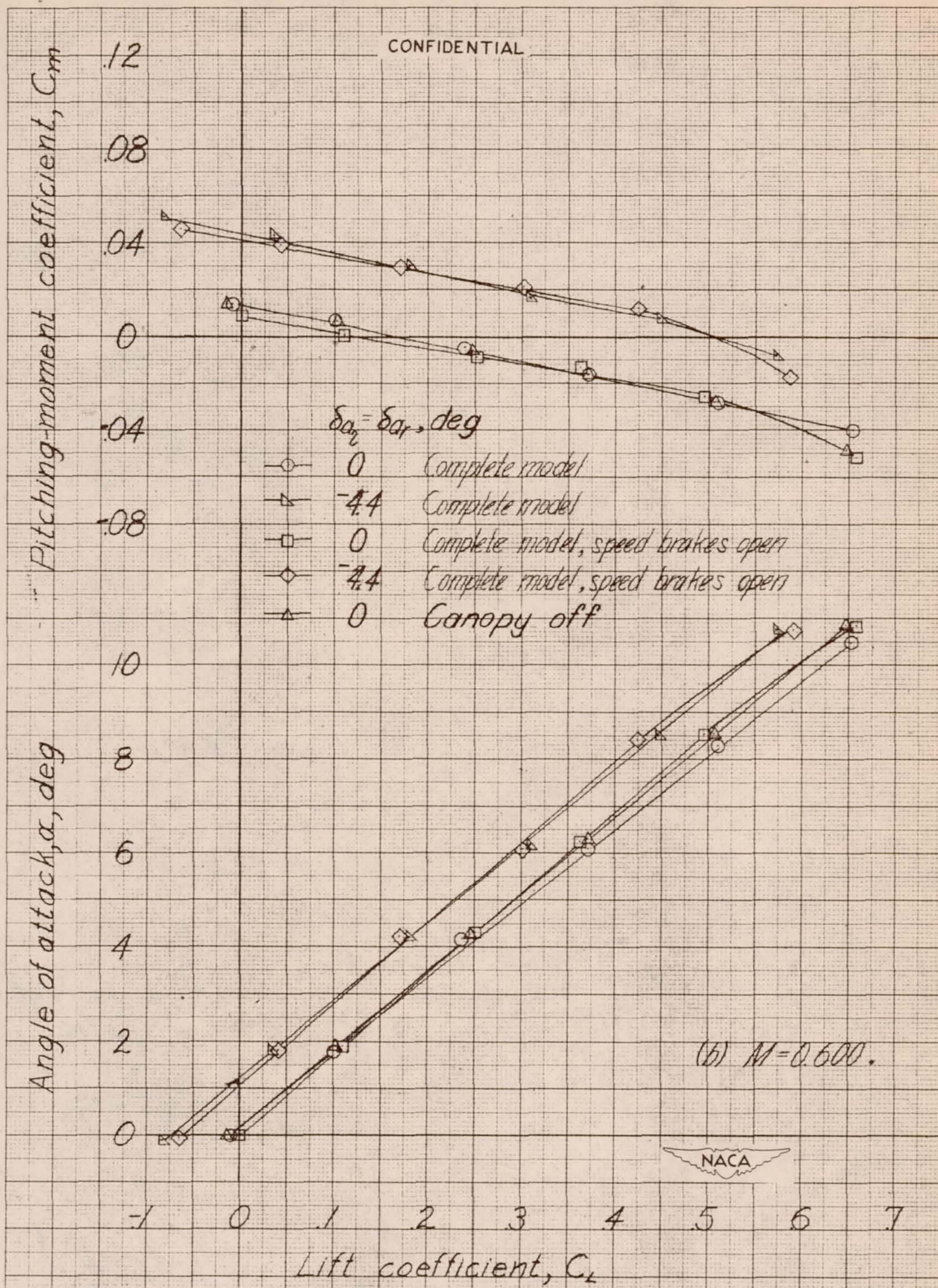

Figure 6. - Continued.

CONFIDENTIAL

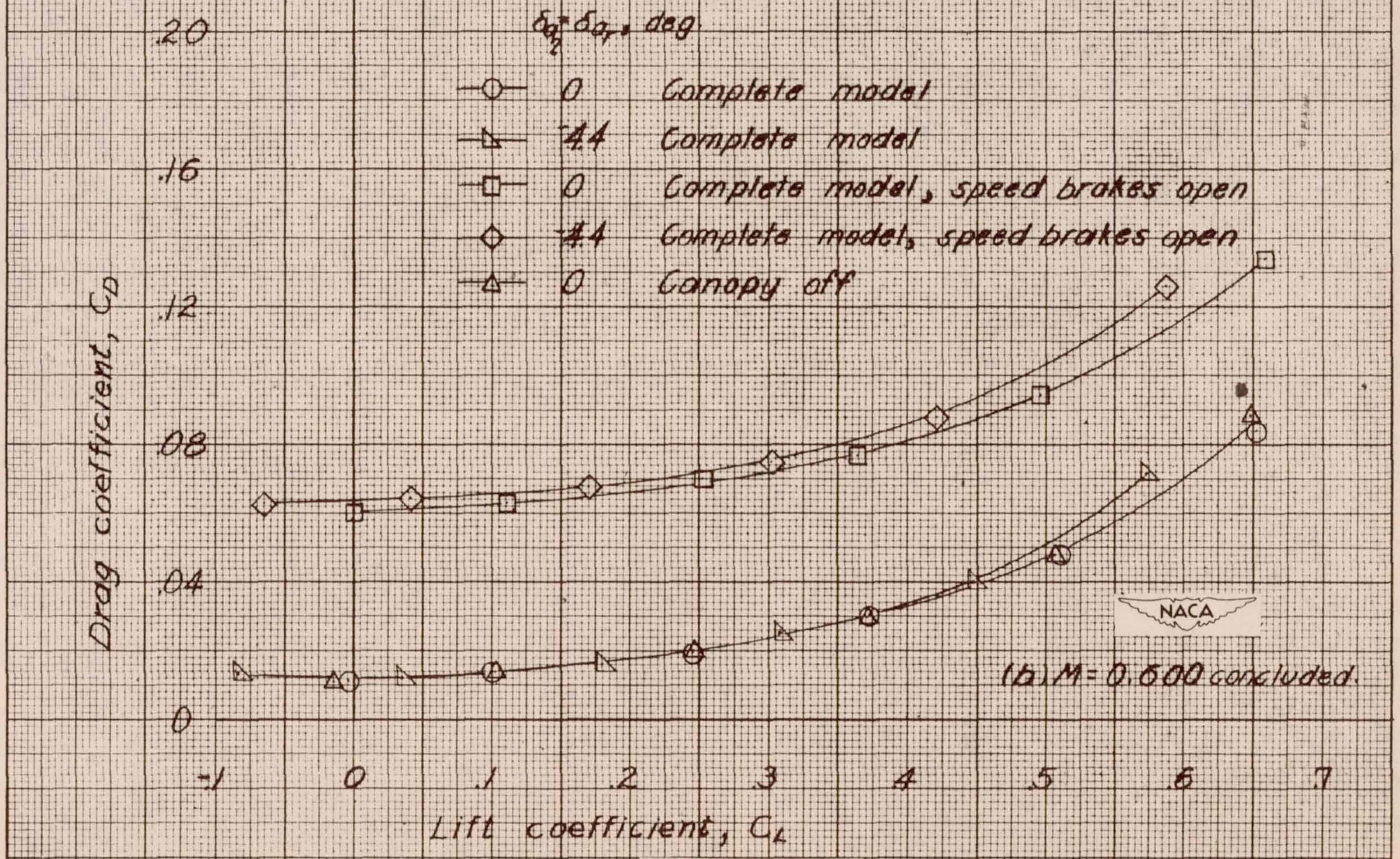

Figure 6. - Continued.

CONFIDENTIAL

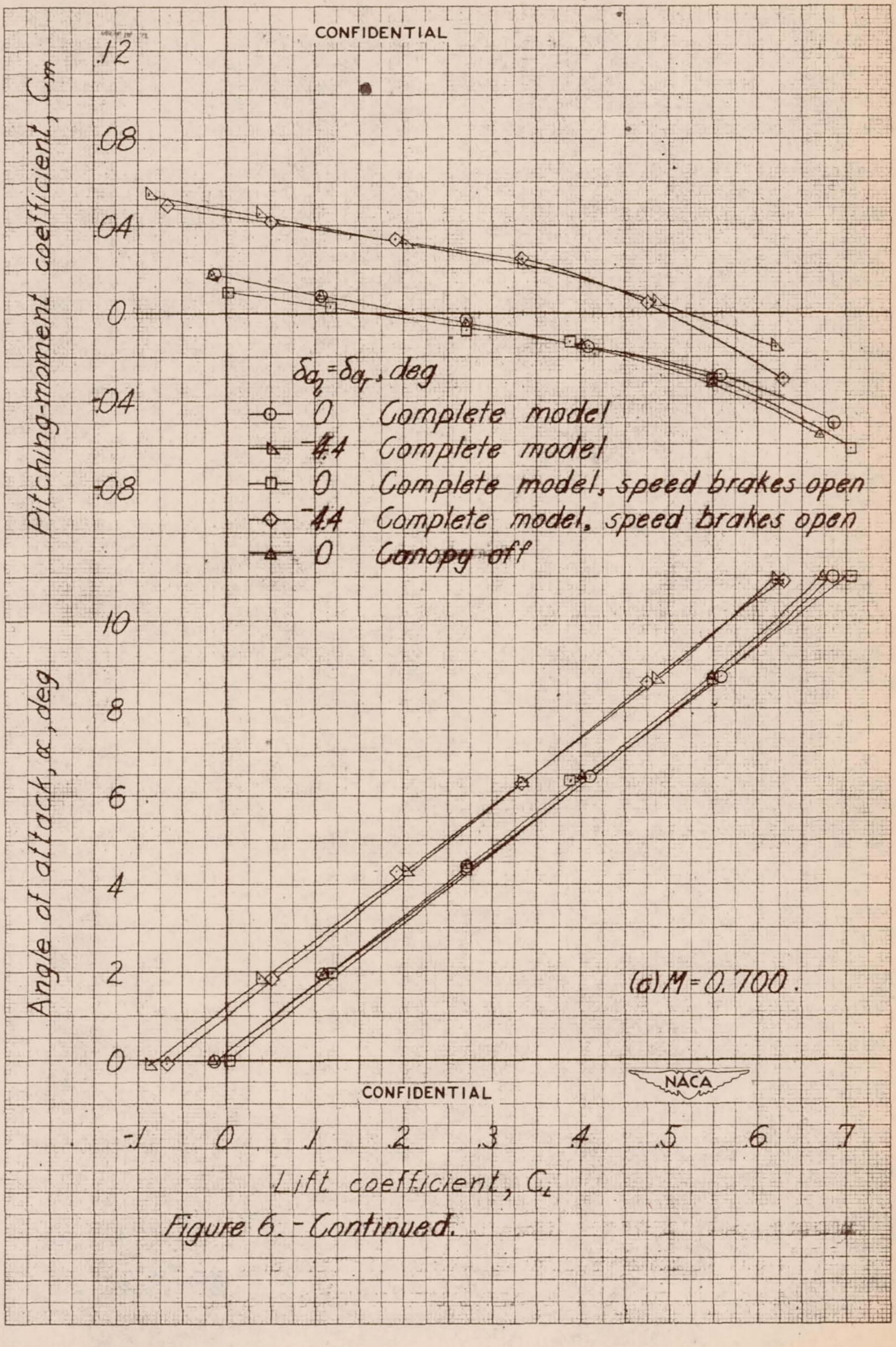

Figure 6. - Continued.

CONFIDENTIAL

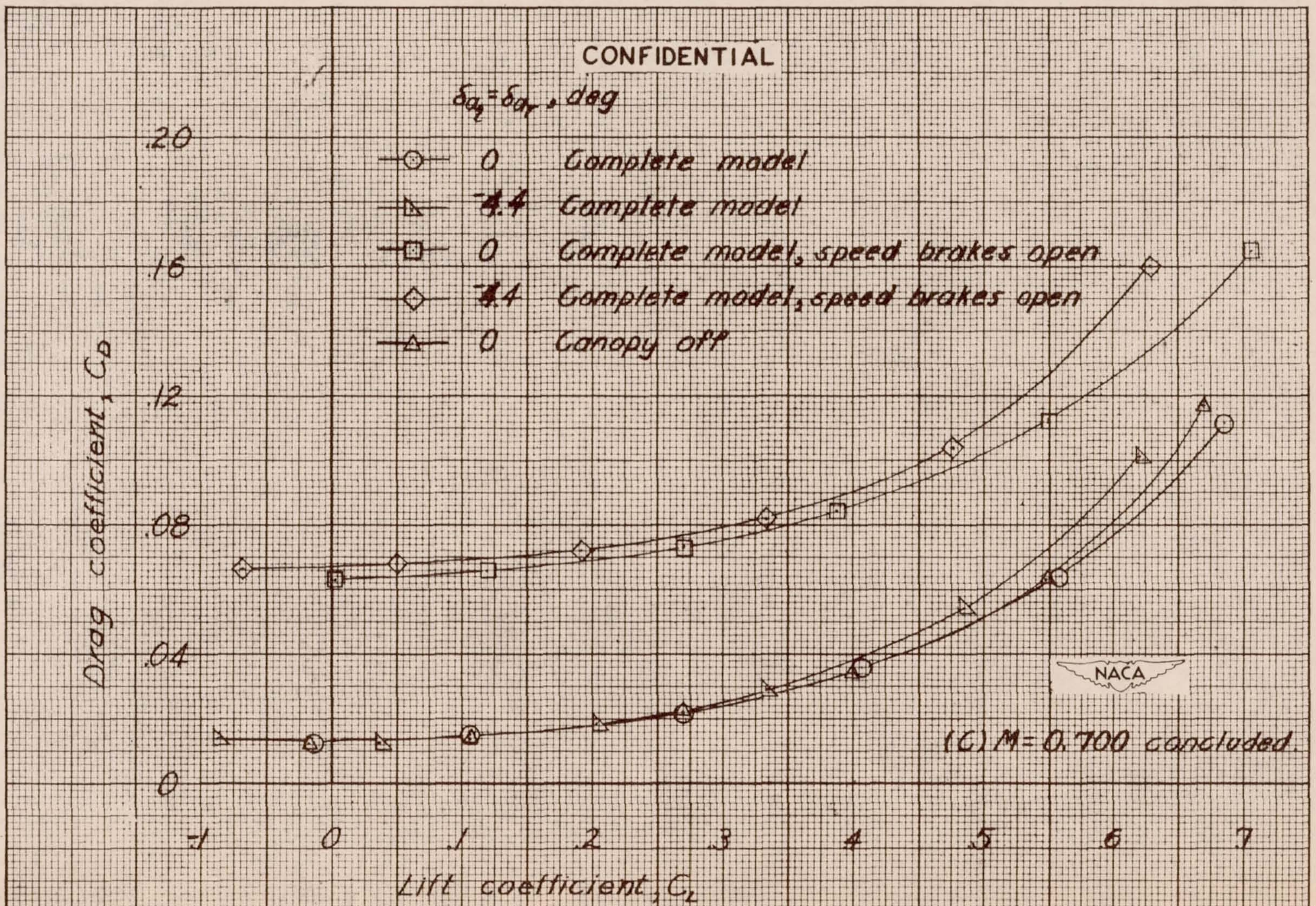

Figure 6. - Continued.

CONFIDENTIAL

CONFIDENTIAL

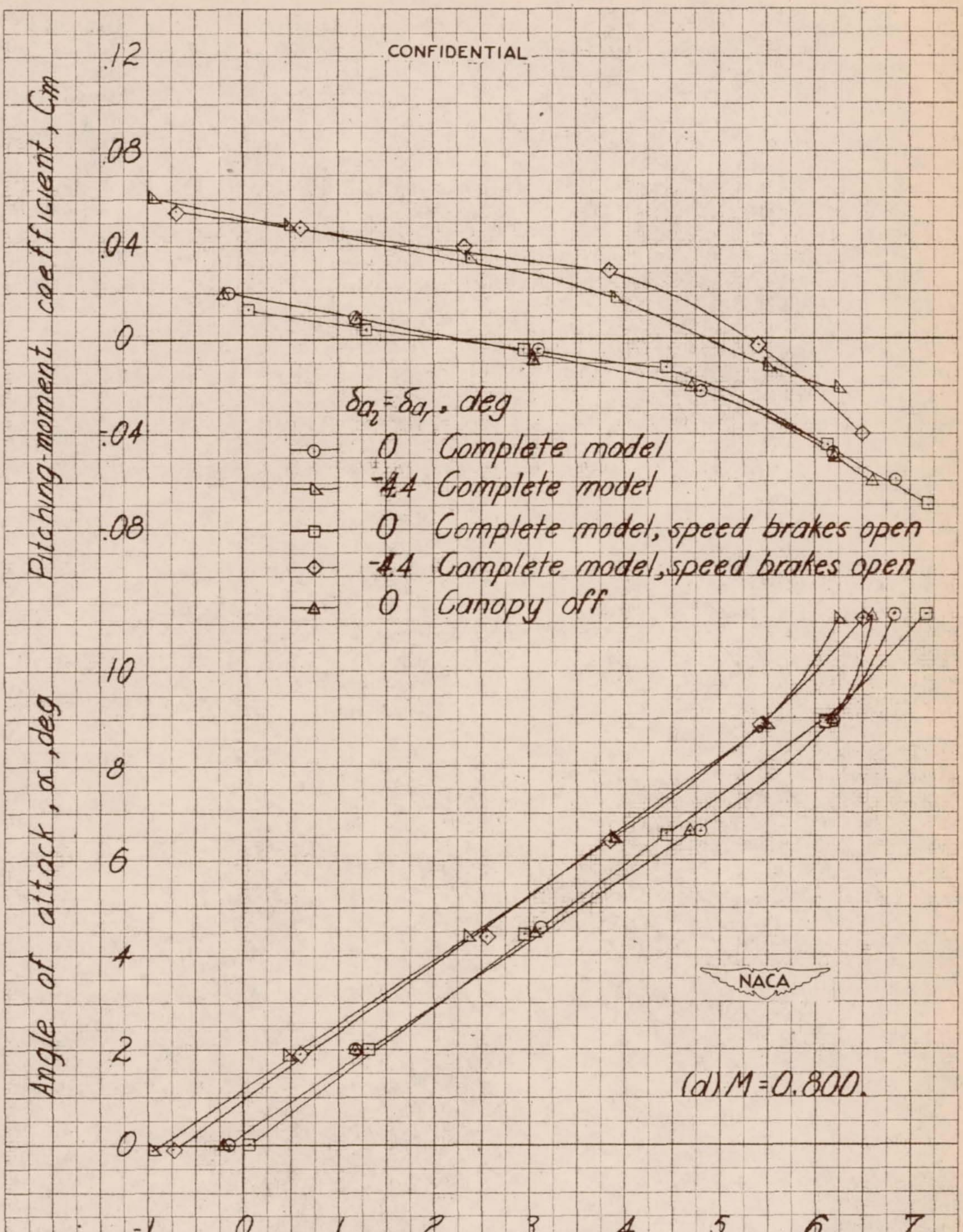

Figure 6.- Continued.

CONFIDENTIAL

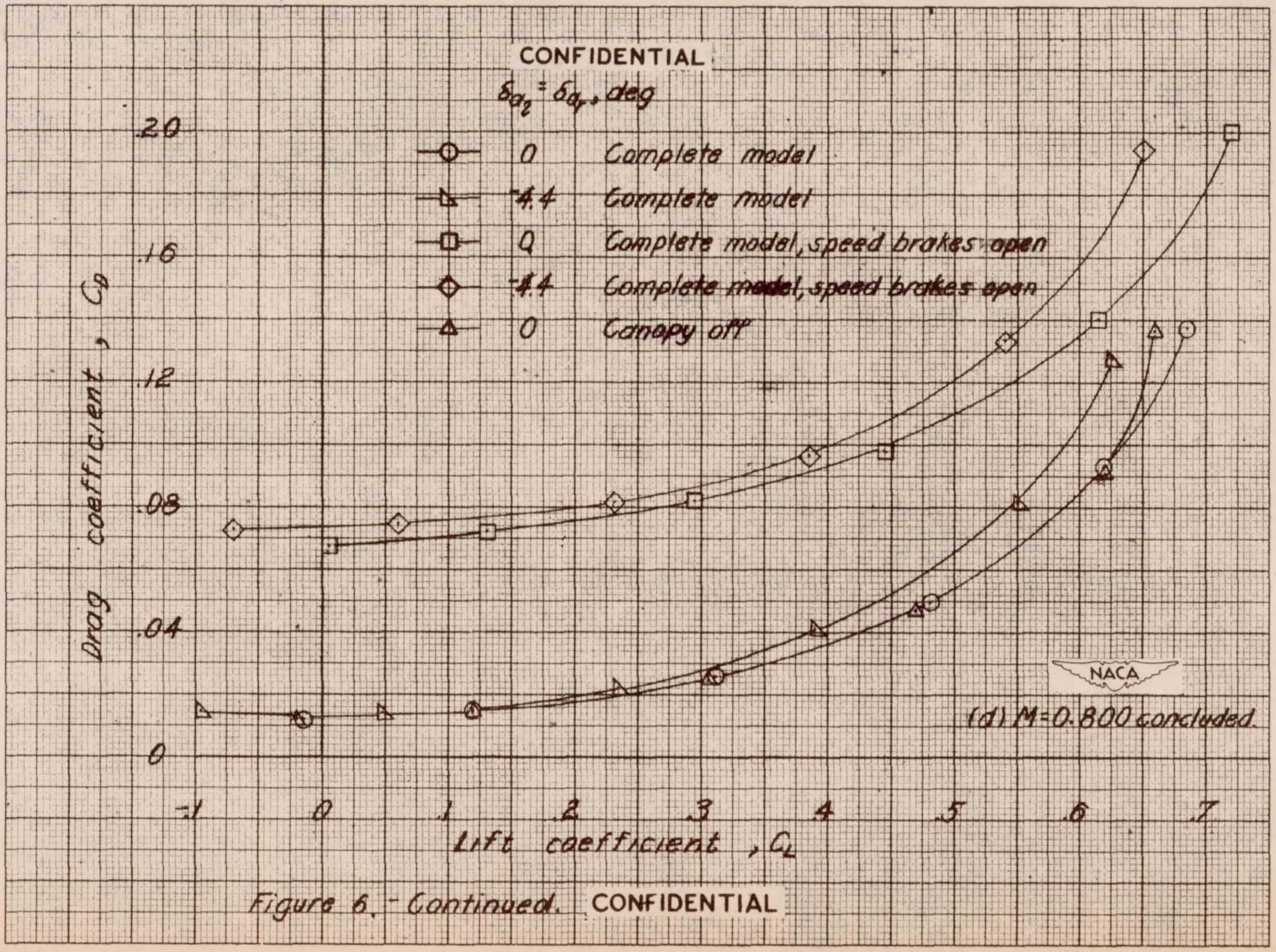

Figure 6. - Continued. CONFIDENTIAL

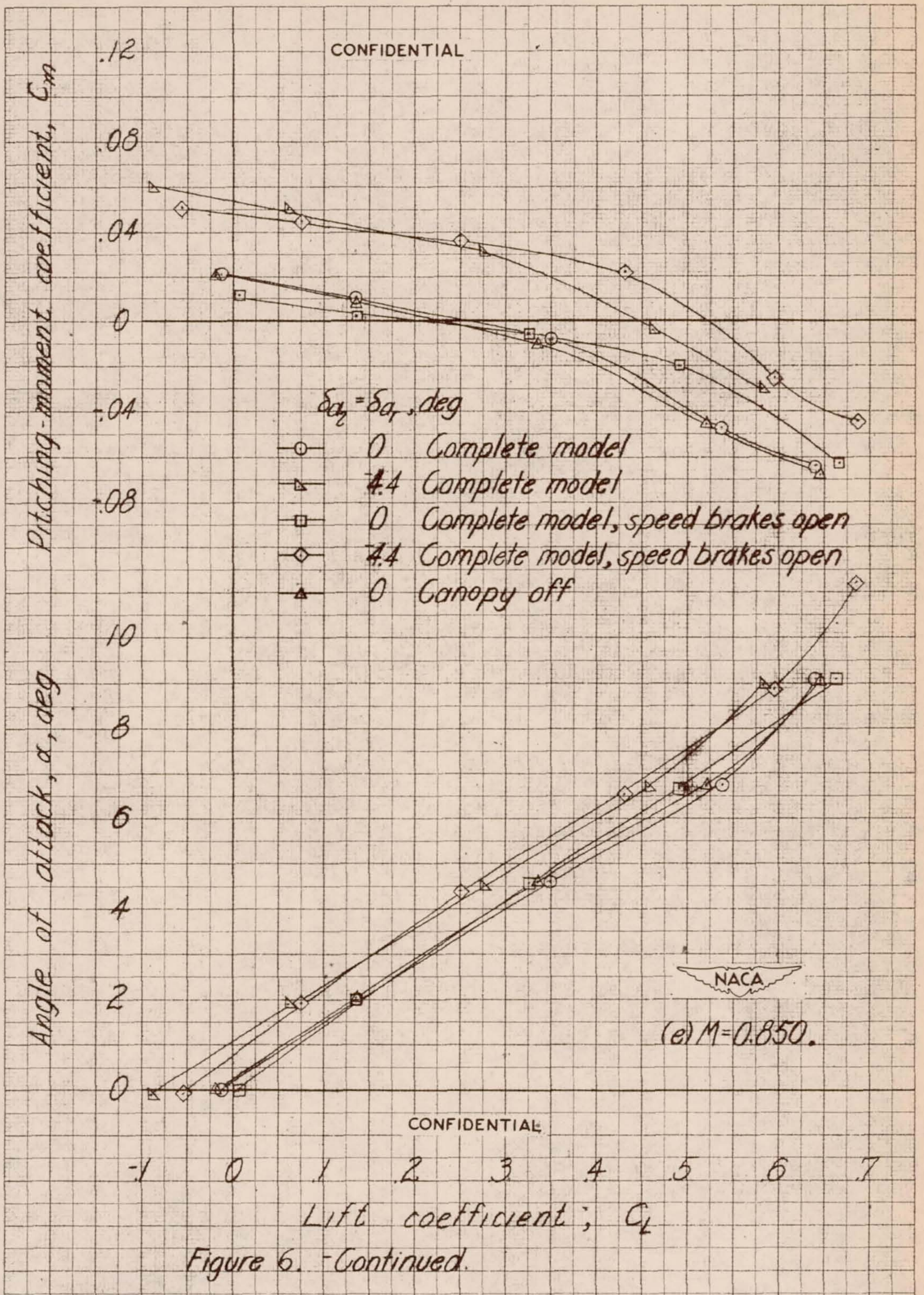

Figure 6. - Continued.

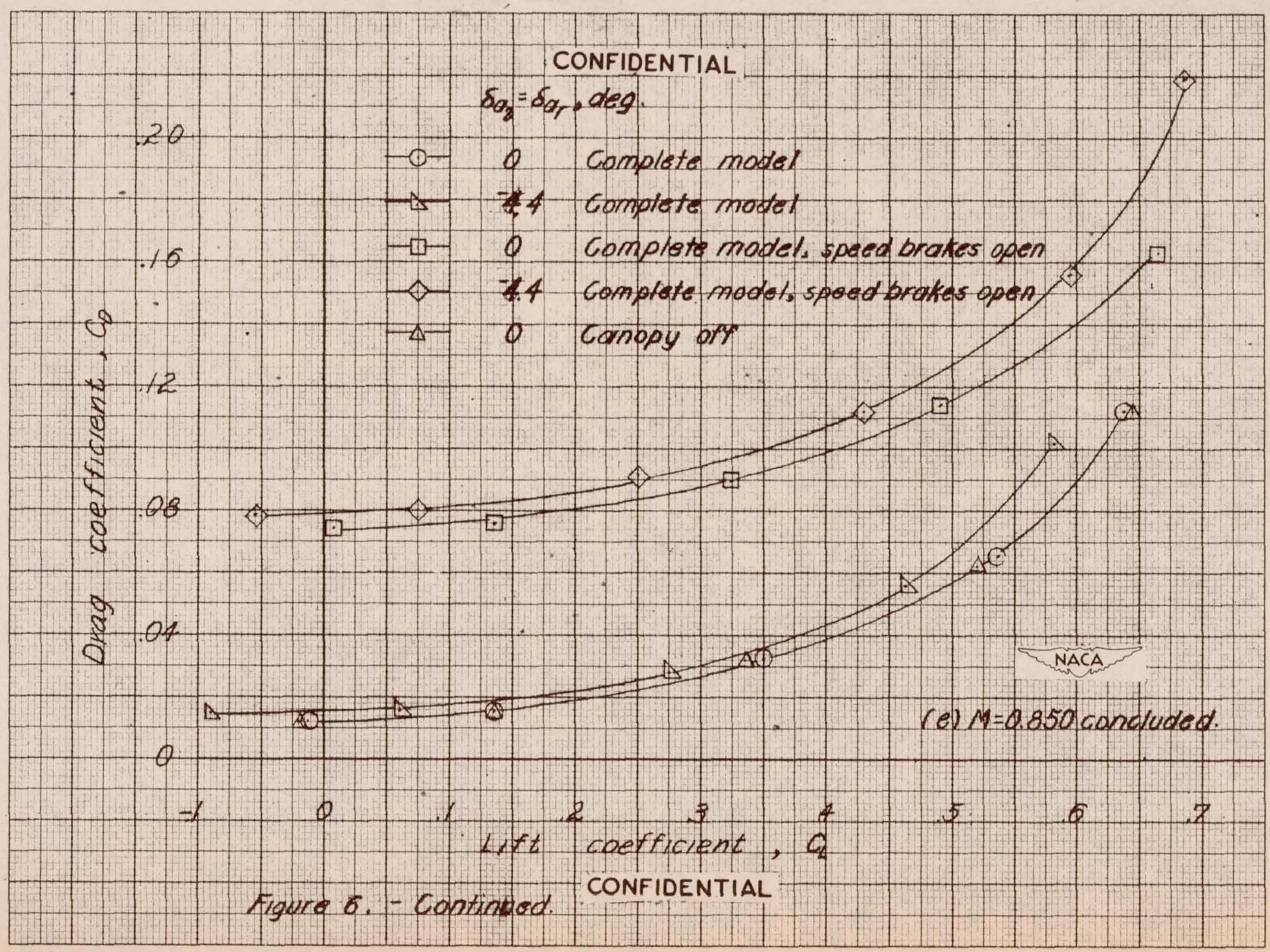

Figure 6. - Continued.

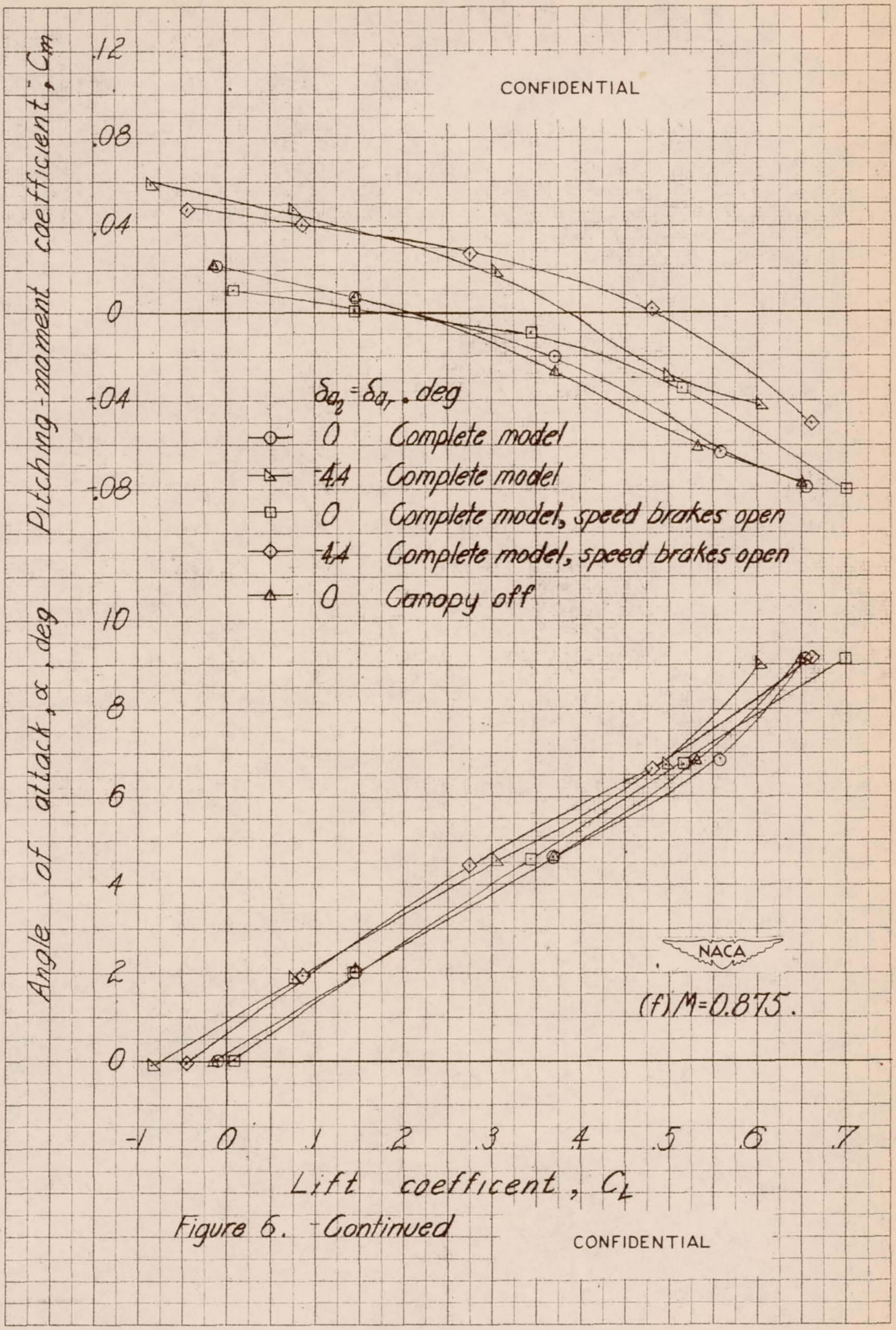

Figure 6. - Continued

CONFIDENTIAL

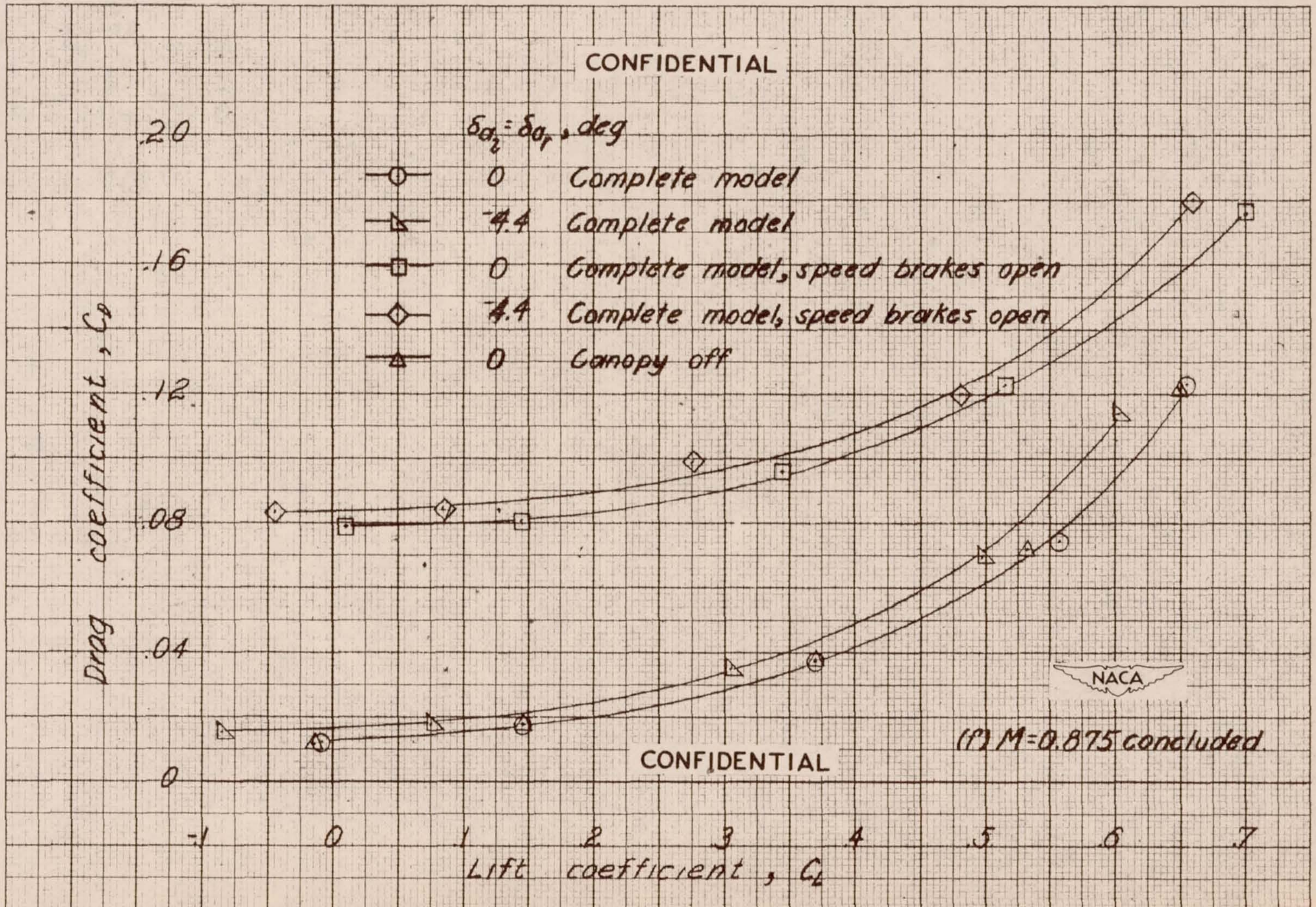

Figure 6. - Continued.

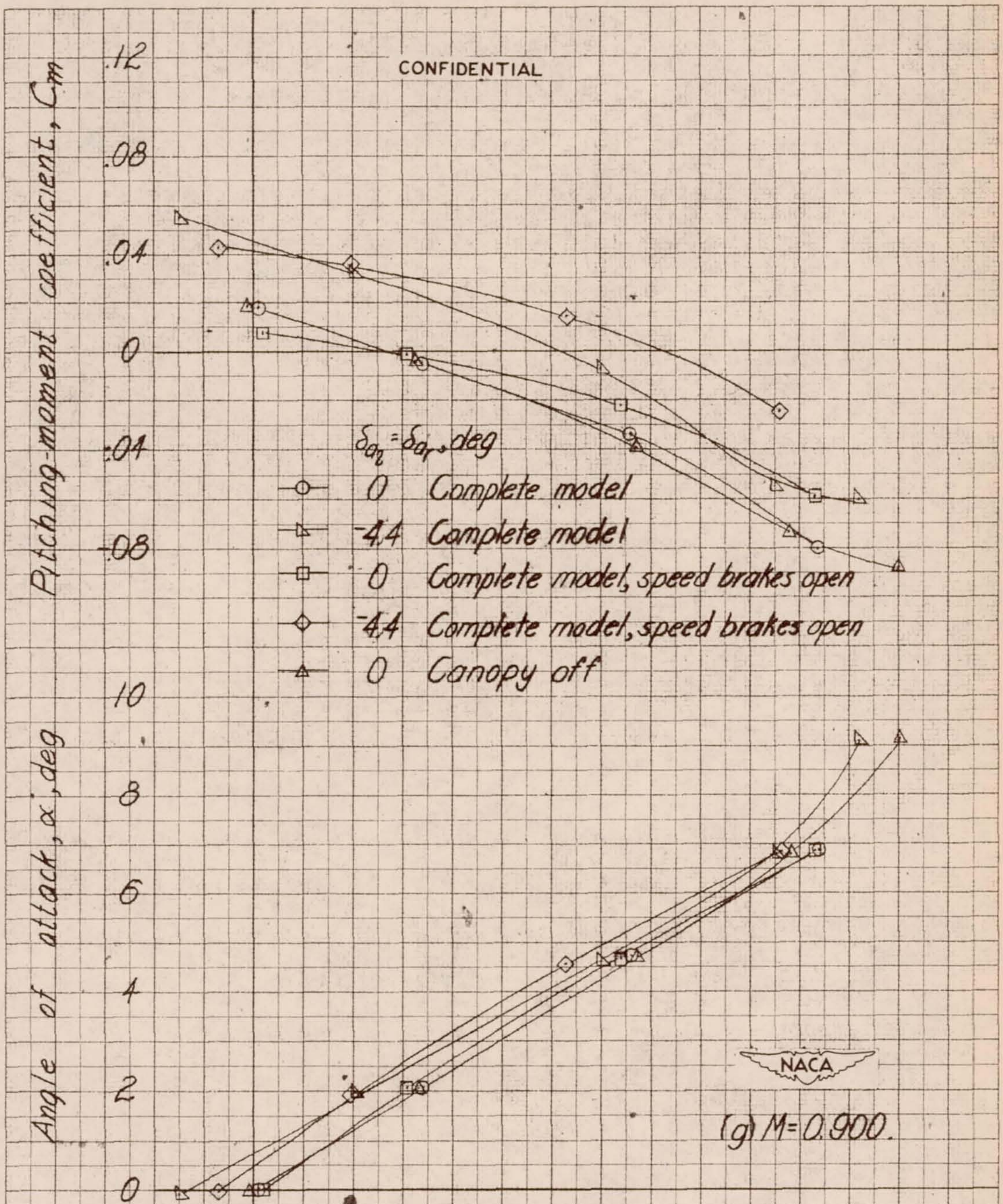

Figure 6. - Continued.

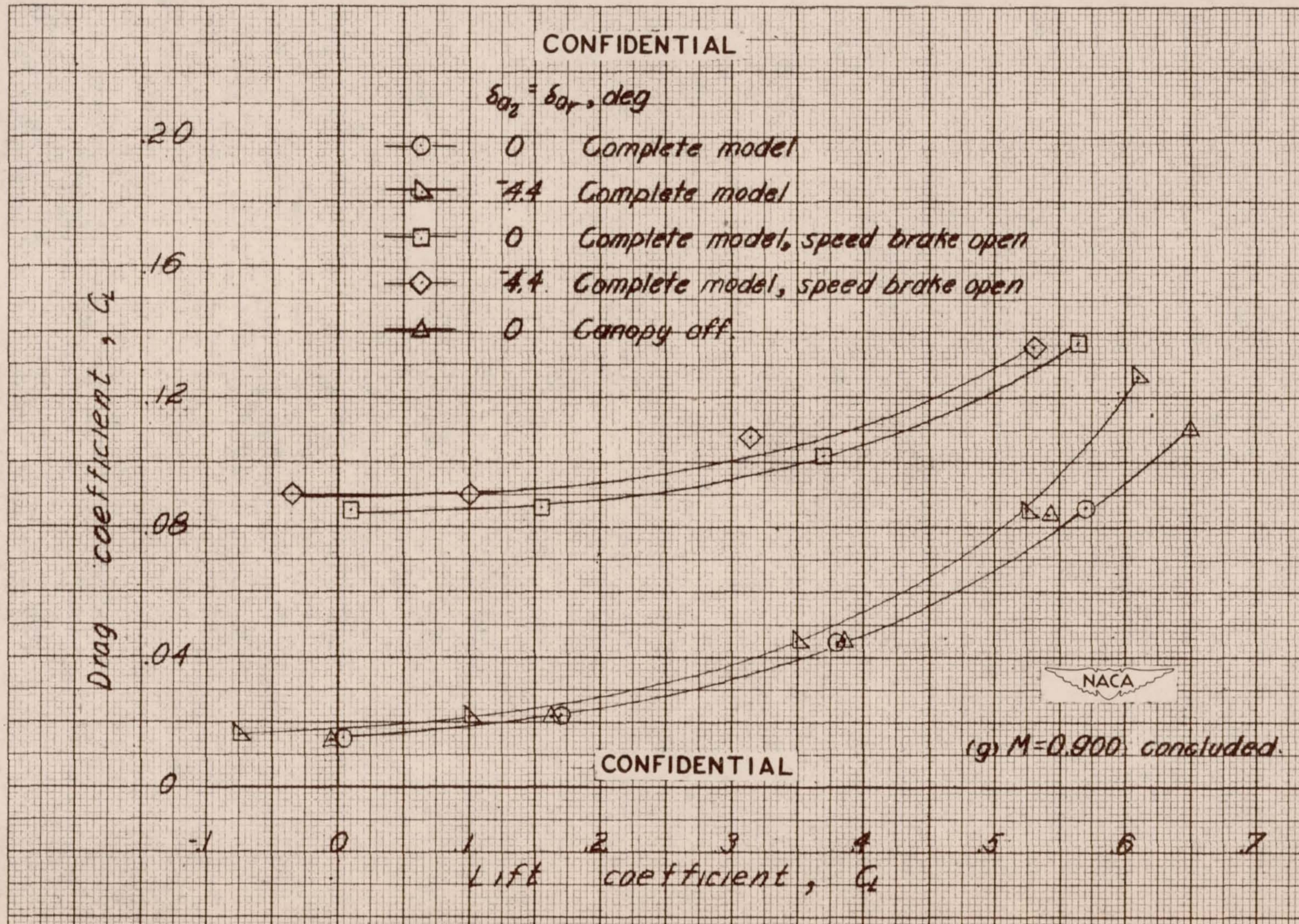

(g) M = 0.900; concluded.

Figure 6. - Continued.

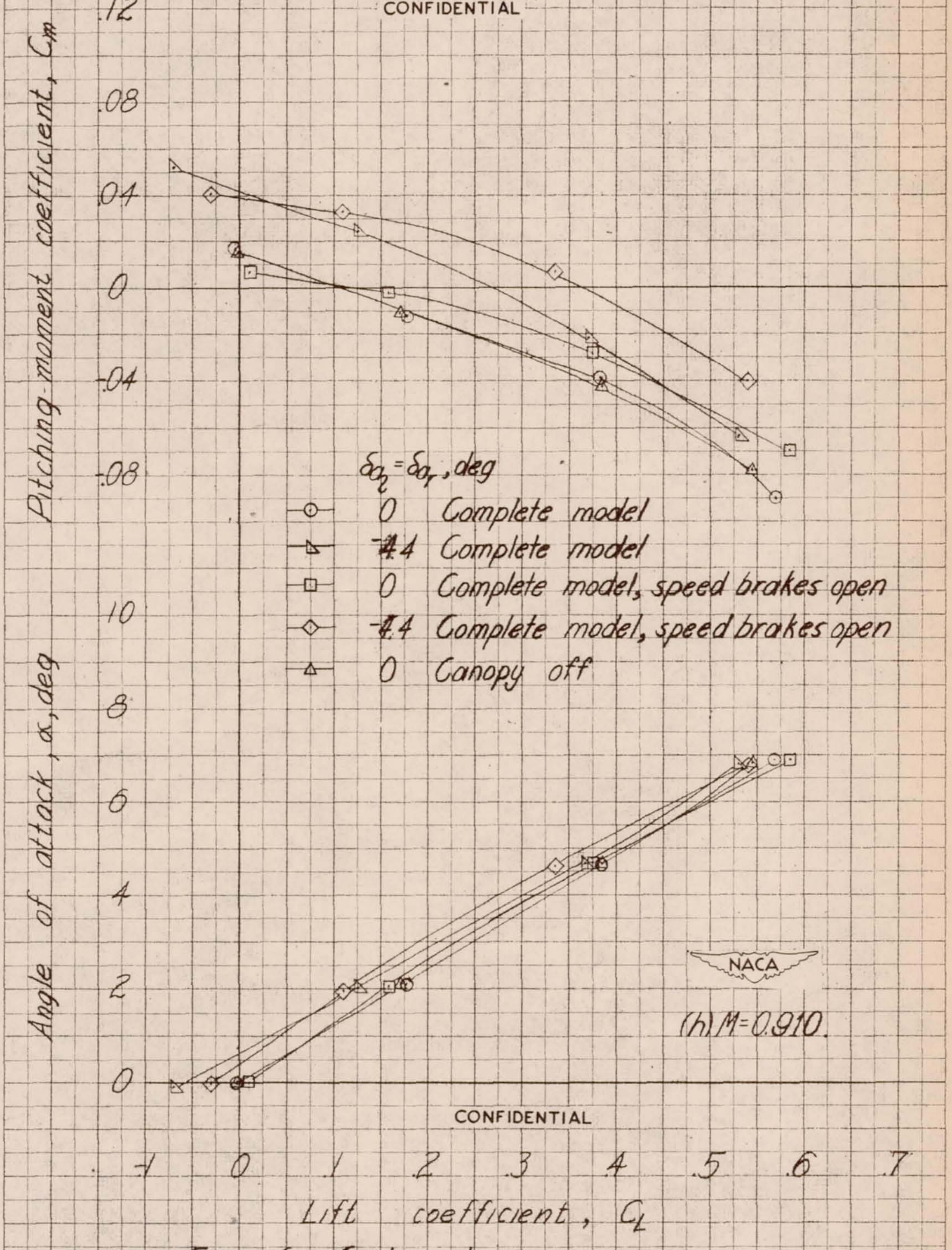

Figure 6. - Continued.

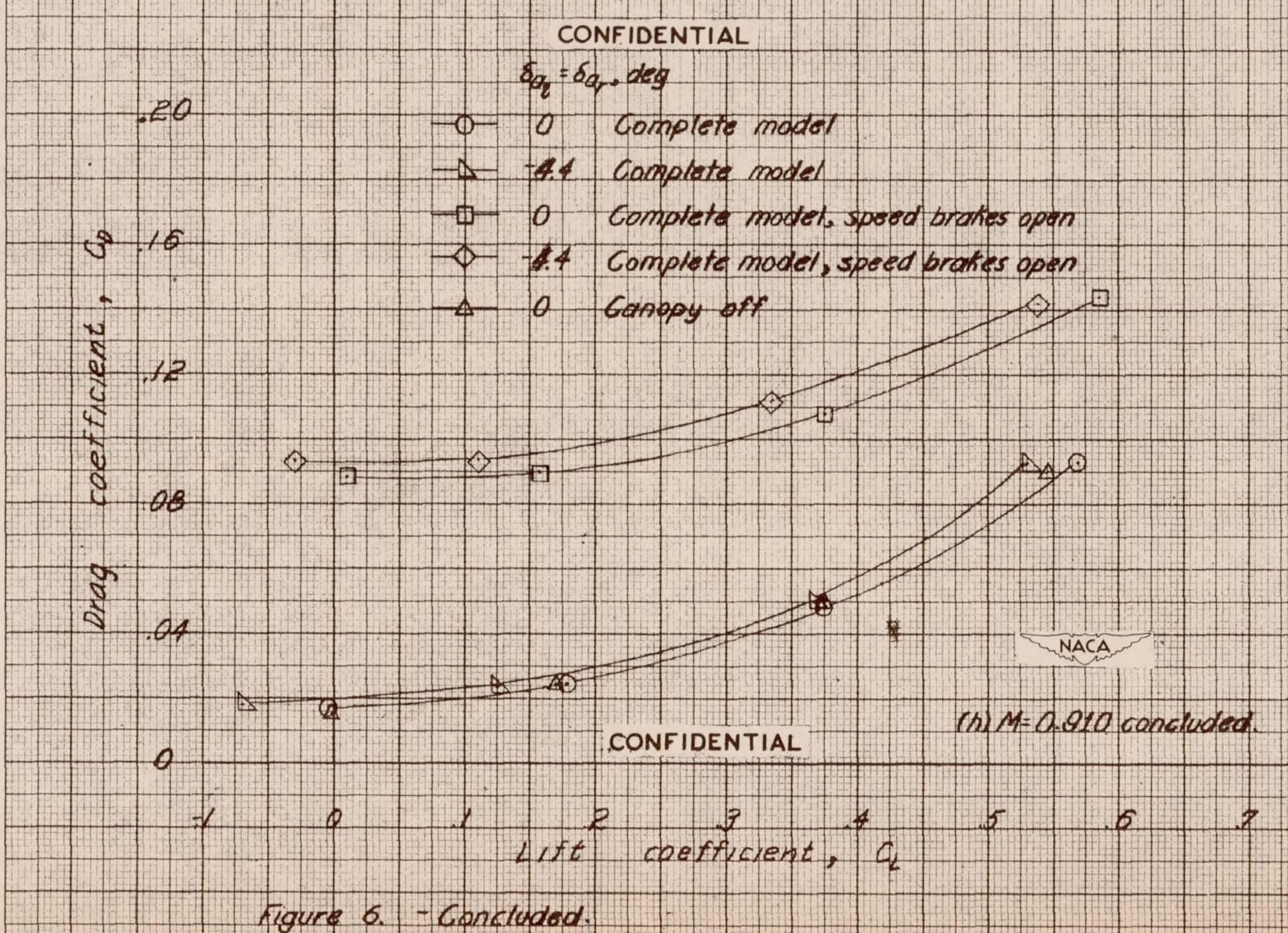

Figure 6. - Concluded.

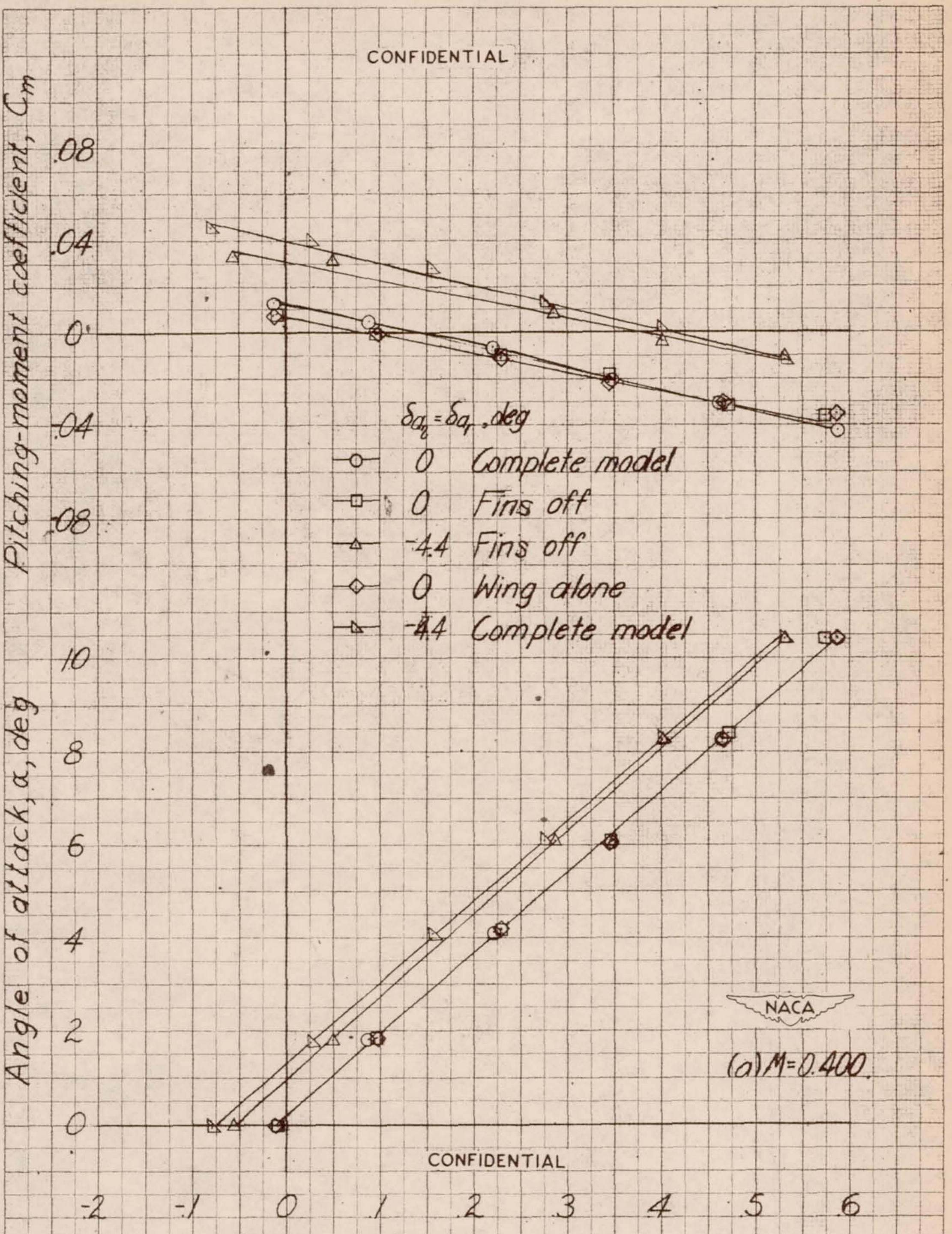

Figure 7. - Fins off and wing alone characteristics of the 0.08-scale model of the Chance Vought XF7U-1 airplane.

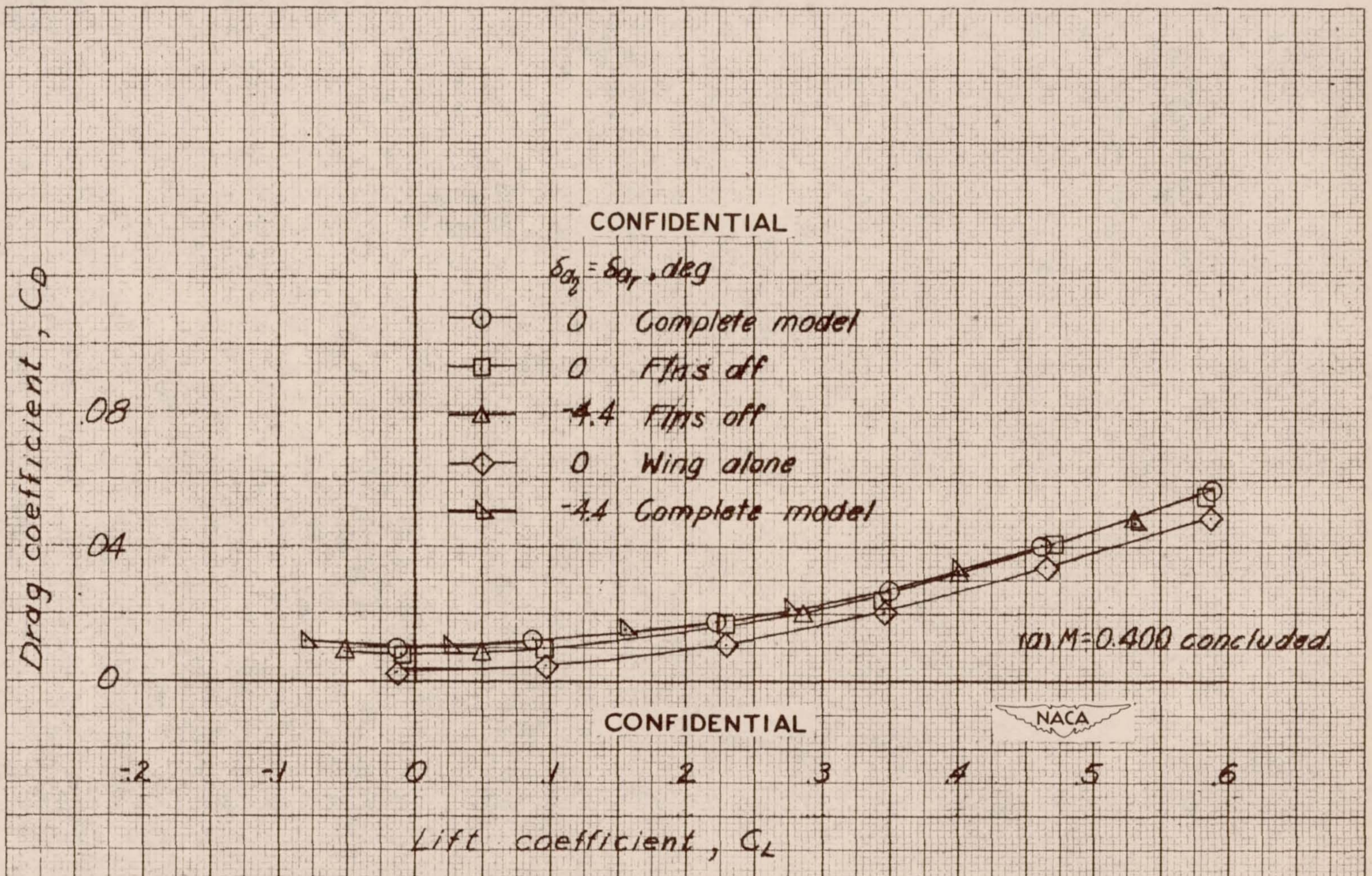

Figure 7. - Continued.

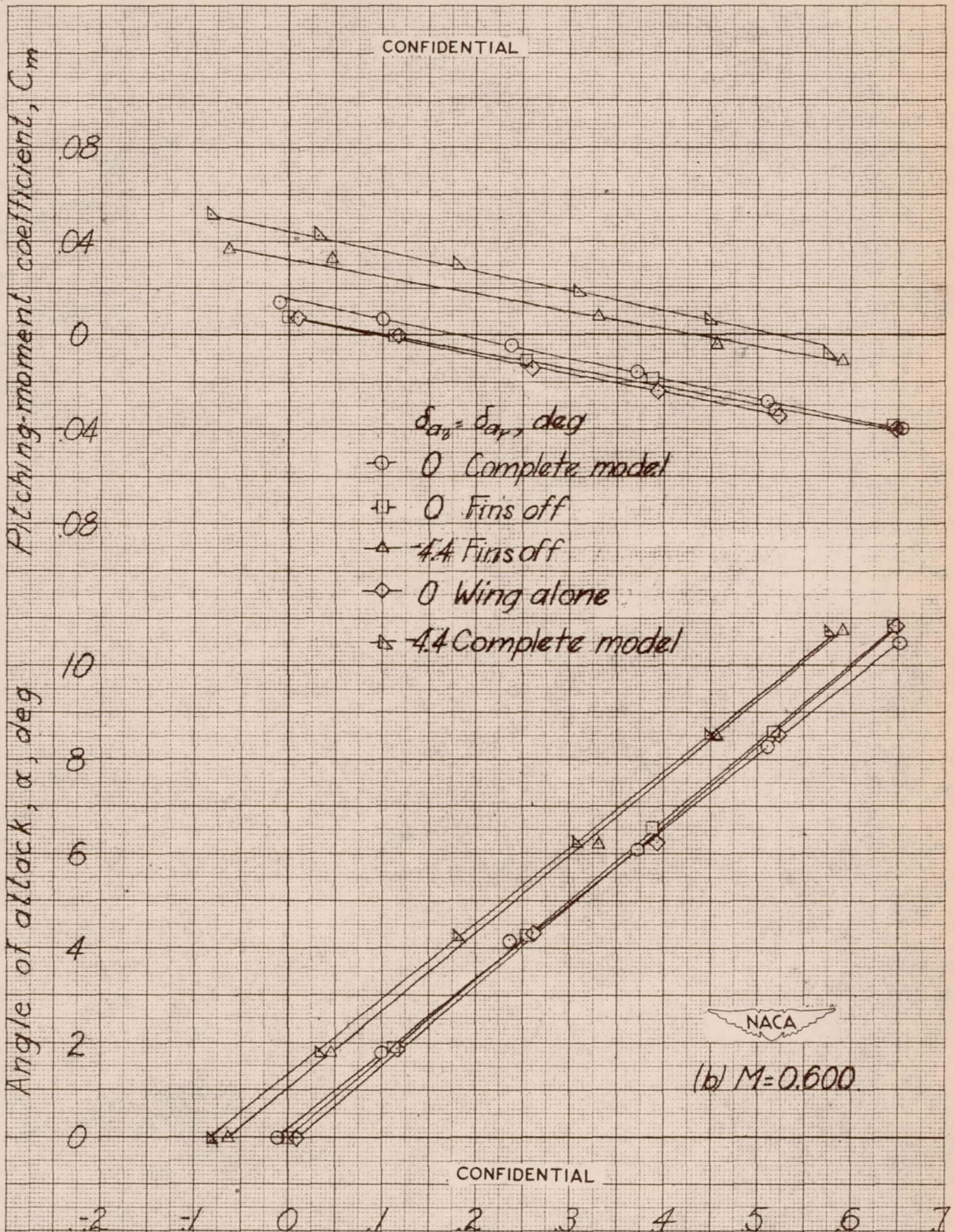

Figure 7. -Continued.

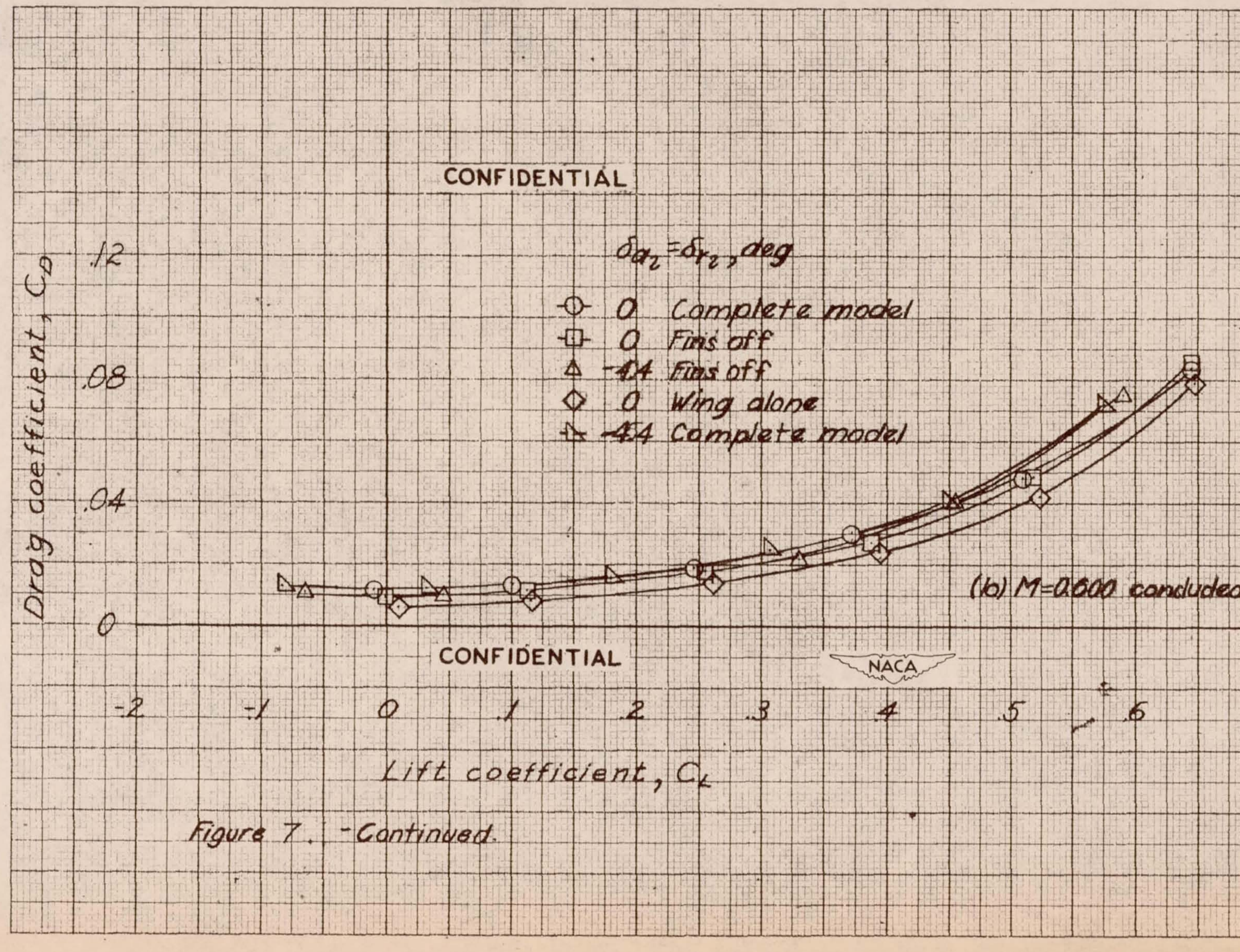

Figure 7. - Continued.

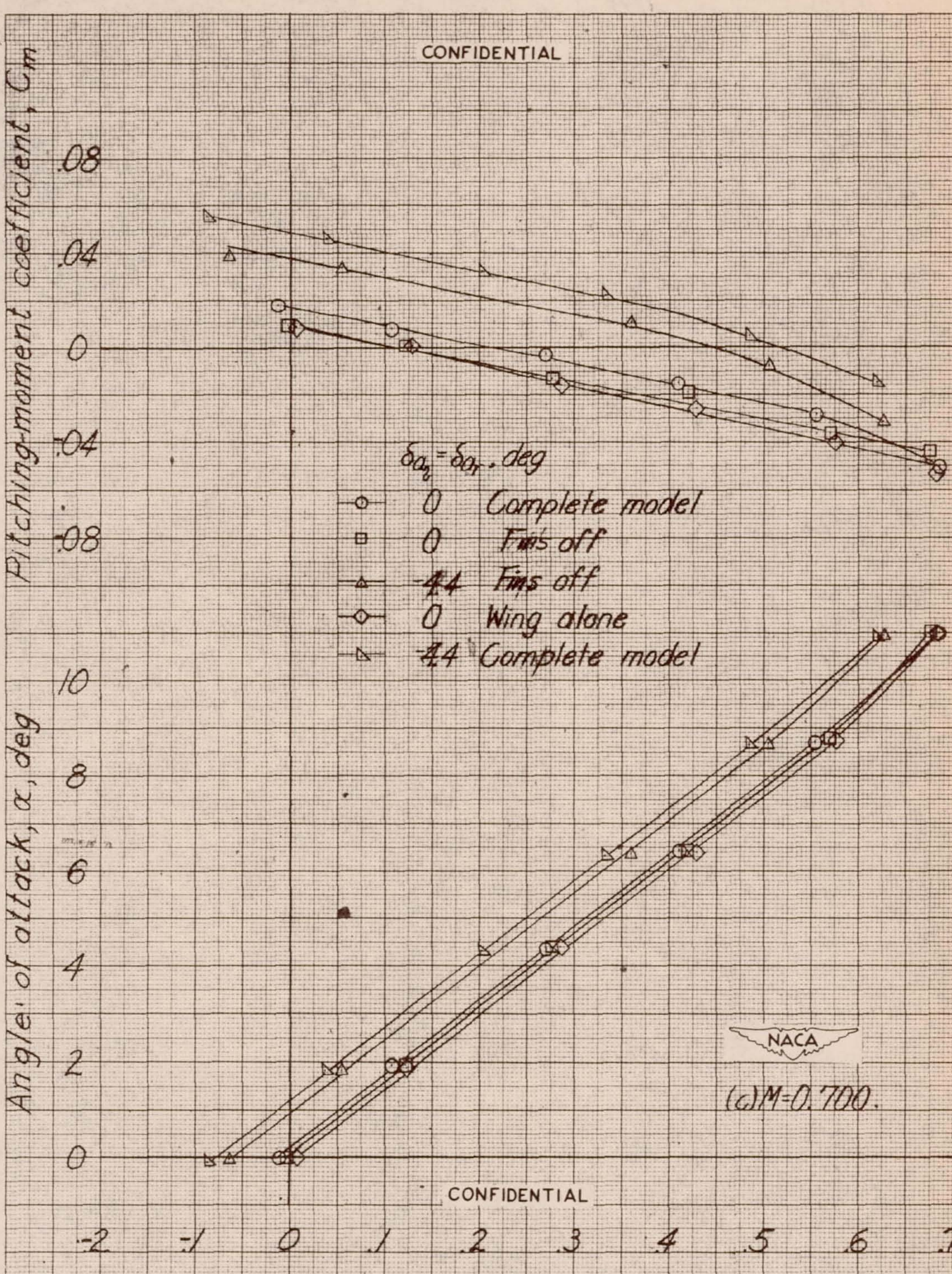

Figure 7.- Continued.

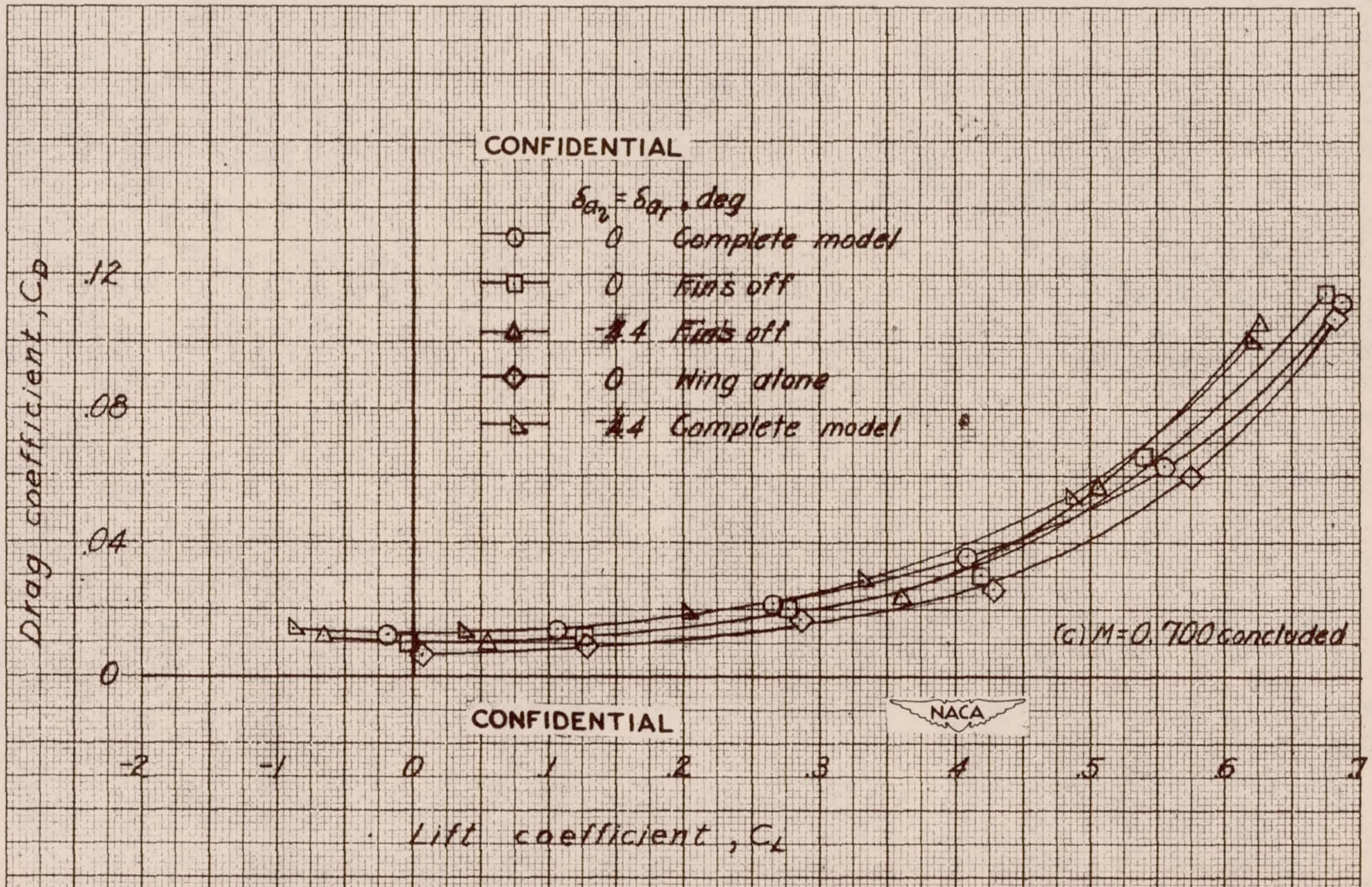

Figure 7. - Continued.

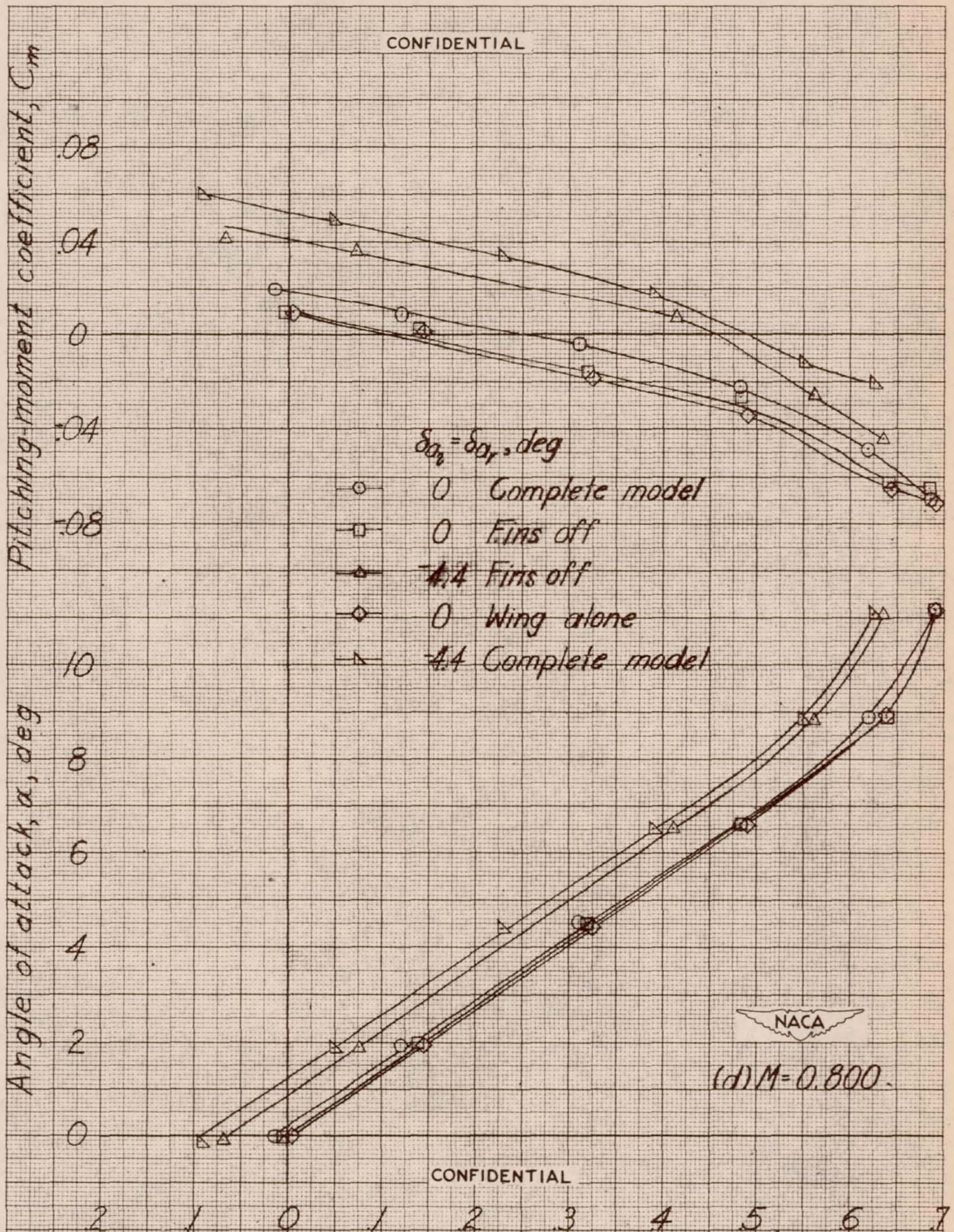

Figure 7. -Continued.

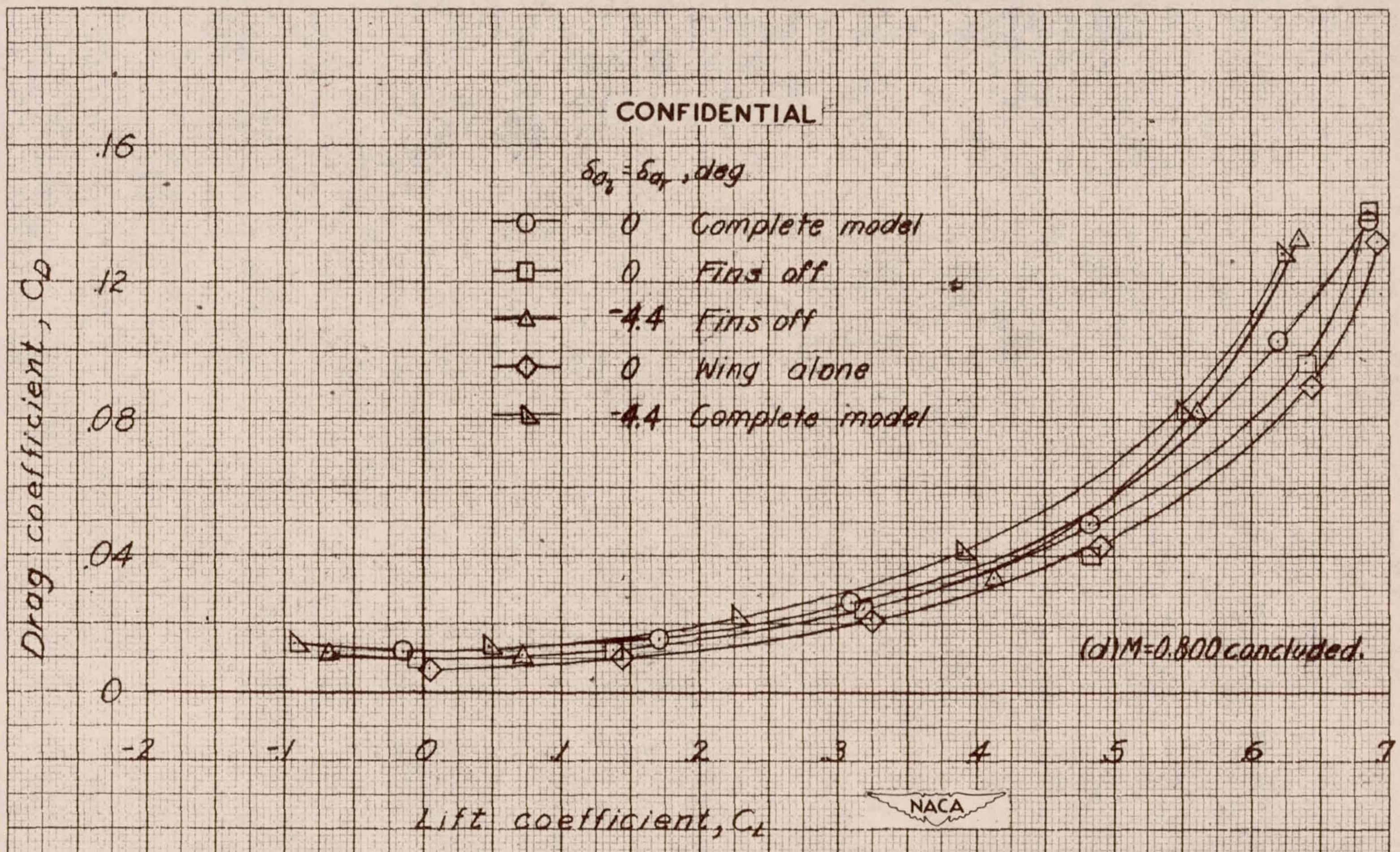

Figure 7. - Continued.

CONFIDENTIAL

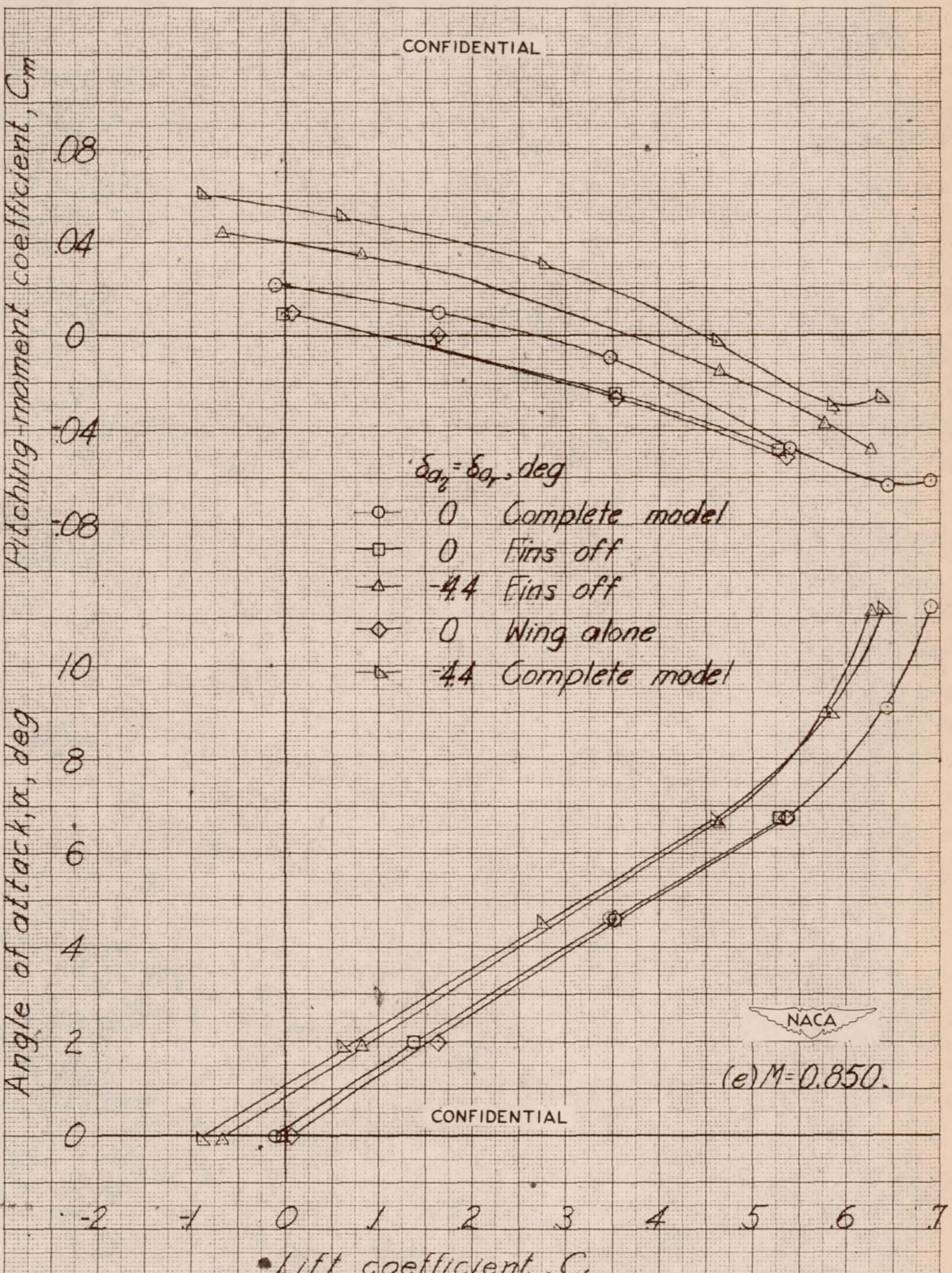

Figure 7. - Continued.

CONFIDENTIAL

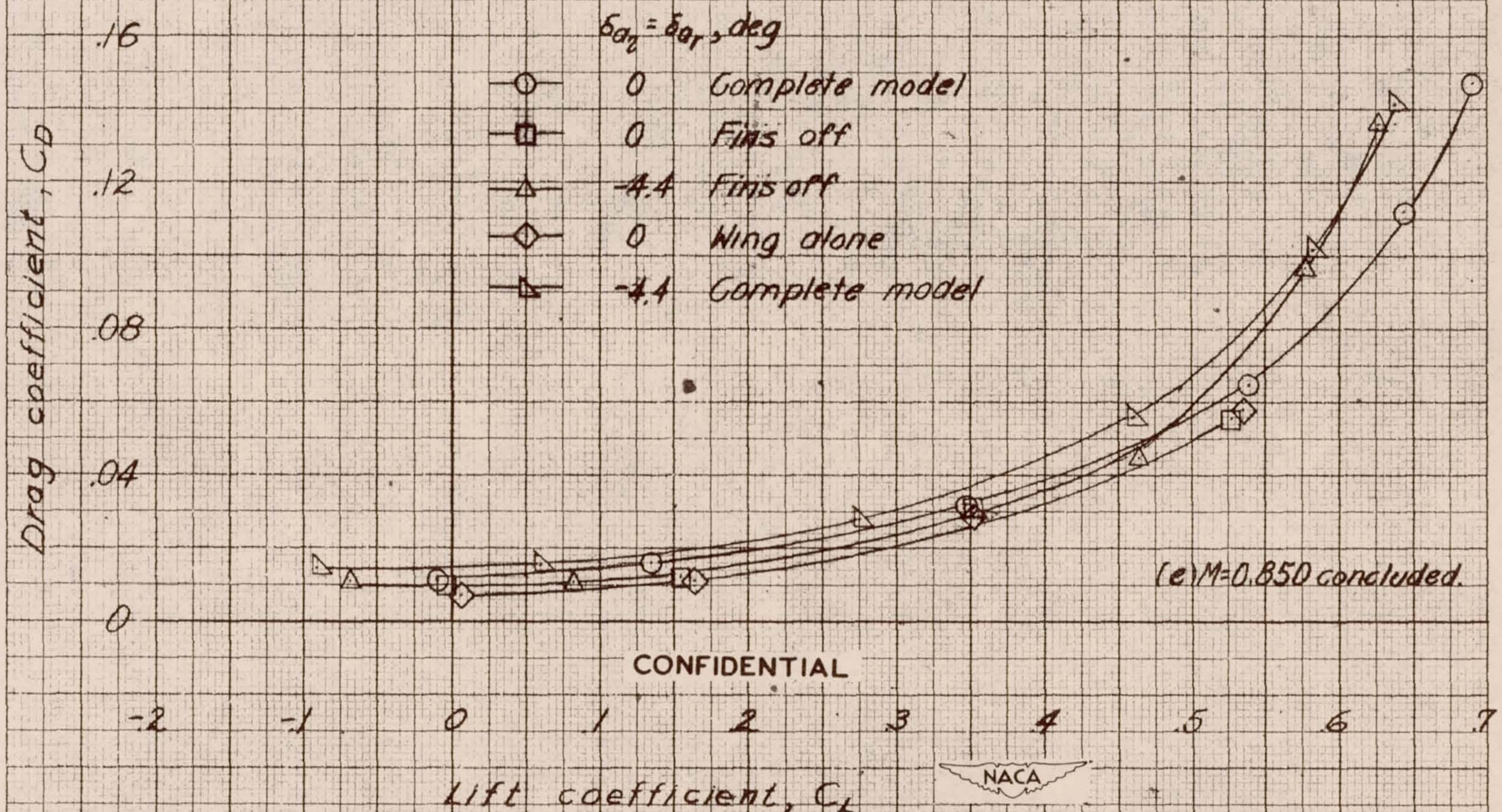

CONFIDENTIAL

Figure 7. -Continued.

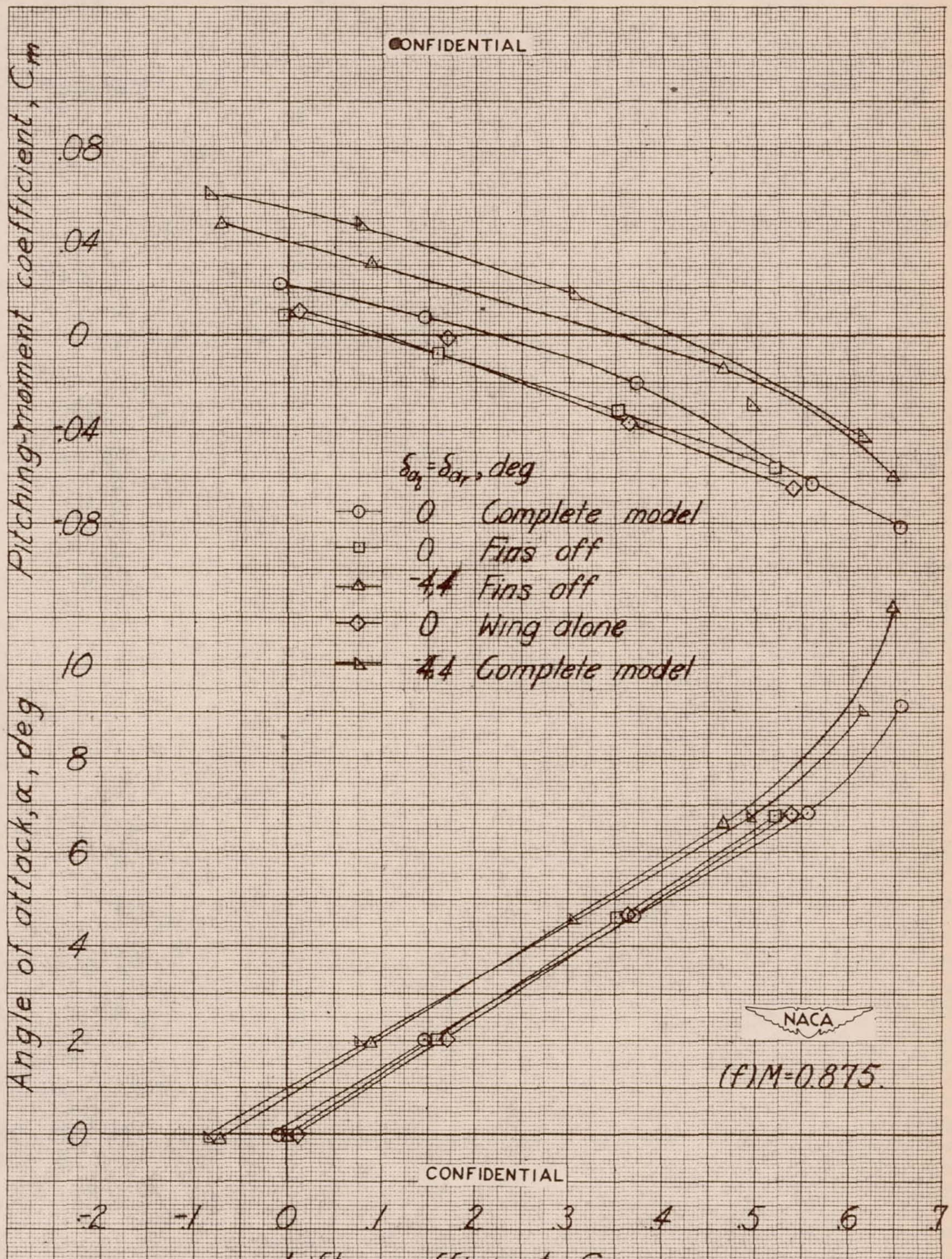

Figure 7.- Continued.

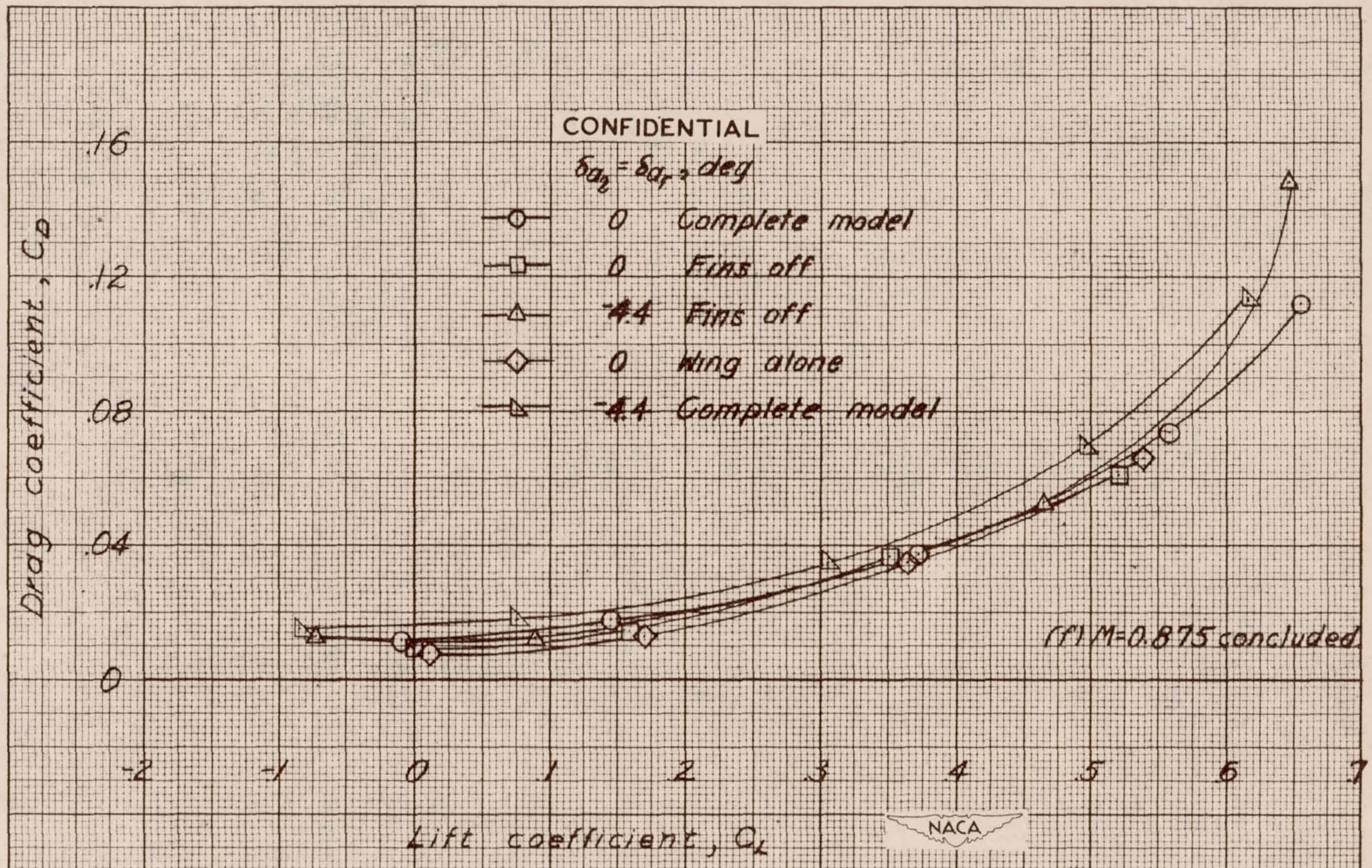

Figure 7. - Continued.

CONFIDENTIAL

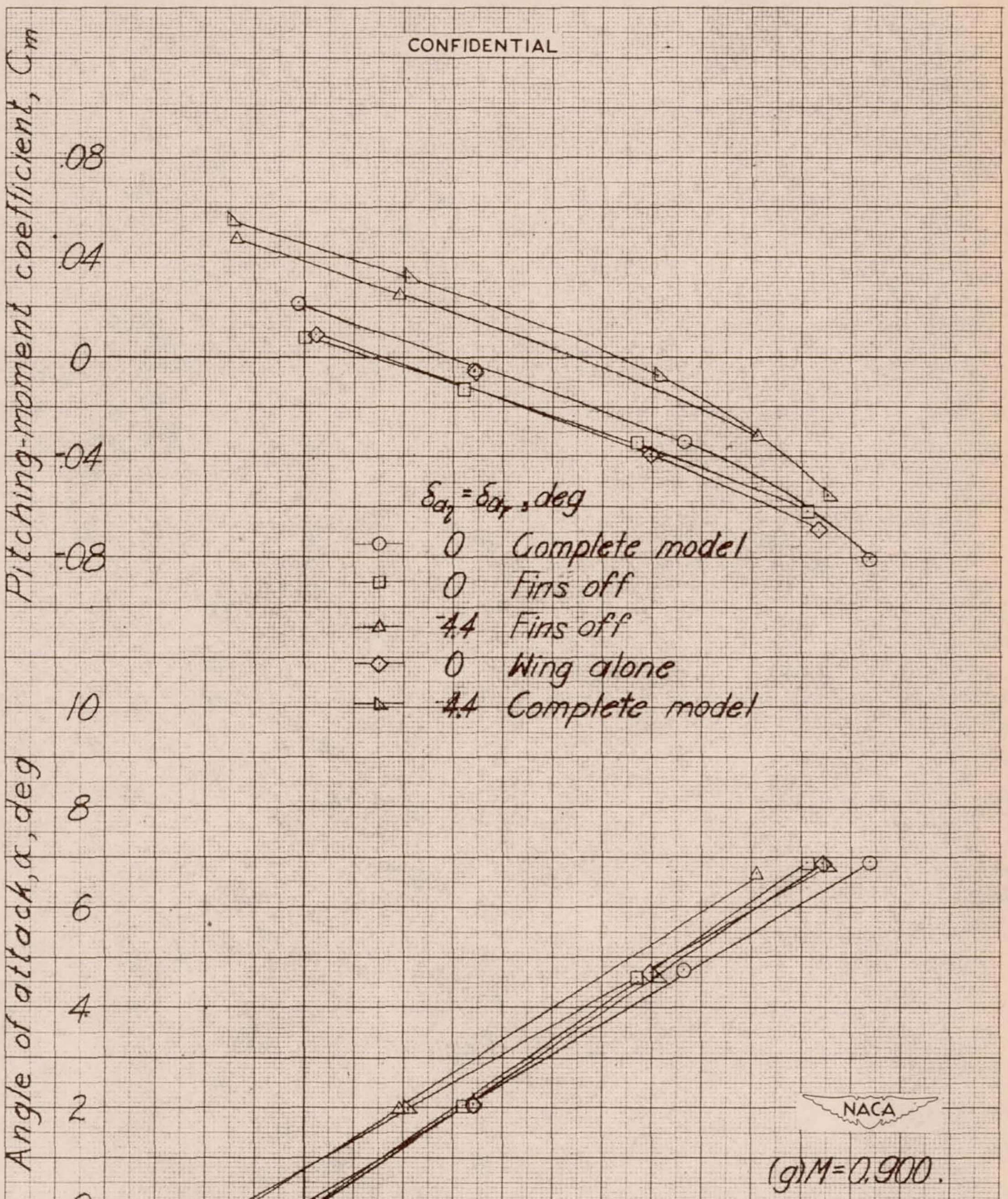

Figure 7. - Continued.

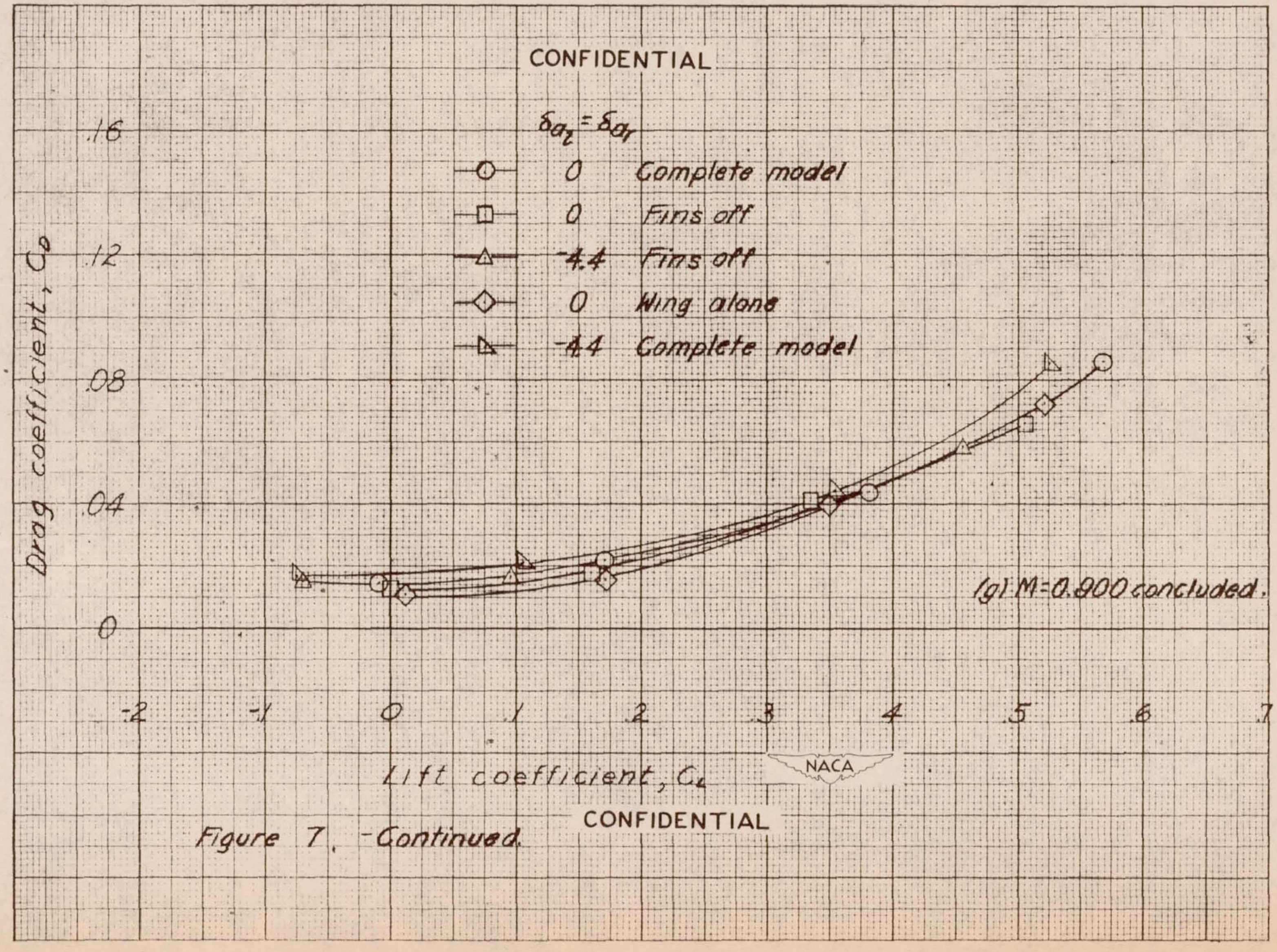

Figure 7. - Continued.

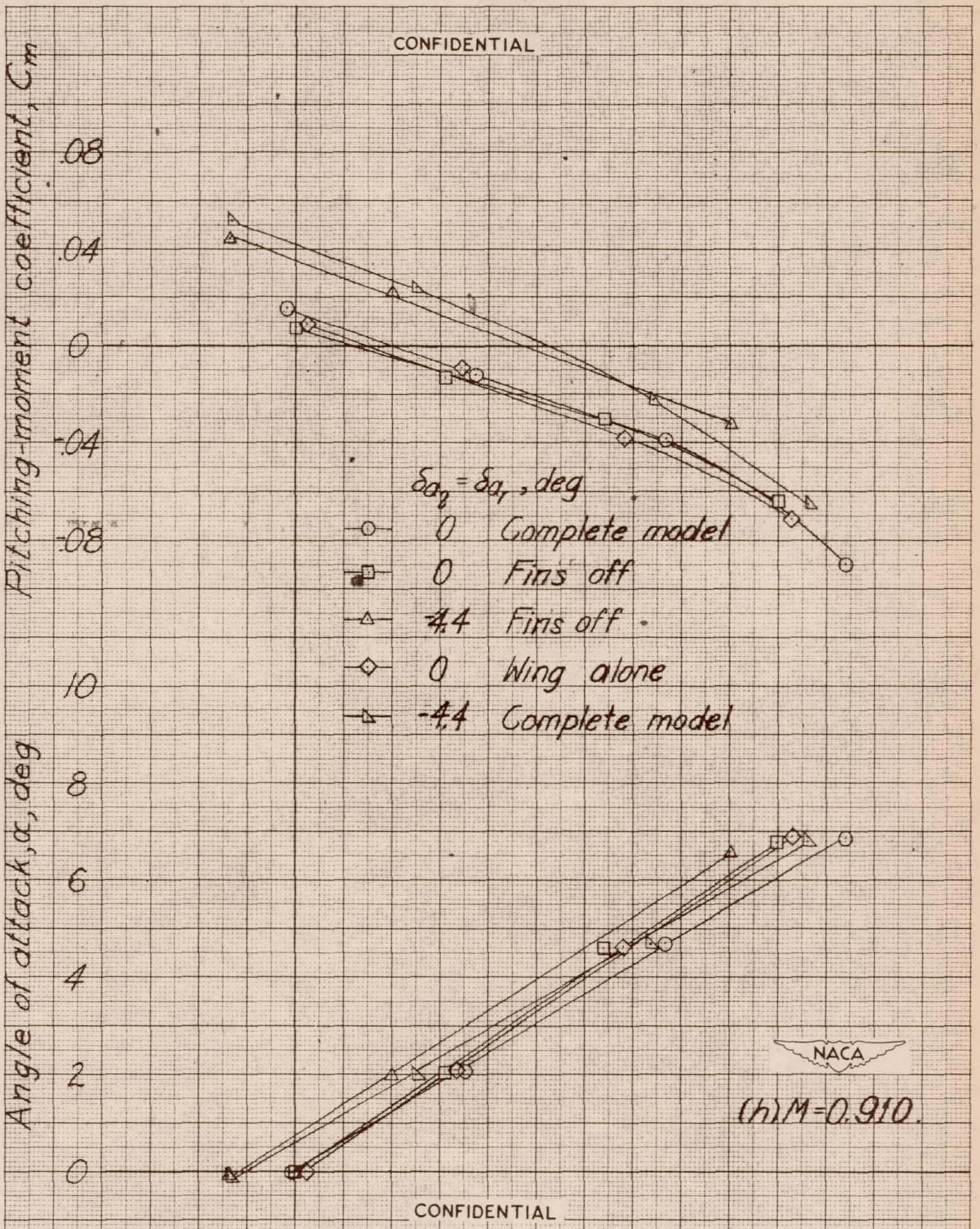

Figure 7 - Continued.

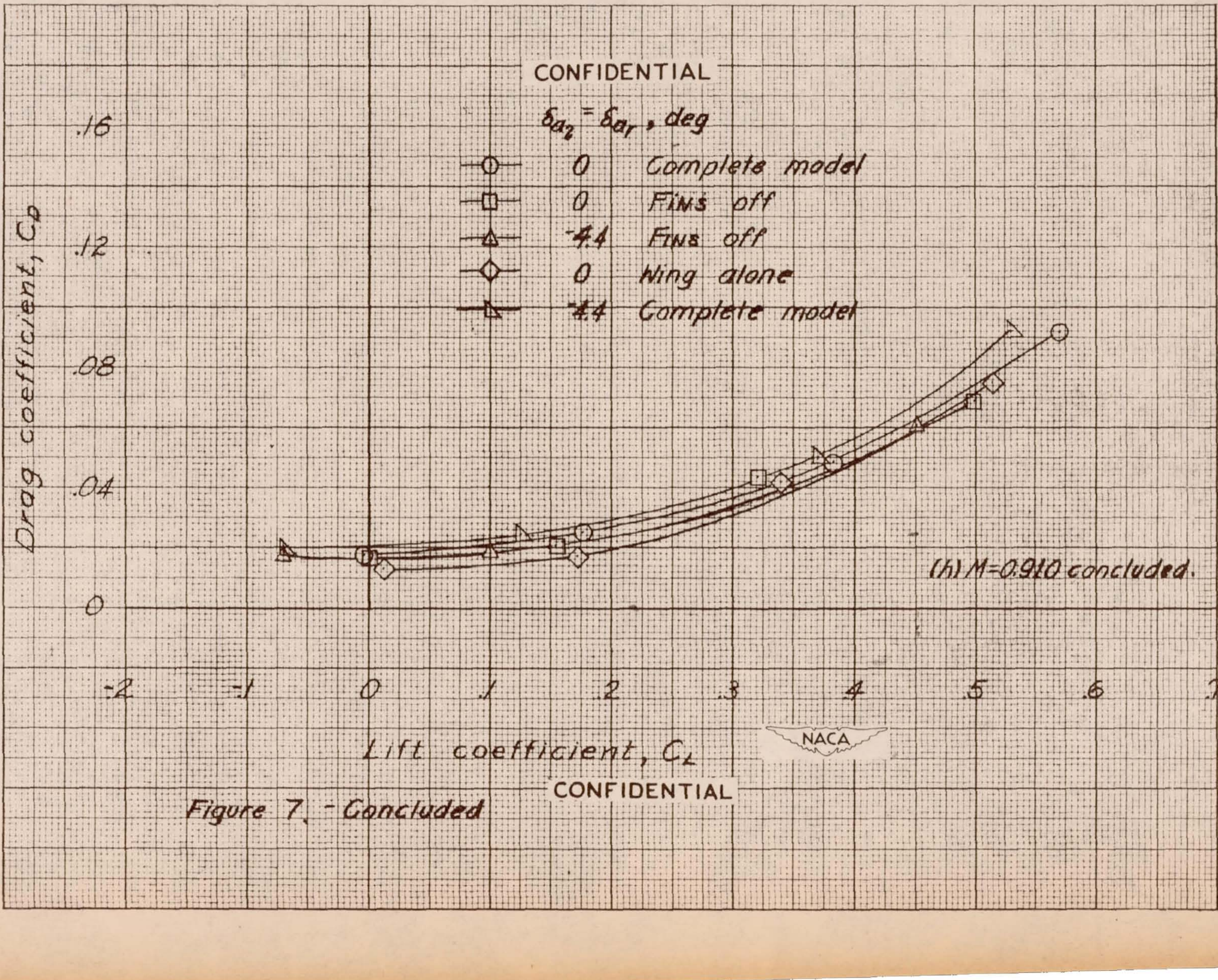

Figure 7. - Concluded

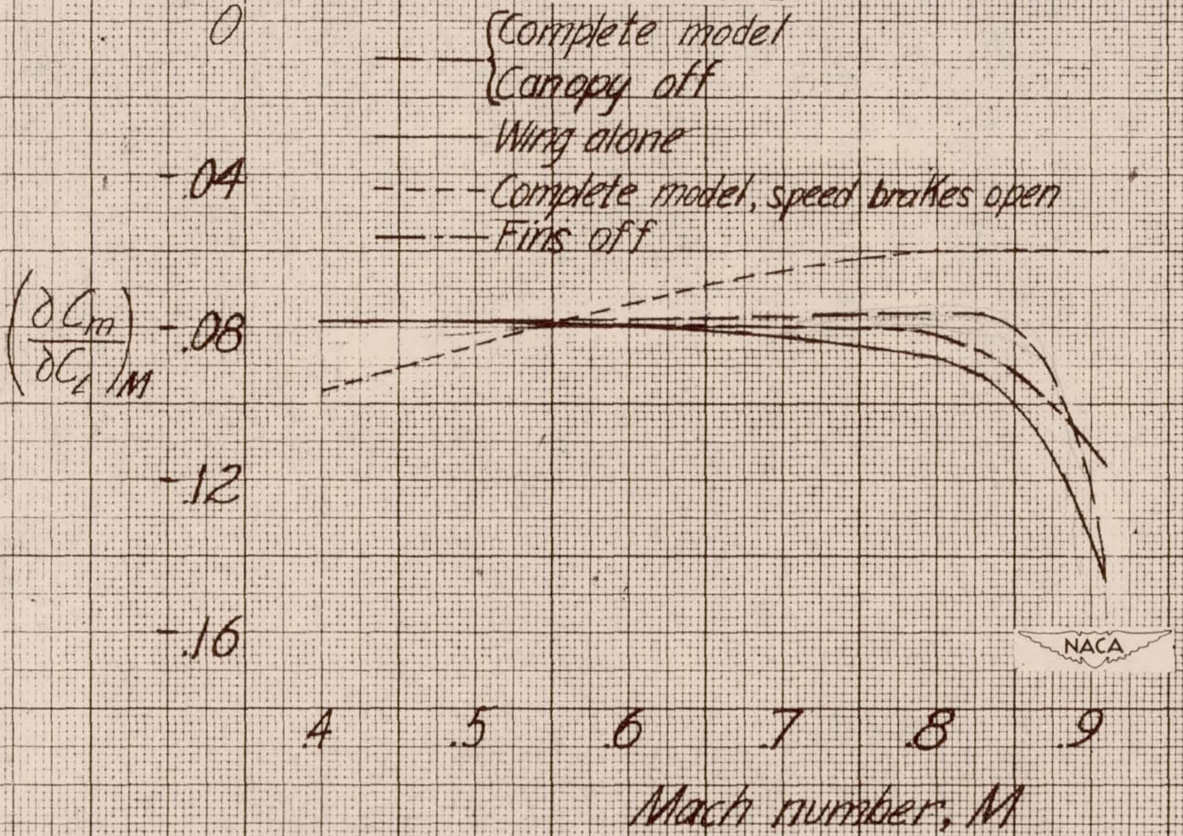

Figure 8.- Variation of $\left(\frac{\partial C_m}{\partial C_L}\right)_M$ with Mach number for the low lift coefficient range for various configurations of the 0.08-scale model of the Chance Vought XF7U-1 airplane.

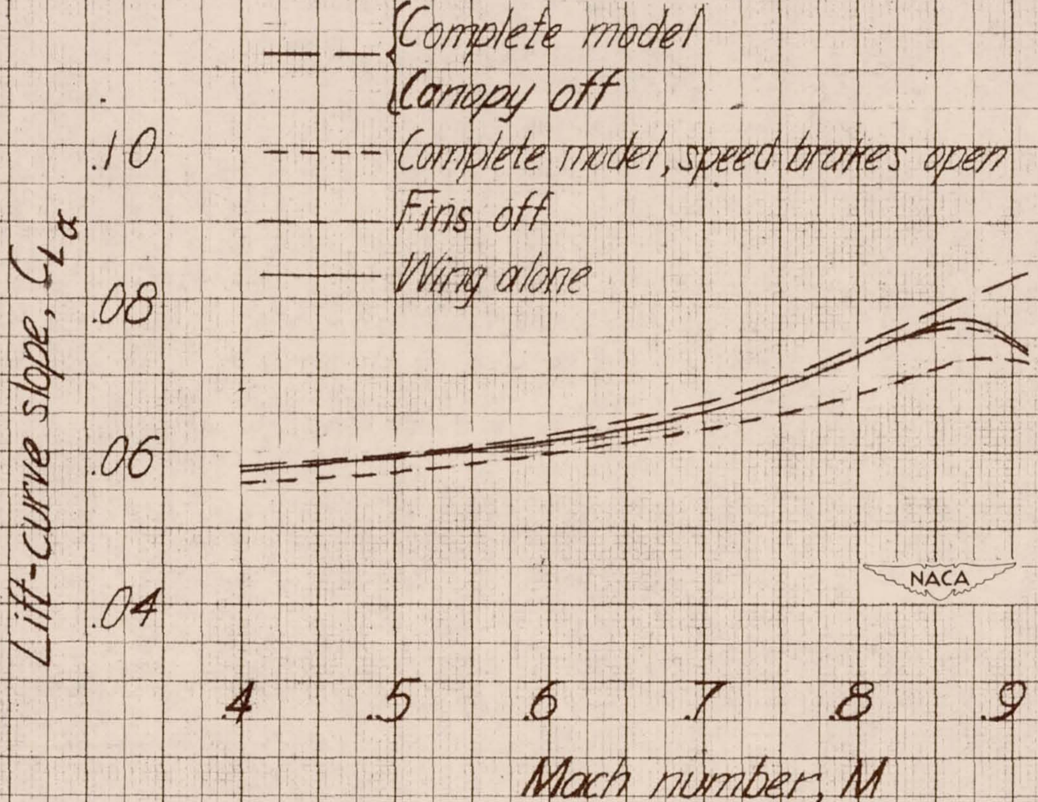

Figure 9. - Variation of lift-curve slope with Mach number for low lift coefficients for various configurations of the 0.08-scale model of the Chance Vought XF7U-1 airplane.

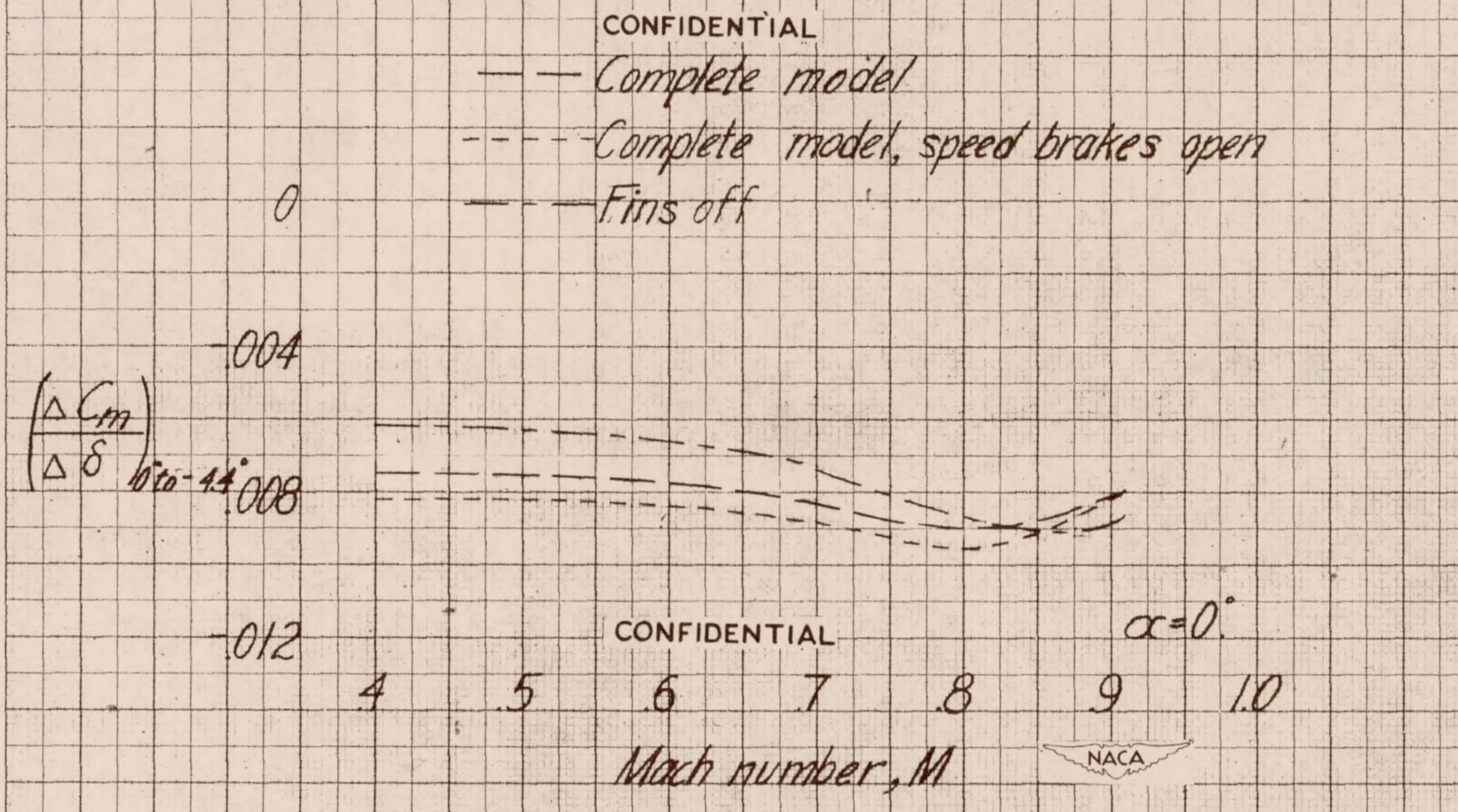

Figure 10.- Variation of the control effectiveness parameter, C_{m_δ}, with Mach number for several configurations of the 0.08-scale model of the Chance Vought XF7U-1 airplane.

CONFIDENTIAL

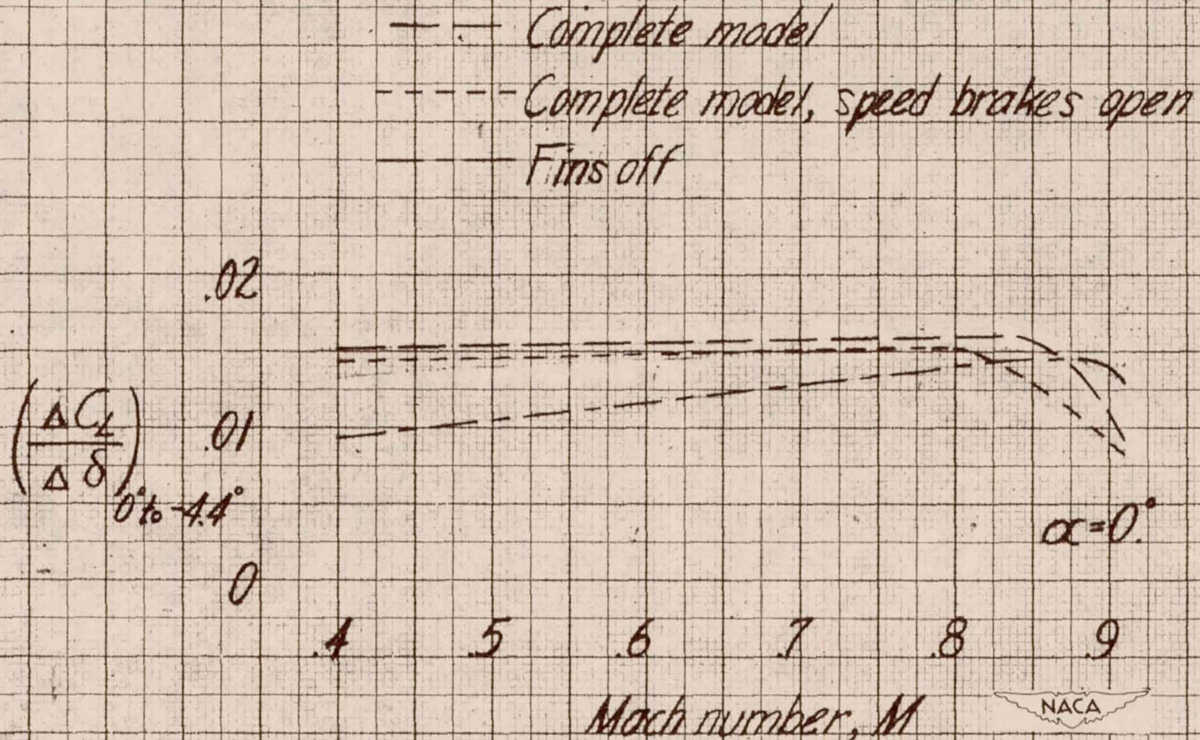

Figure 11. - Variation of C_{l_δ} with Mach number for constant angle of attack for various configurations of the 0.08 - scale model of the Chance Vought XF7U-1 airplane.

CONFIDENTIAL

CONFIDENTIAL

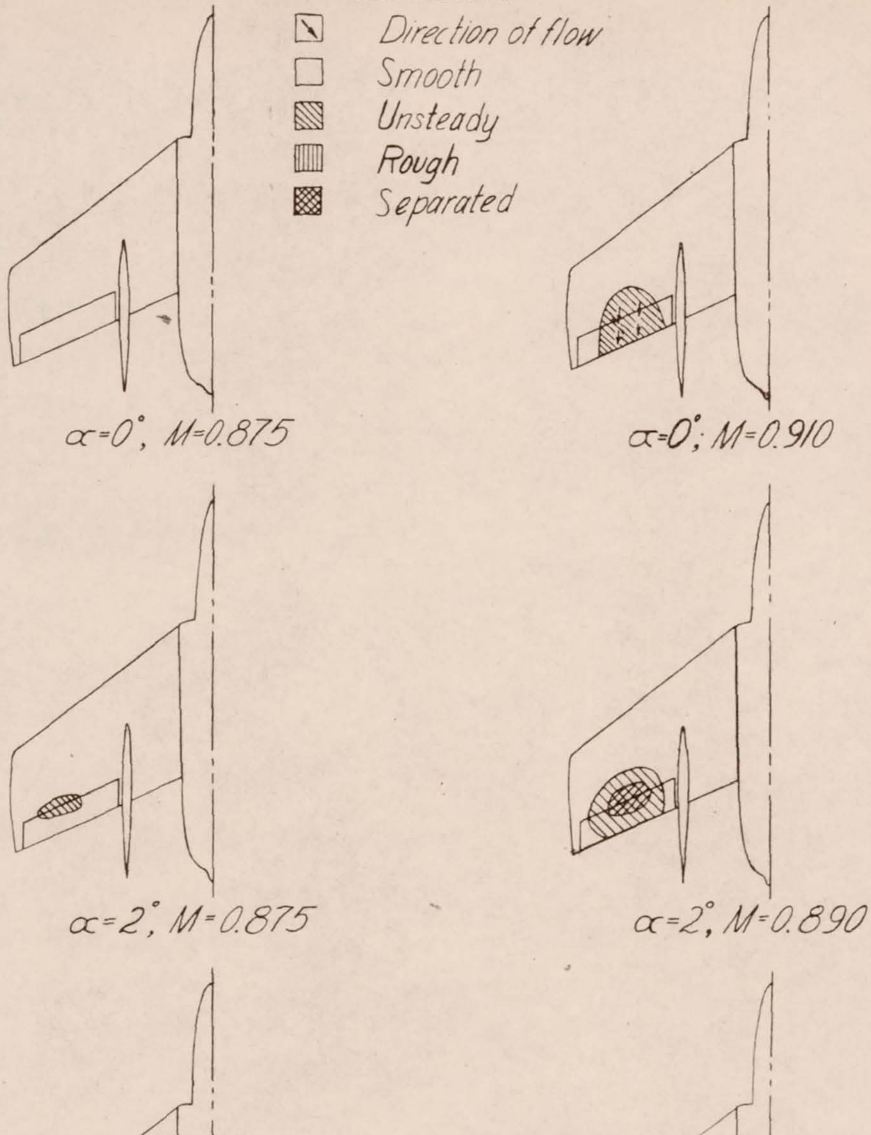

Figure 12.- Tuft studies over the wing at various angles of attack and Mach numbers of the 0.08-scale model of the Chance Vought XF7U-1 airplane; $\psi = 0°$.

CONFIDENTIAL

CONFIDENTIAl

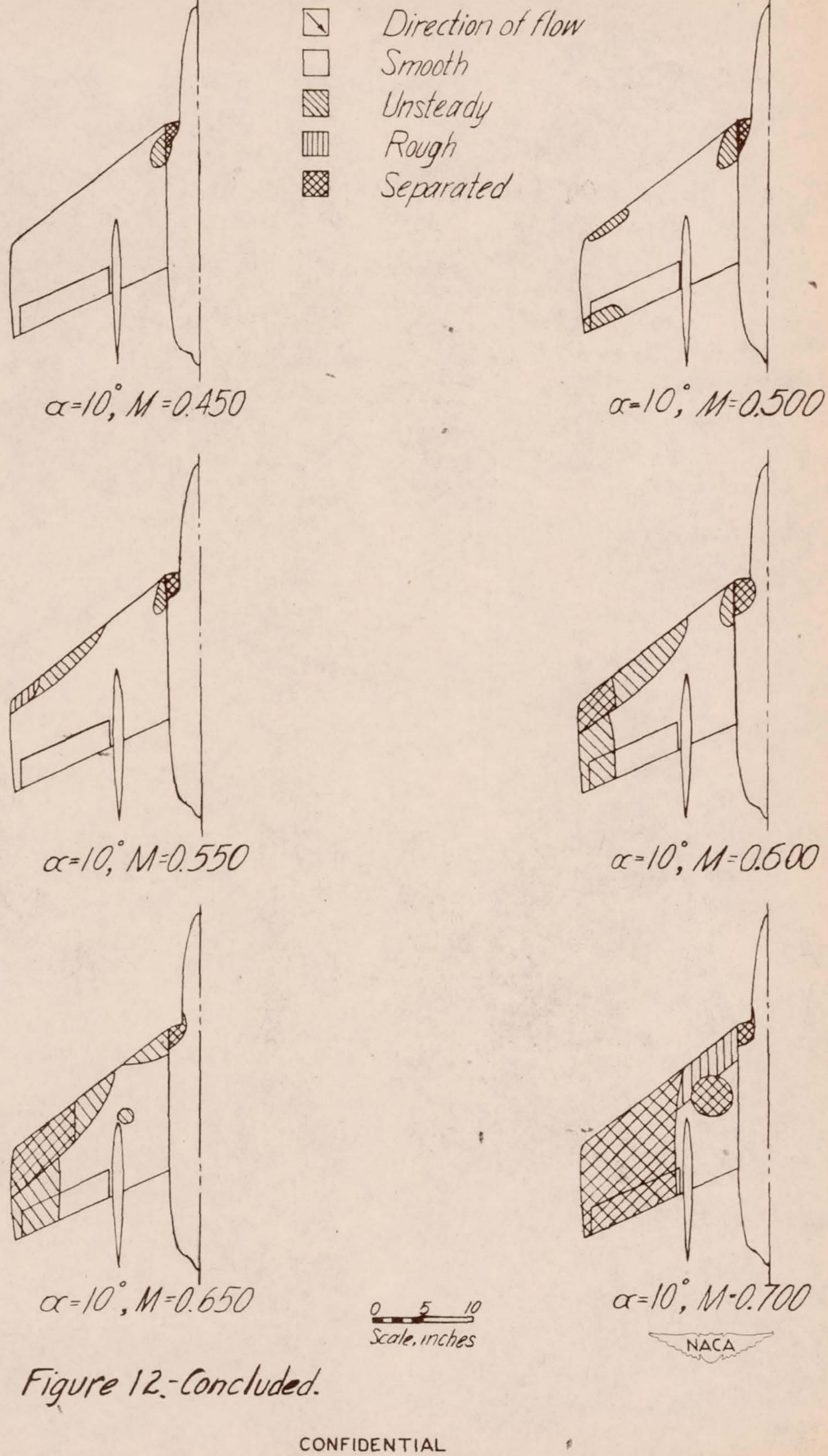

Figure 12.- Concluded.

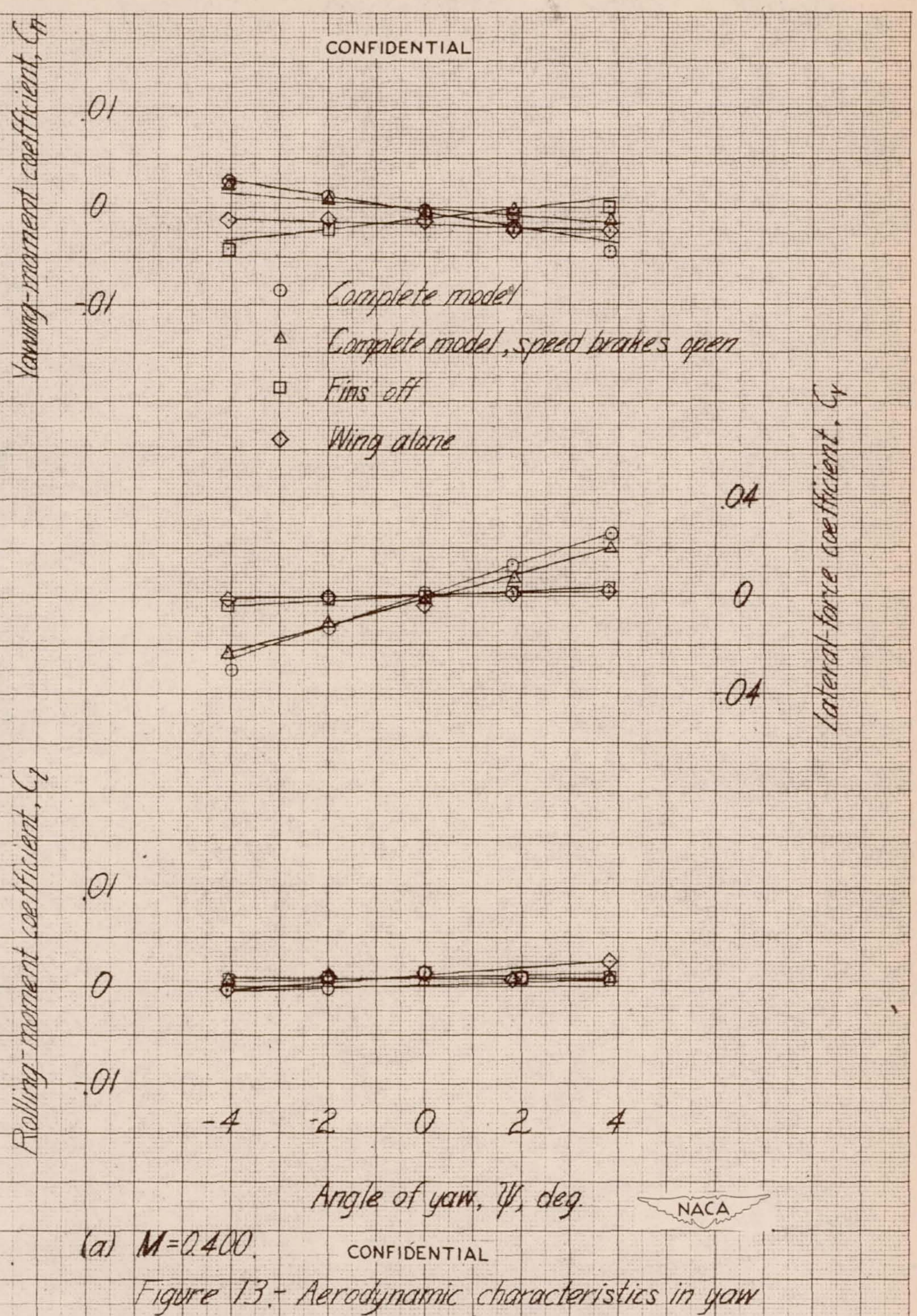

(a) $M = 0.400$.

Figure 13.- Aerodynamic characteristics in yaw for several configurations of the 0.08-scale model of the Chance Vought XF7U-1 airplane; $\alpha_{static} = 0^{\circ}$.

CONFIDENTIAL

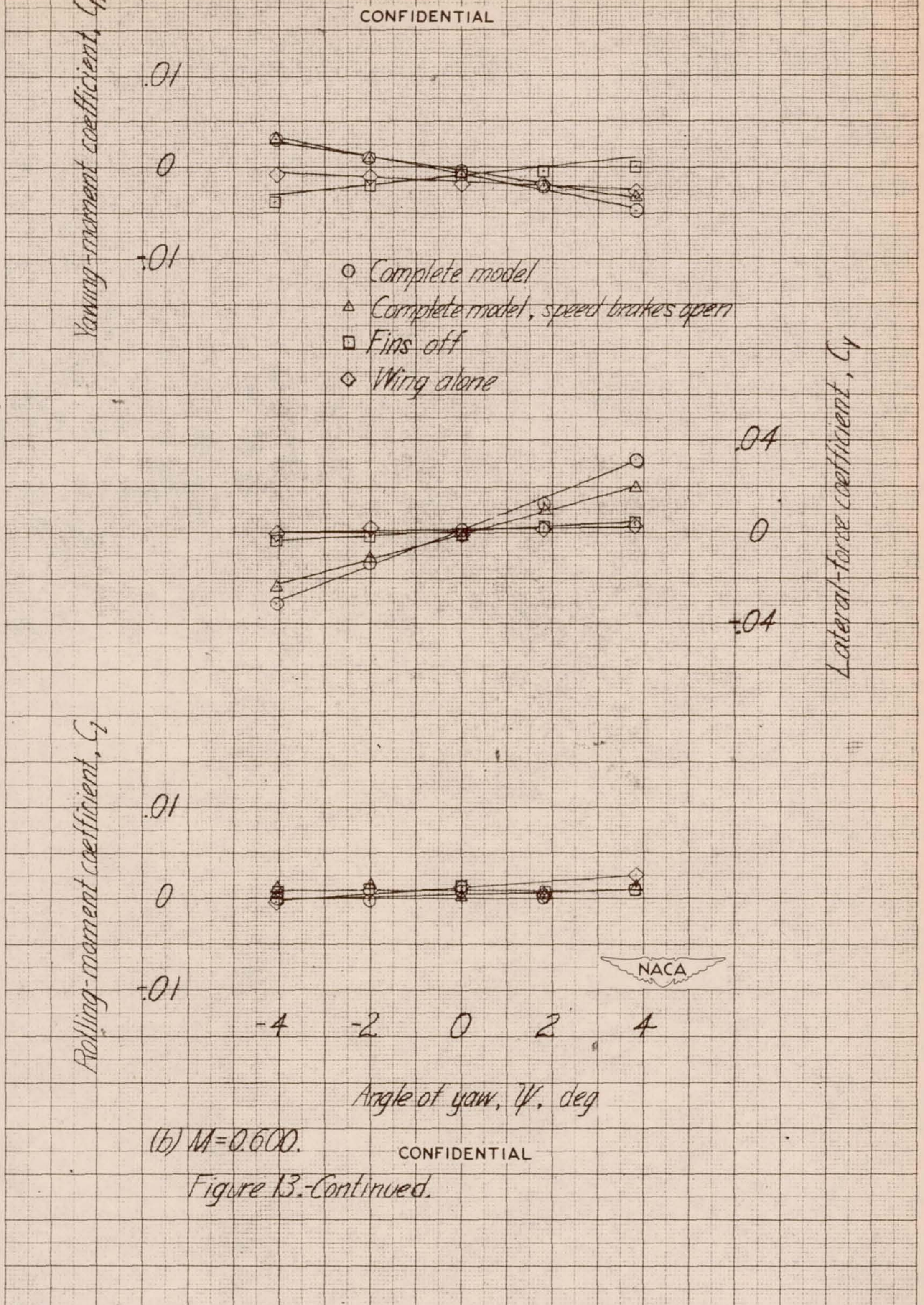

(b) $M = 0.600$.

CONFIDENTIAL

Figure 13.- Continued.

CONFIDENTIAL

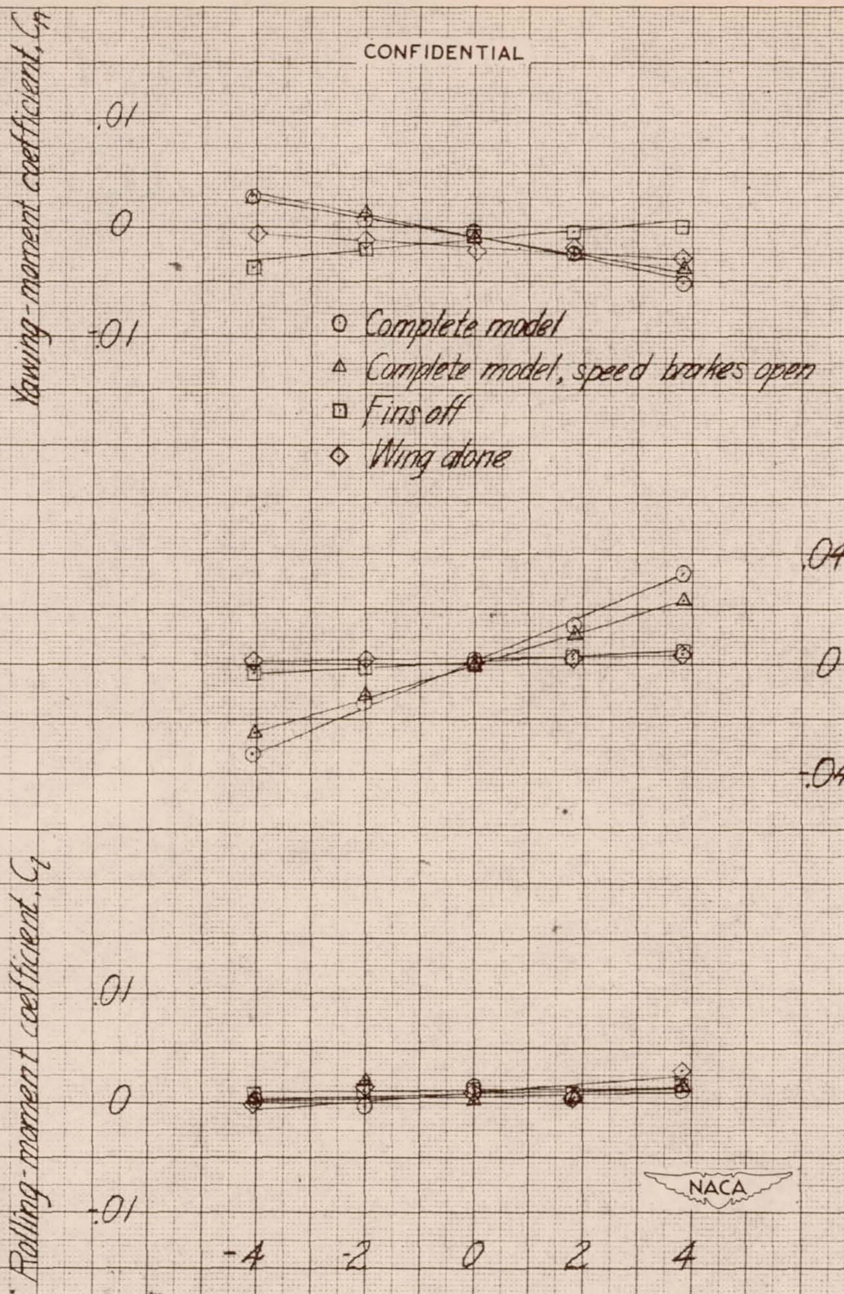

(c) M=0.700.

CONFIDENTIAL

Figure 13.-Continued.

CONFIDENTIAL

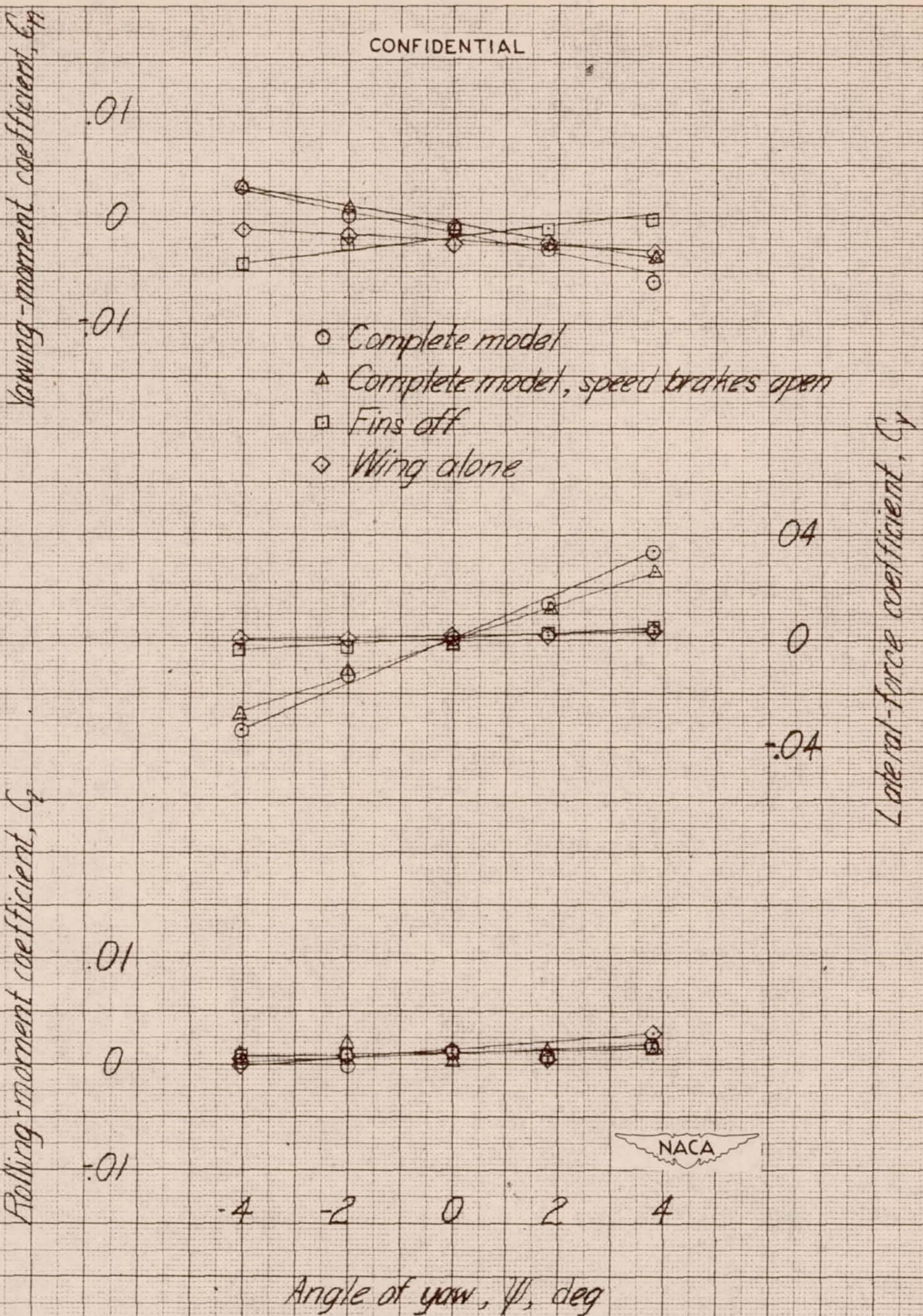

(d) M = 0.800.

Figure 13.- Continued.

CONFIDENTIAL

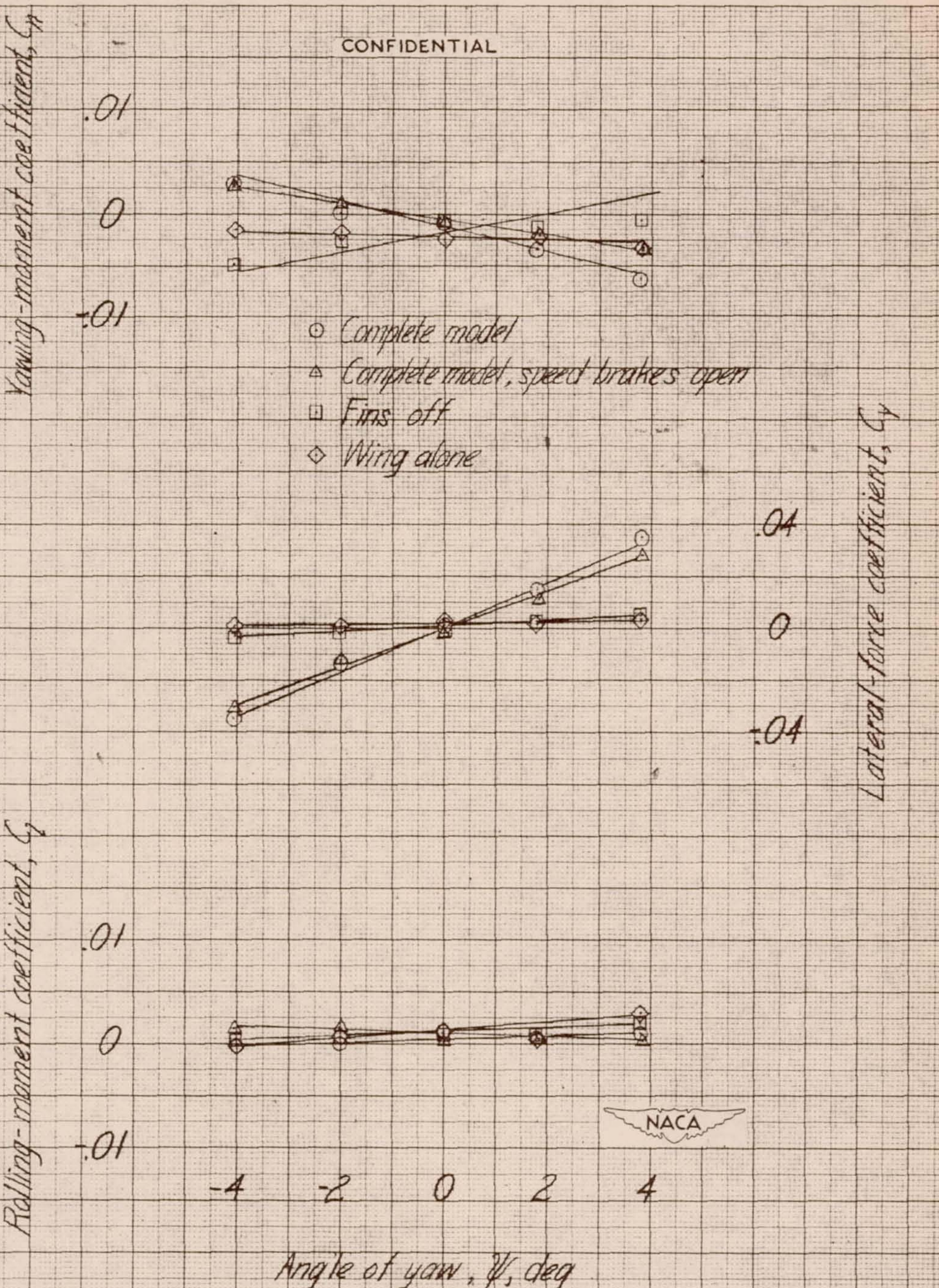

(e) M=0.850.

Figure 13.-Continued.

CONFIDENTIAL

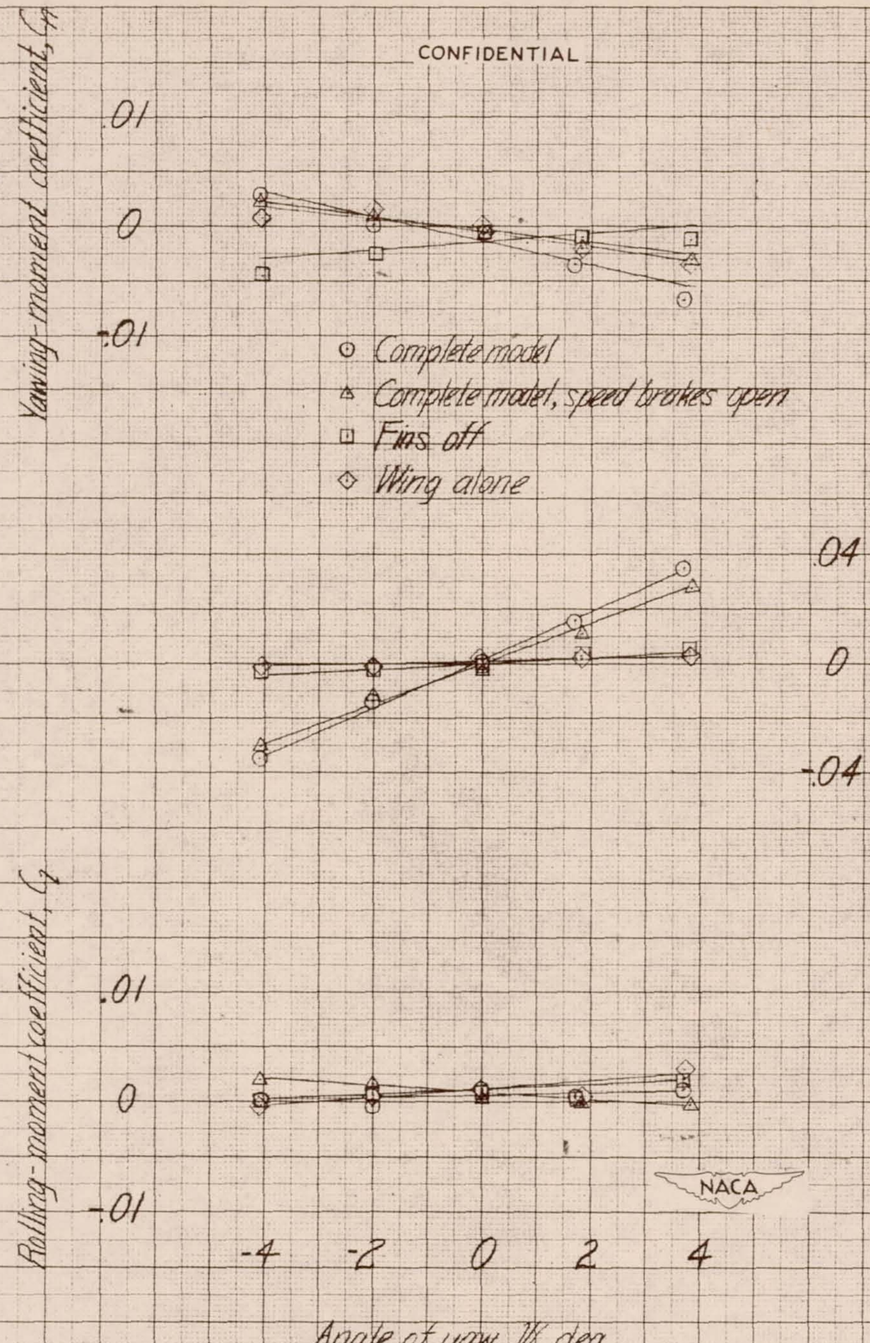

(f) $M=0.875$.

CONFIDENTIAL

Figure 13-Continued.

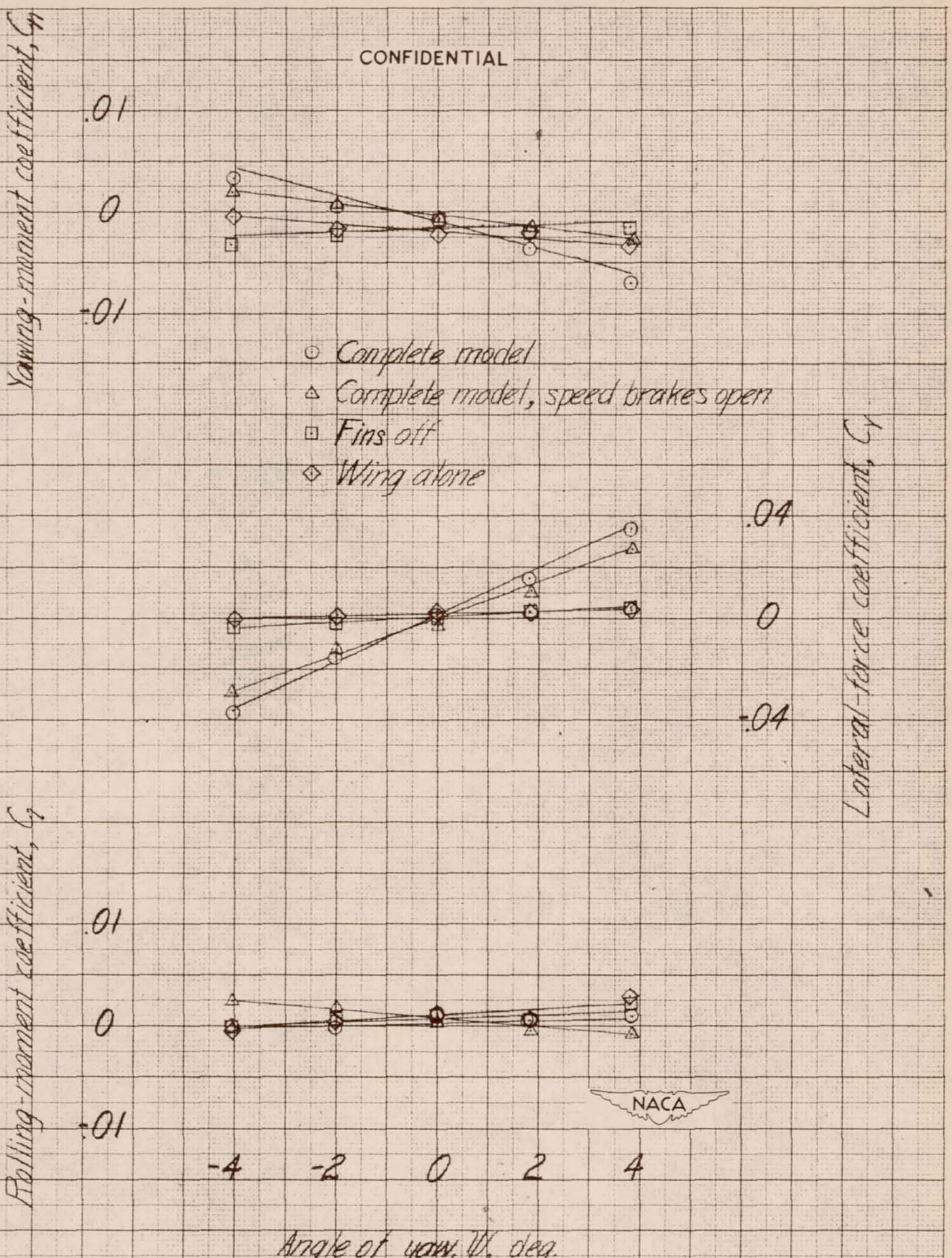

(g) $M=0.900$.

CONFIDENTIAL

Figure 13.- Continued.

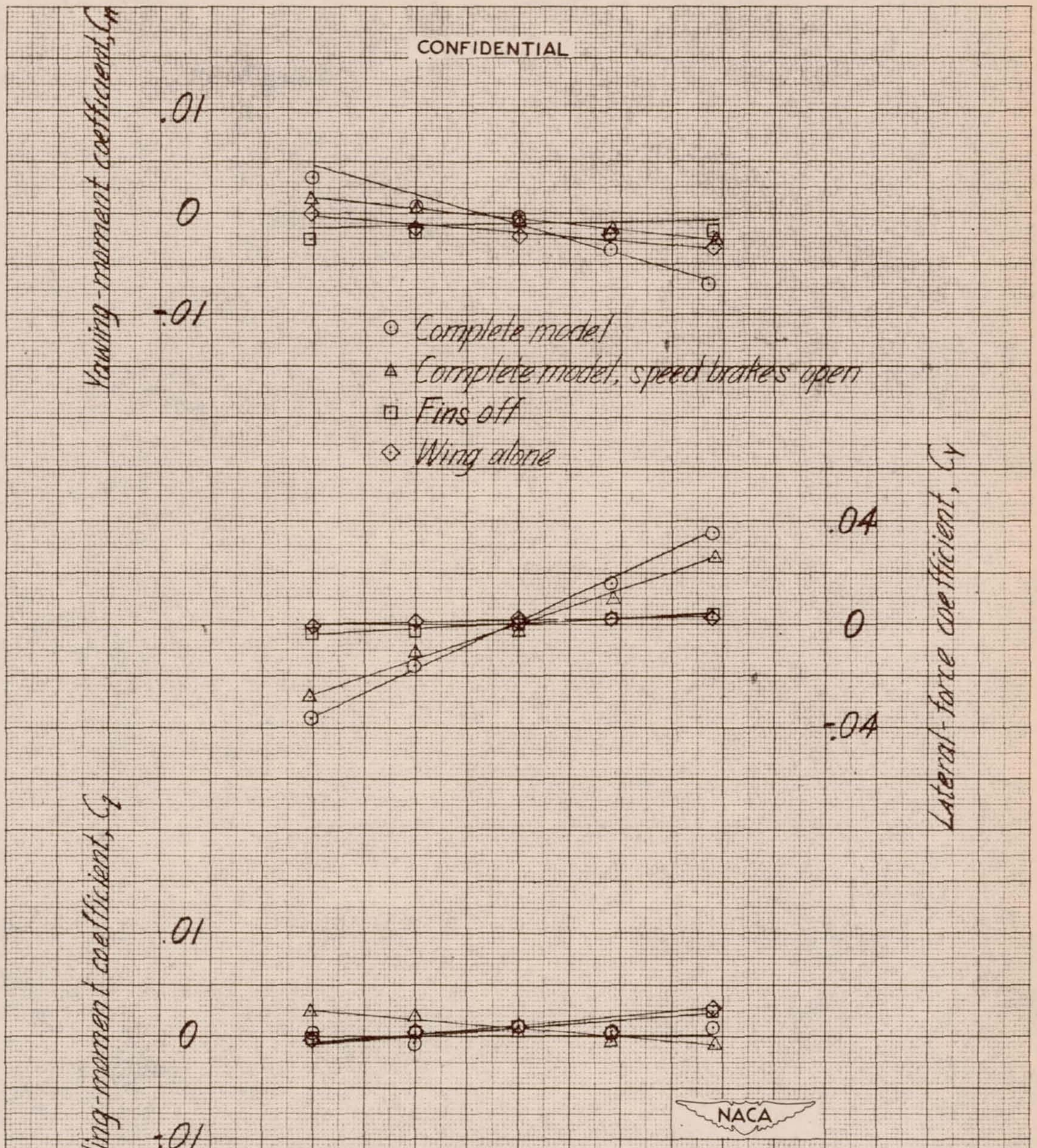

(h) M=0.910.

Figure 13.-Concluded.

CONFIDENTIAL

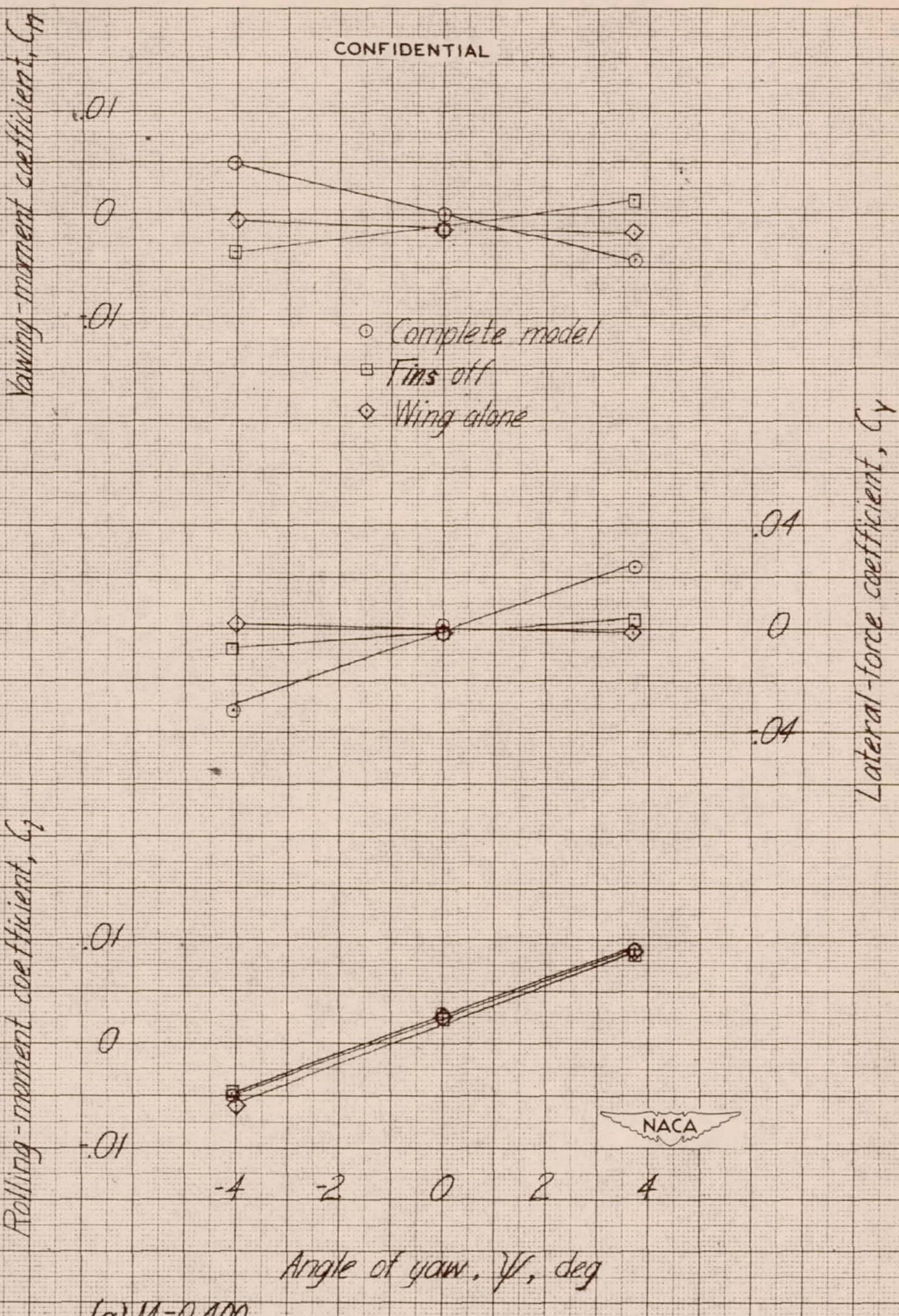

(a) $M = 0.400$.

CONFIDENTIAL

Figure 14.- Aerodynamic characteristics in yaw for several configurations of the 0.08-scale model of the Chance Vought XF7U-1 airplane ; $\alpha_{static} = 6°$.

CONFIDENTIAL

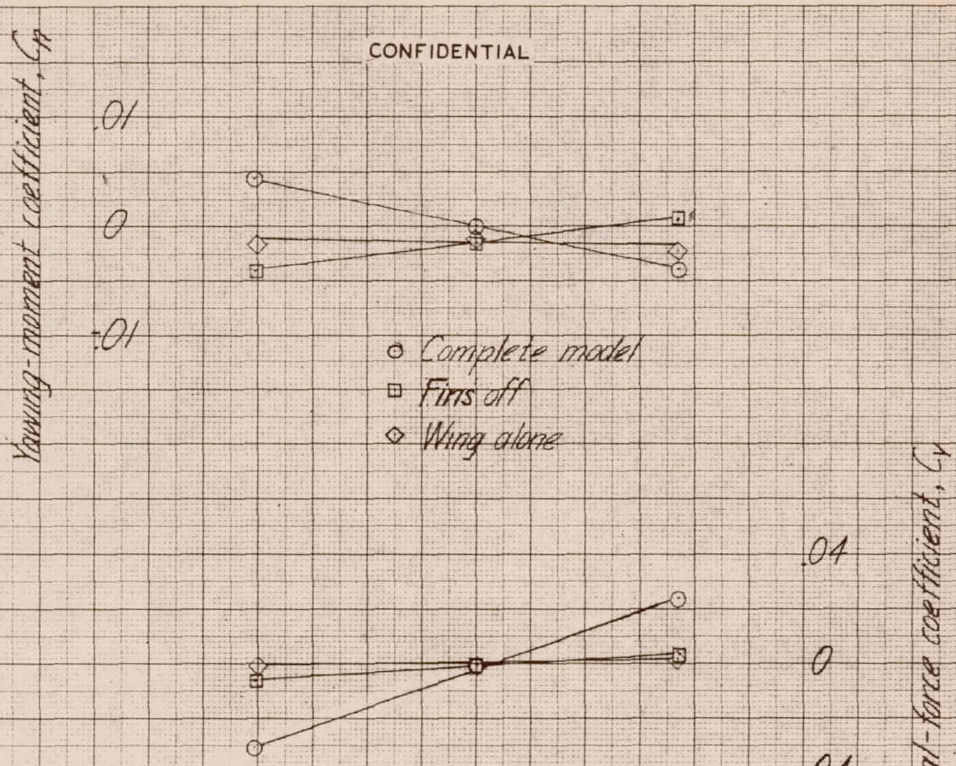

(b) $M = 0.600$.

CONFIDENTIAL

Figure 14-Continued.

CONFIDENTIAL

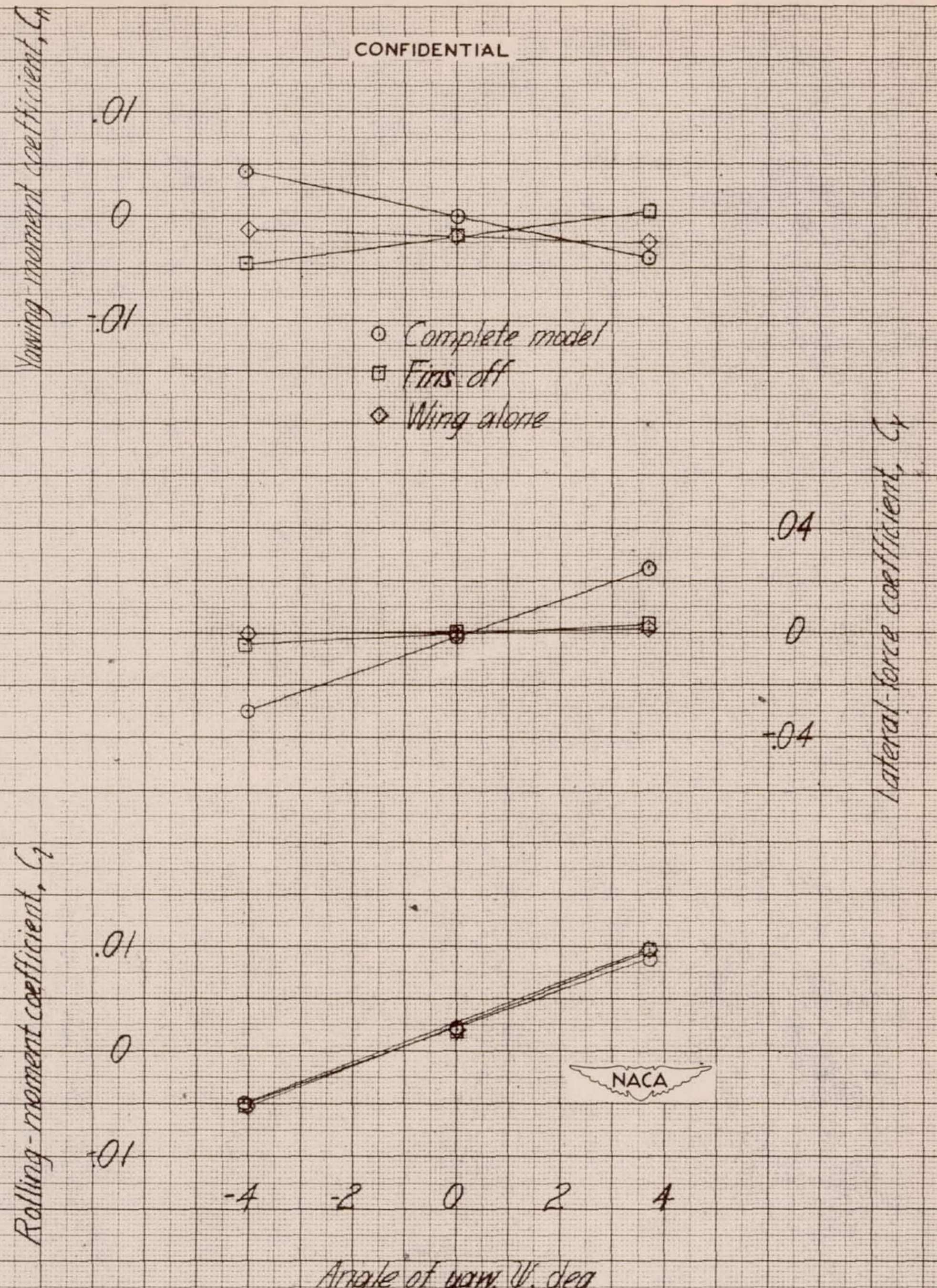

(c) $M=0.700$.

CONFIDENTIAL

Figure 14-Continued.

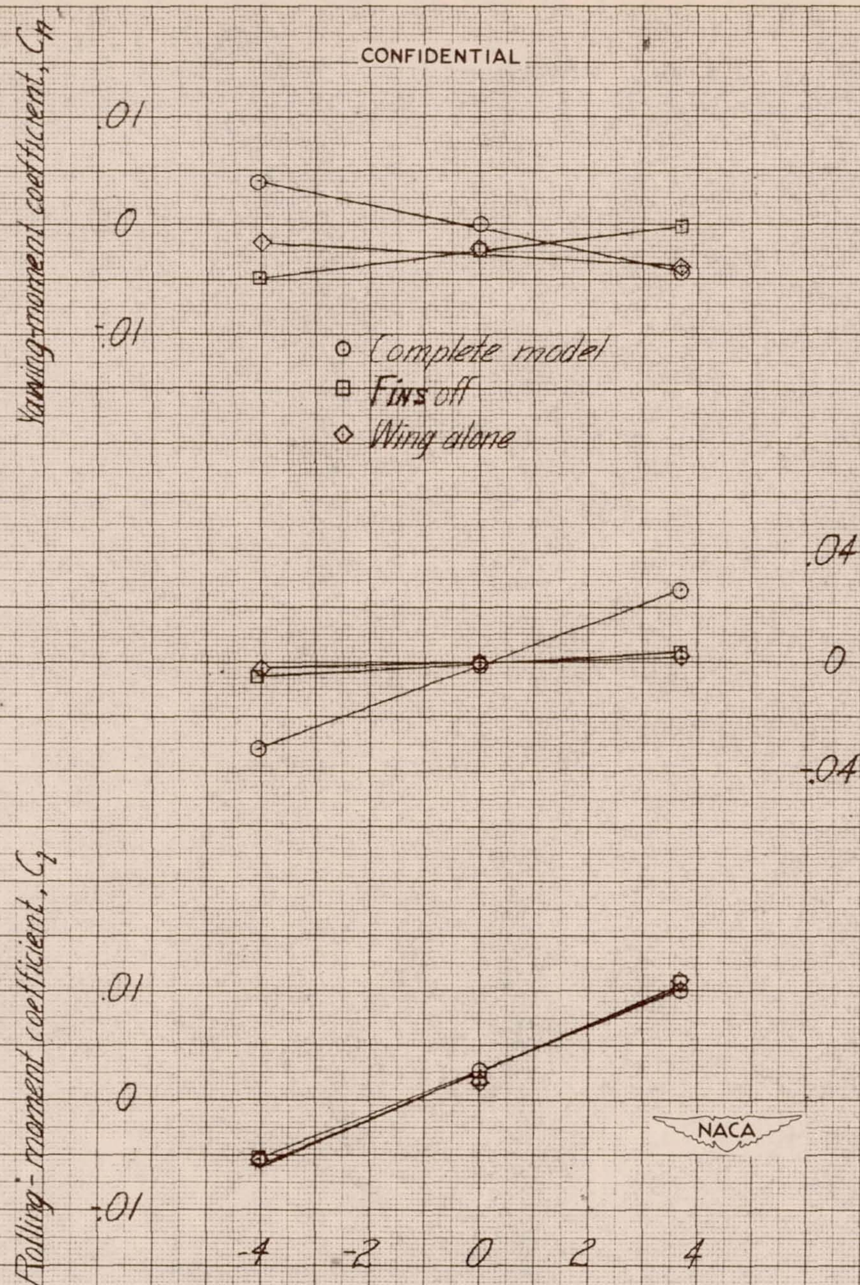

(d) $M = 0.800$.

Figure 14.- Continued.

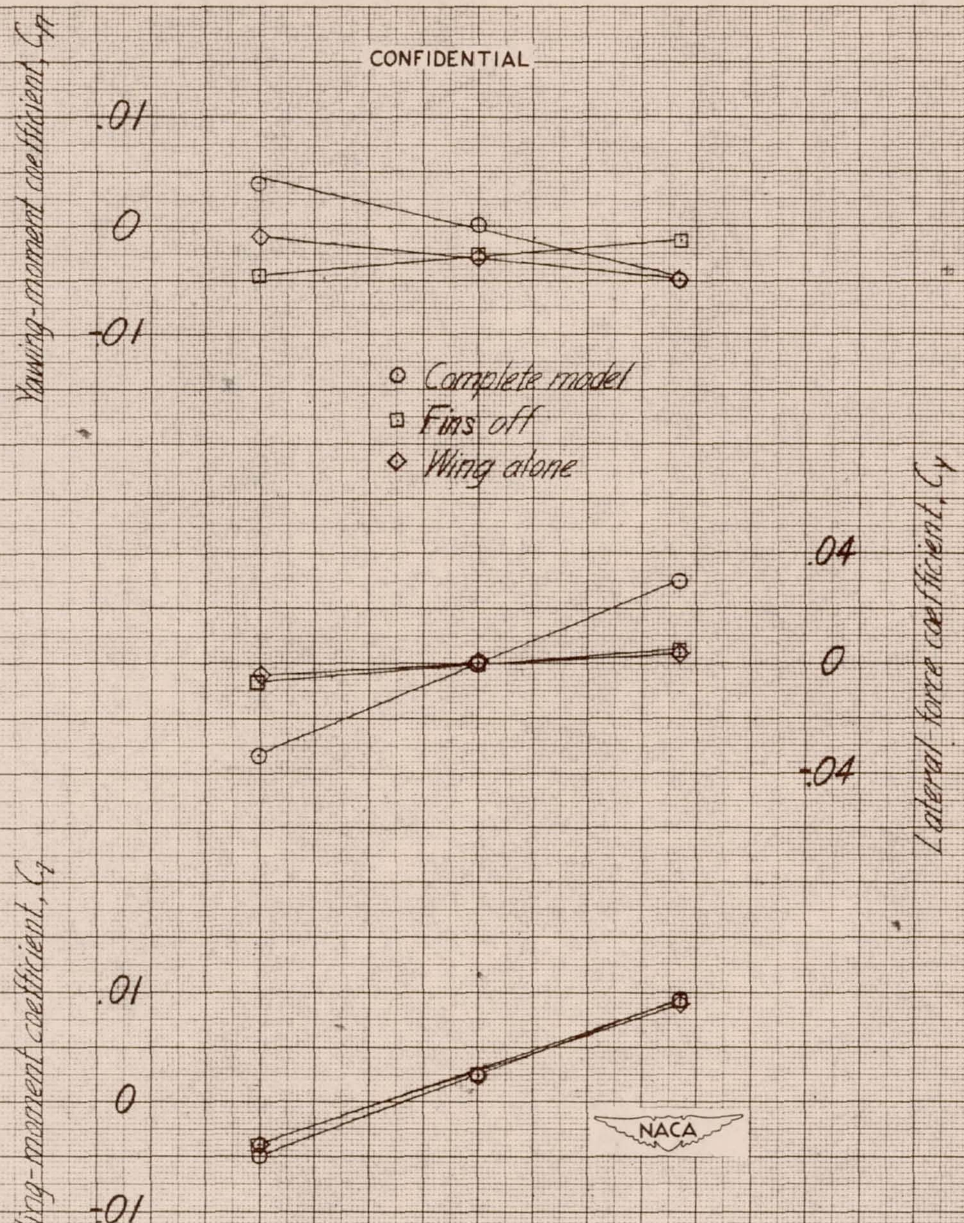

(e) $M = 0.850$.

CONFIDENTIAL

Figure 14.- Continued.

CONFIDENTIAL

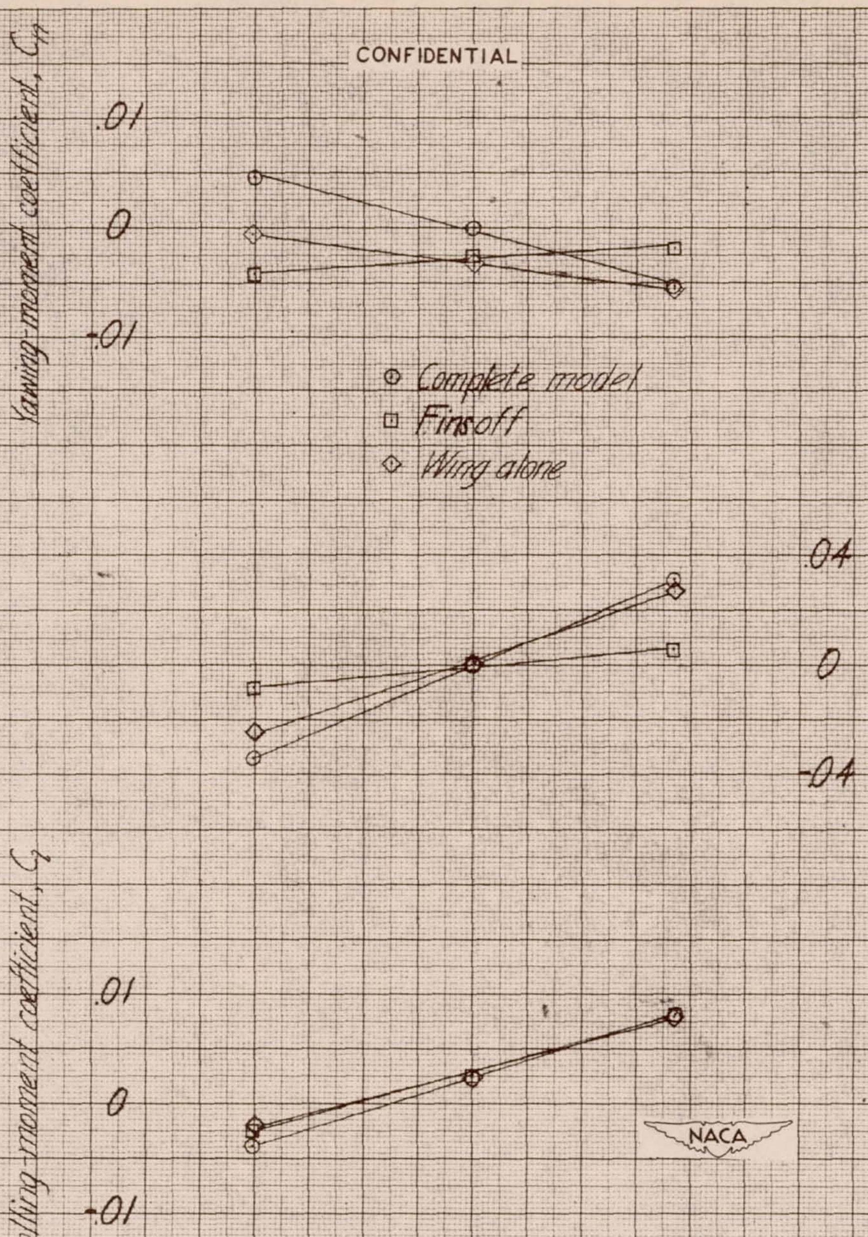

(f) M=0.875.

CONFIDENTIAL

Figure 14.-Continued.

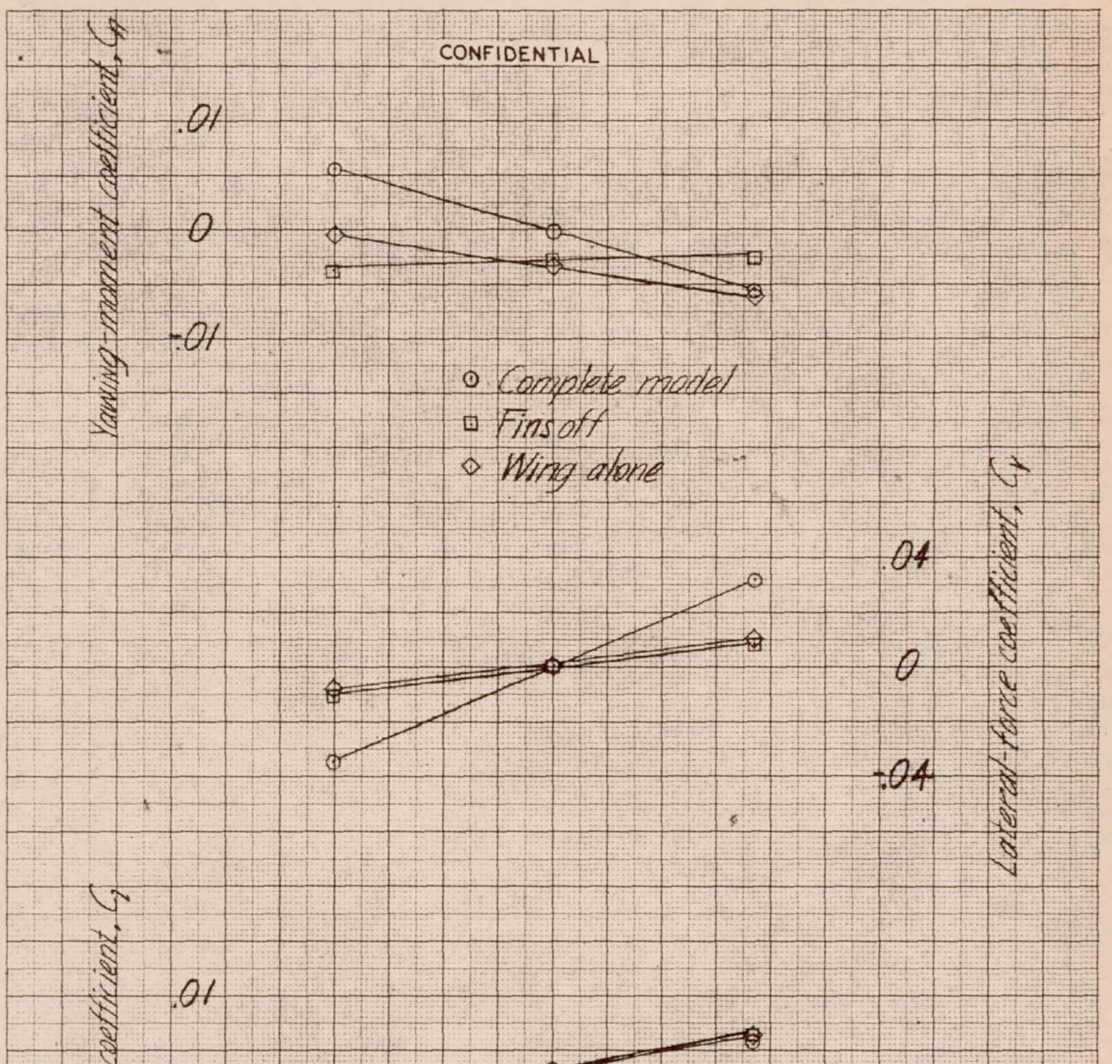

(g) $M = 0.900$.

CONFIDENTIAL

Figure 14.- Concluded.

CONFIDENTIAL

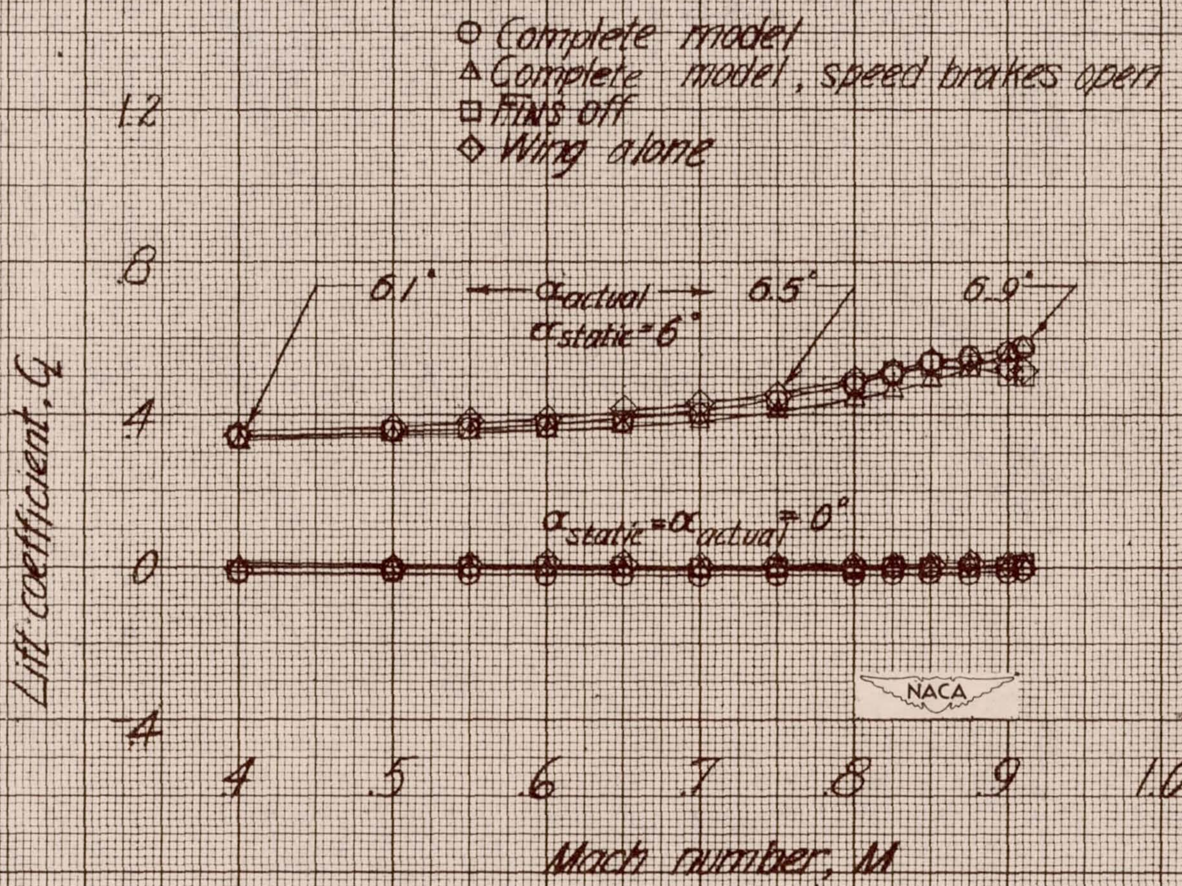

Figure 15 - Variation of lift coefficient with Mach number at constant values of static angle of attack for several different model configurations of the 0.08-scale model of the Chance Vought XF7U-1 airplane.

CONFIDENTIAL

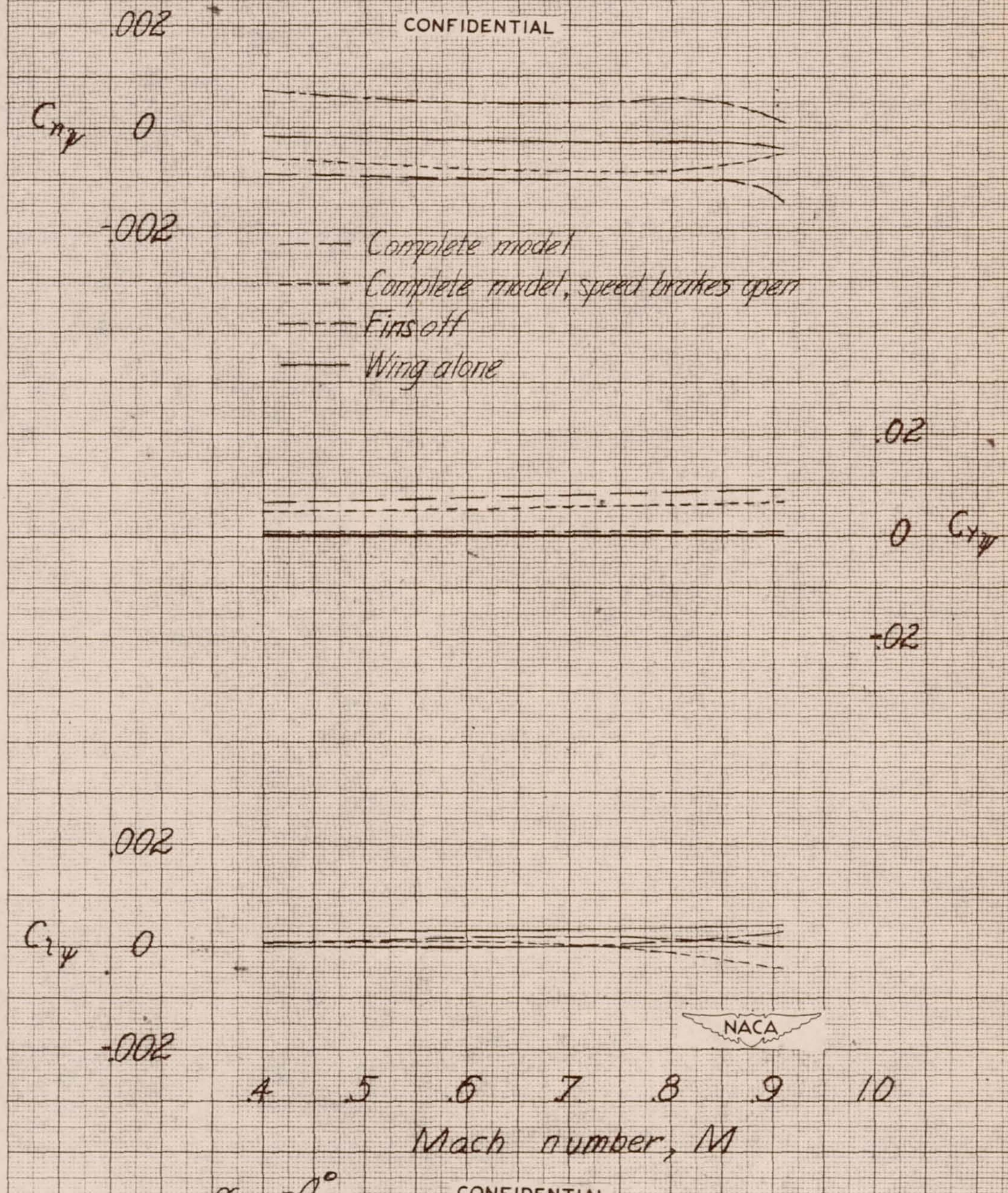

Figure 16.- Variation with Mach number of the lateral stability characteristics for several configurations of the 0.08-scale model of the Chance Vought XF7U-1 airplane.

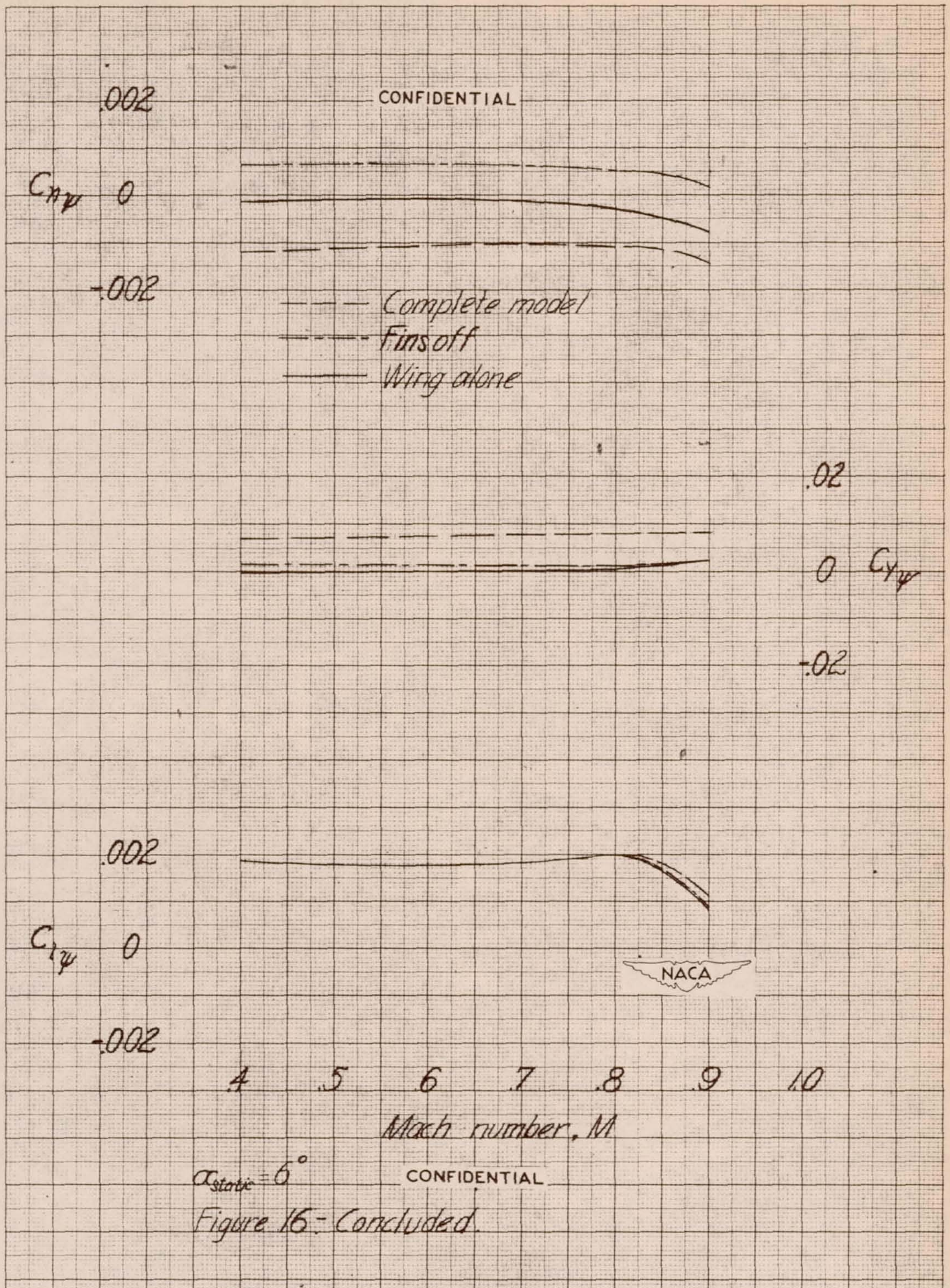

$\alpha_{static} = 6°$

Figure 16.- Concluded.

CONFIDENTIAL

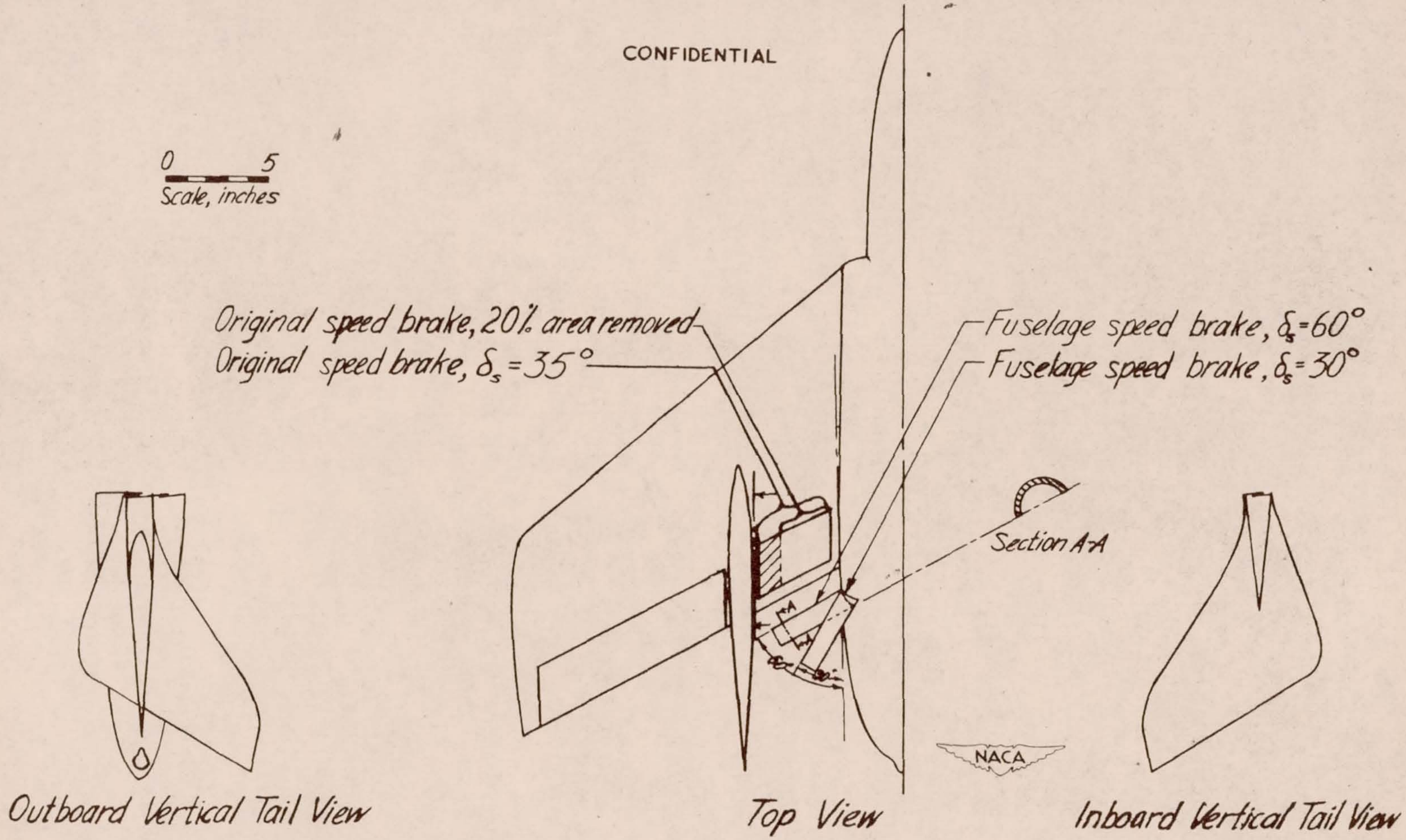

Figure 17.- General arrangement of views for tuft study presentation and the various speed-brake arrangements tested on the 0.08-scale model of the Chance Vought XF7U-1 airplane.

CONFIDENTIAL

CONFIDENTIAL

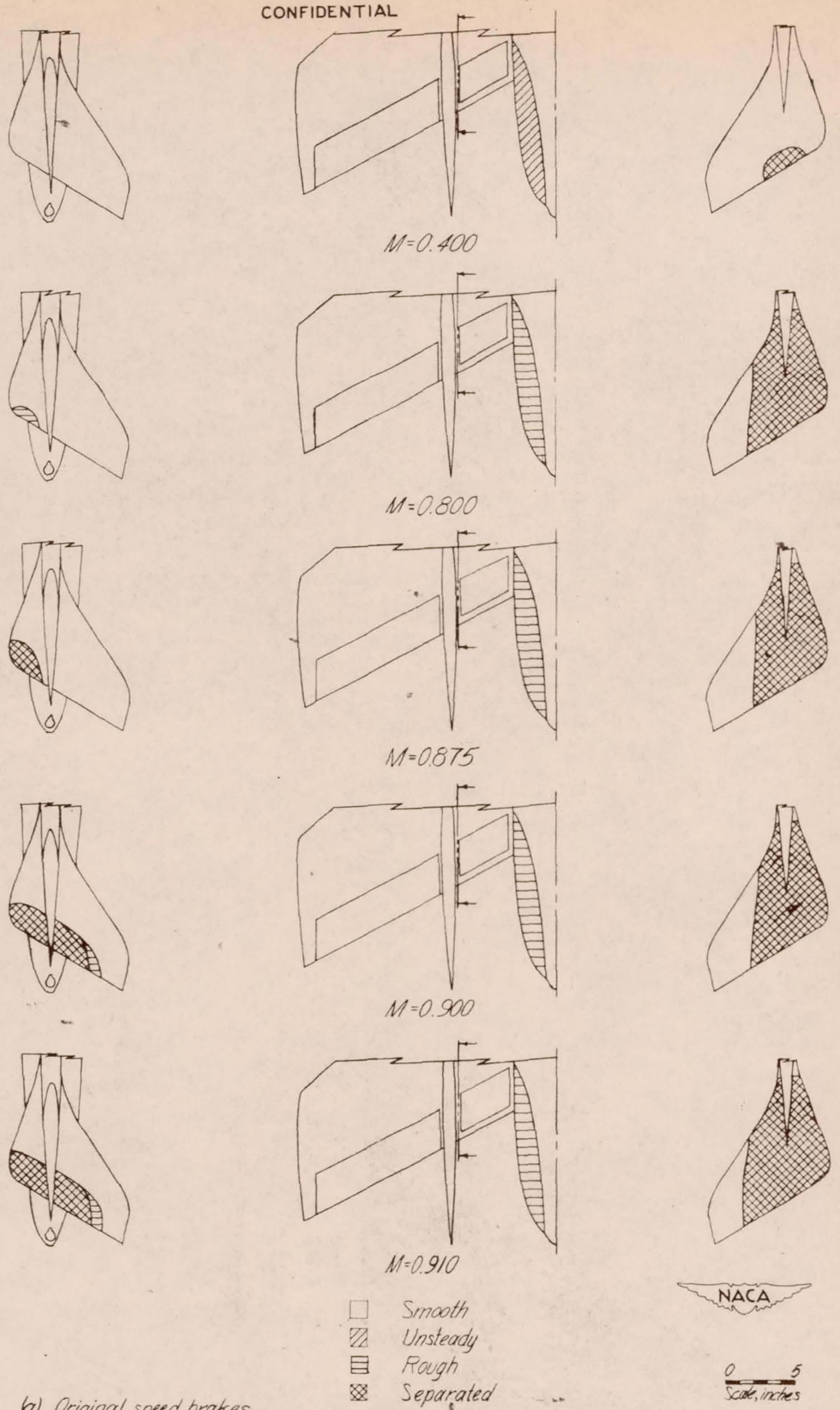

(a) Original speed brakes.

Figure 18.- Tuft studies over the fuselage, outboard vertical fin and inboard vertical fin surfaces at various Mach numbers for the various speed brake configurations of the 0.08-scale model of the Chance Vought XF7U-1 airplane; $\alpha = 2^{\circ}$, $\psi = 0^{\circ}$.

CONFIDENTIAL

CONFIDENTIAL

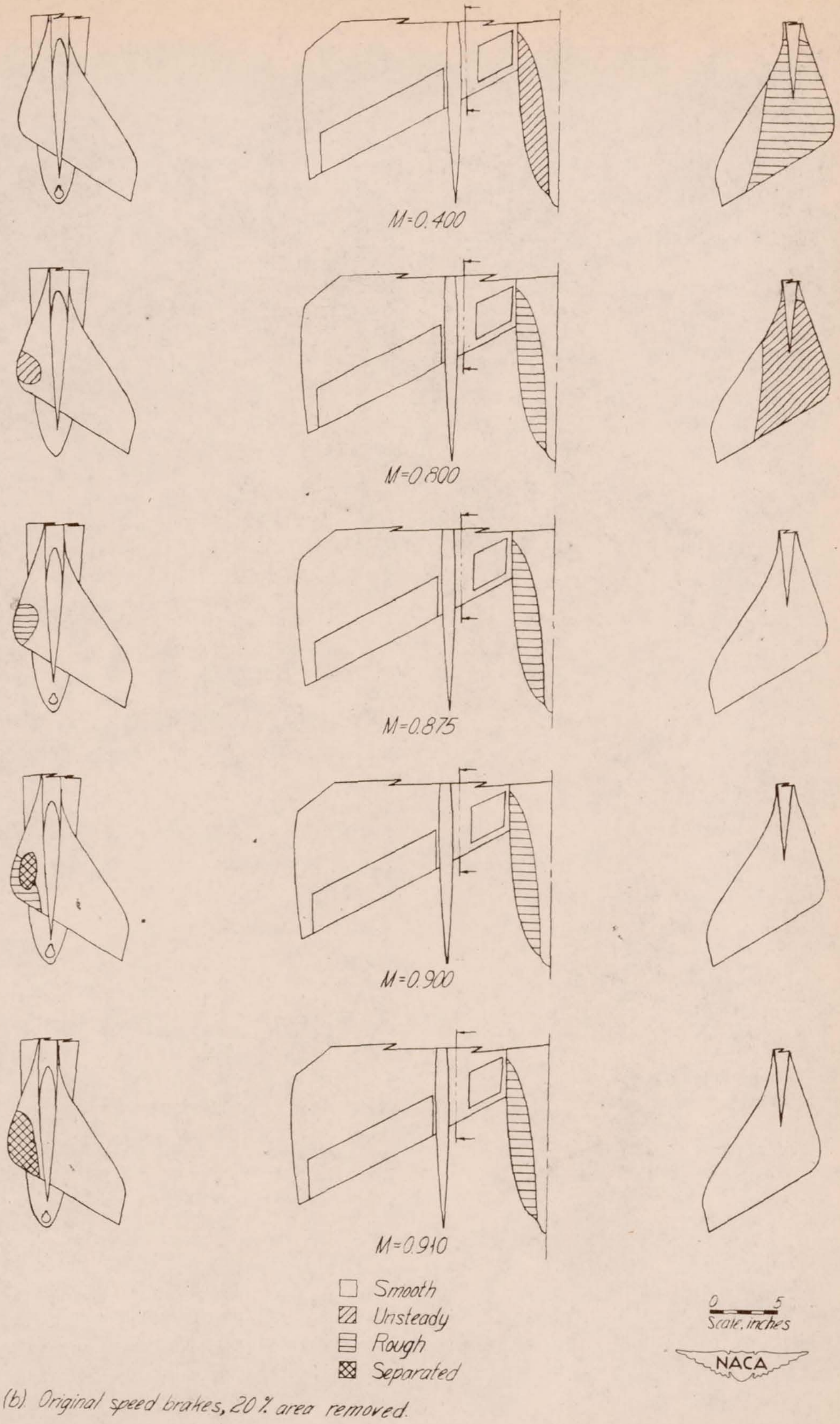

(b) Original speed brakes, 20% area removed.

Figure 18.- Continued.

CONFIDENTIAL

CONFIDENTIAL

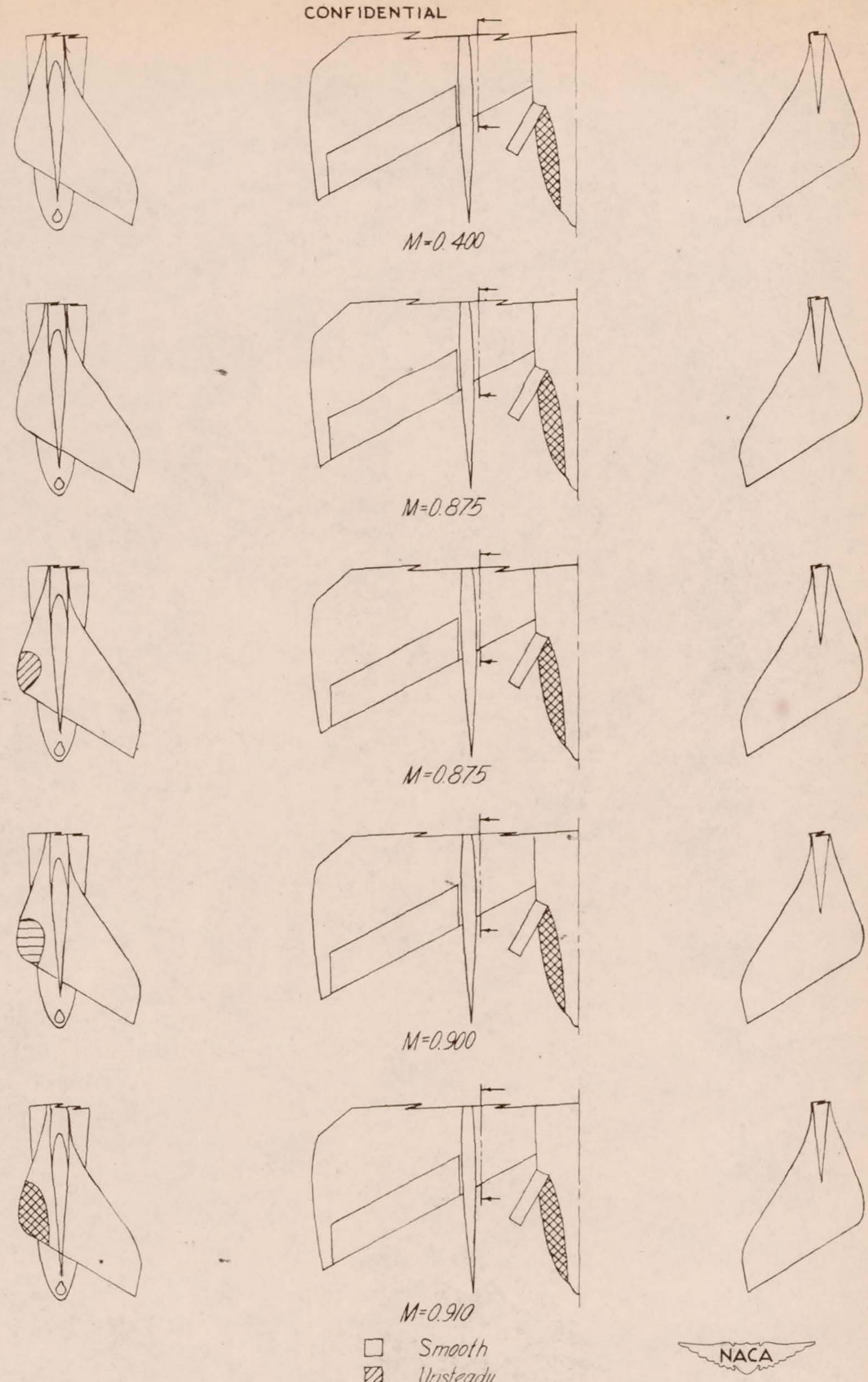

(c) Fuselage speed brakes deflected 30°.

Figure 18. - Continued

CONFIDENTIAL

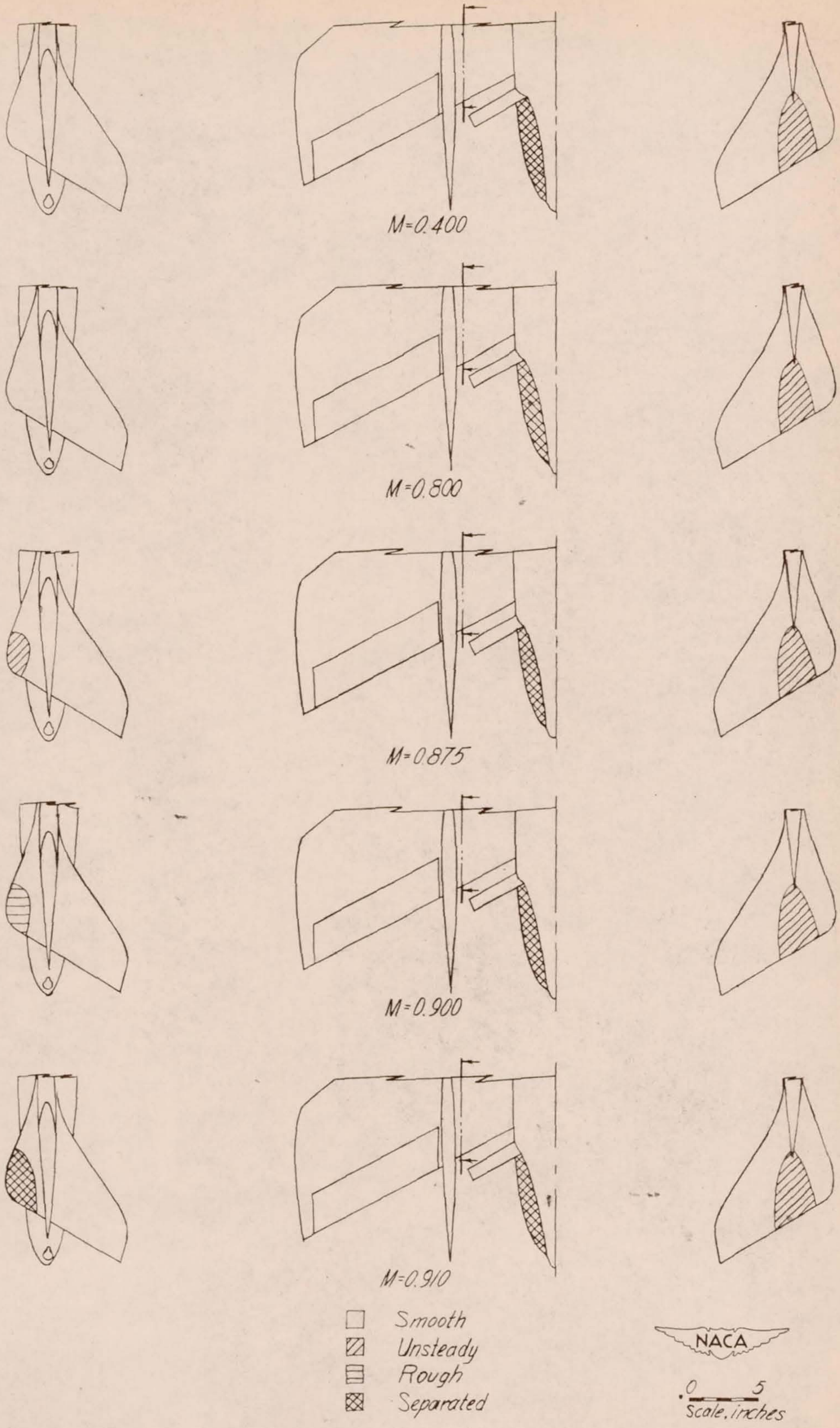

(d) Fuselage speed brakes deflected 60°.

Figure 18.- Concluded.

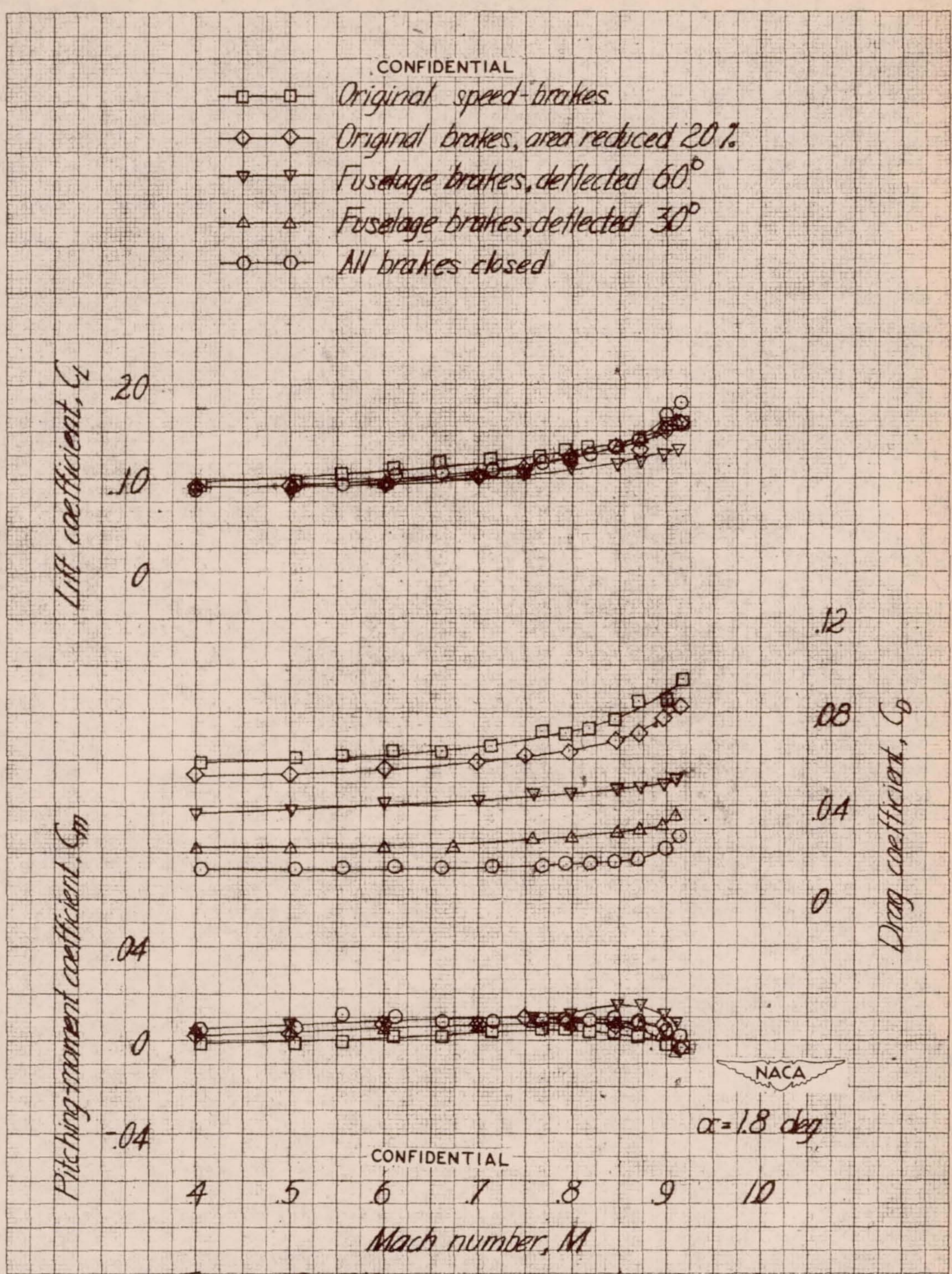

Figure 19.- Effect of various speed-brake configurations on the aerodynamic characteristics in pitch of the 0.08-scale model of the Chance Vought XF7U-1 airplane.

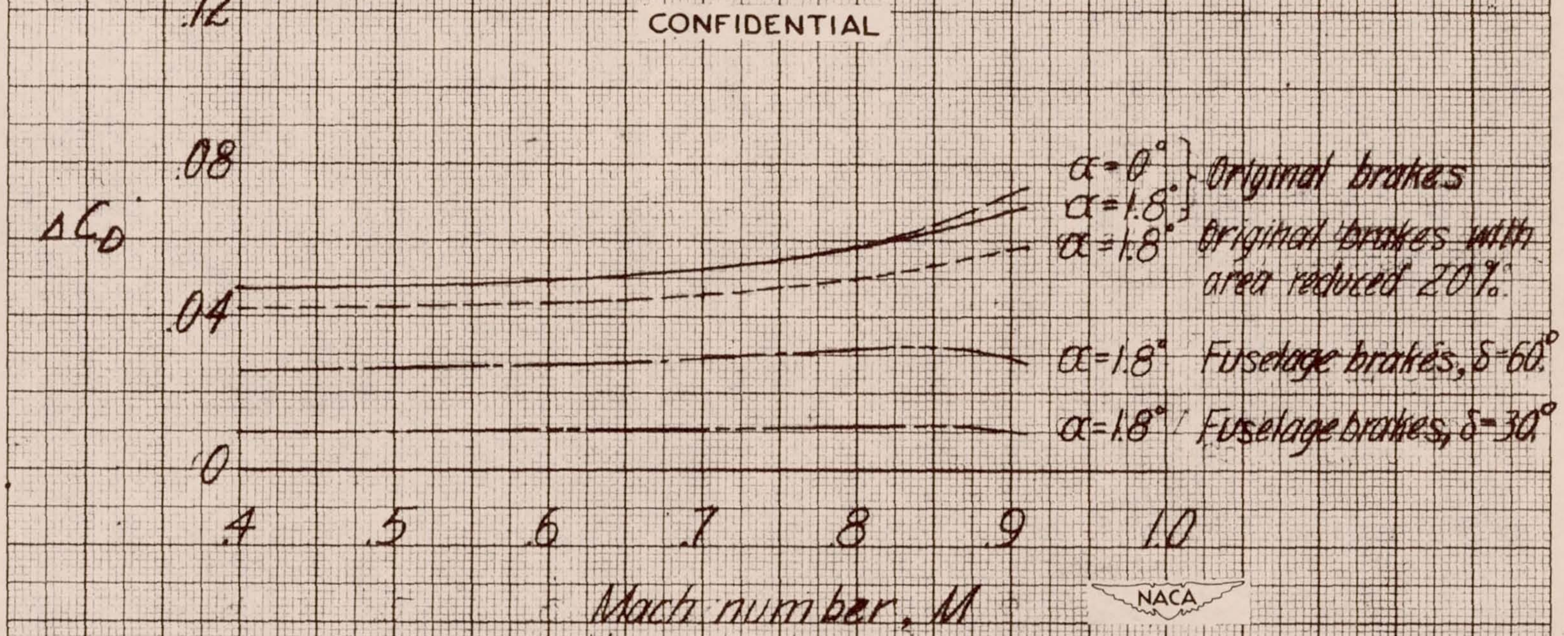

Figure 20.- Variation with Mach number of the drag increments produced by the various speed-brake configurations tested on the 0.08-scale model of the Chance Vought XF7U-1 airplane.

CONFIDENTIAL

CONFIDENTIAL

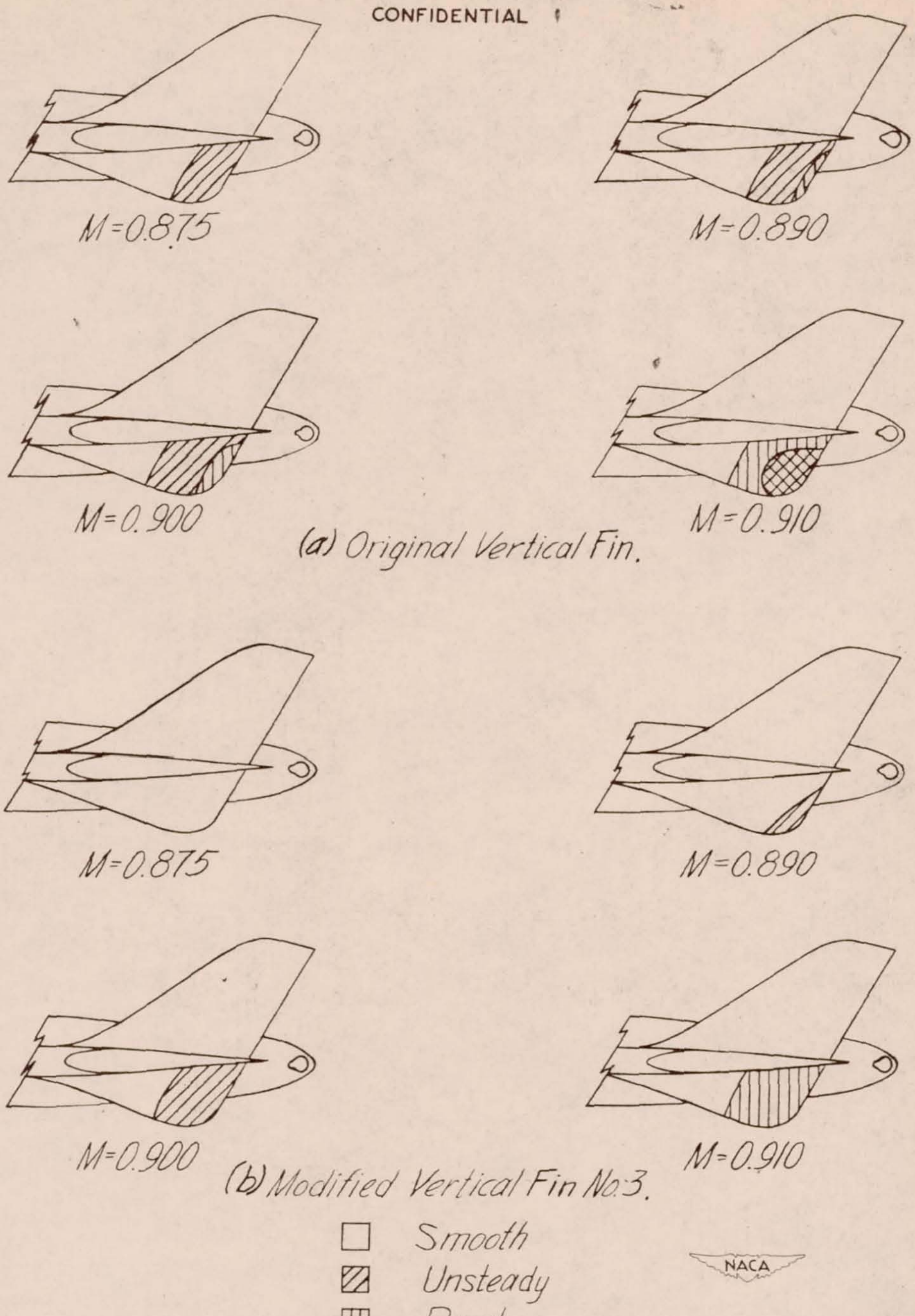

CONFIDENTIAL

Figure 21.- Tuft studies over the outboard surface of the vertical fin for various Mach numbers for the original and a modified vertical tail of the 0.08-scale model of the Chance Vought XF7U-1 airplane; $\alpha = 2^\circ$, $\psi = 0^\circ$.

CONFIDENTIAL

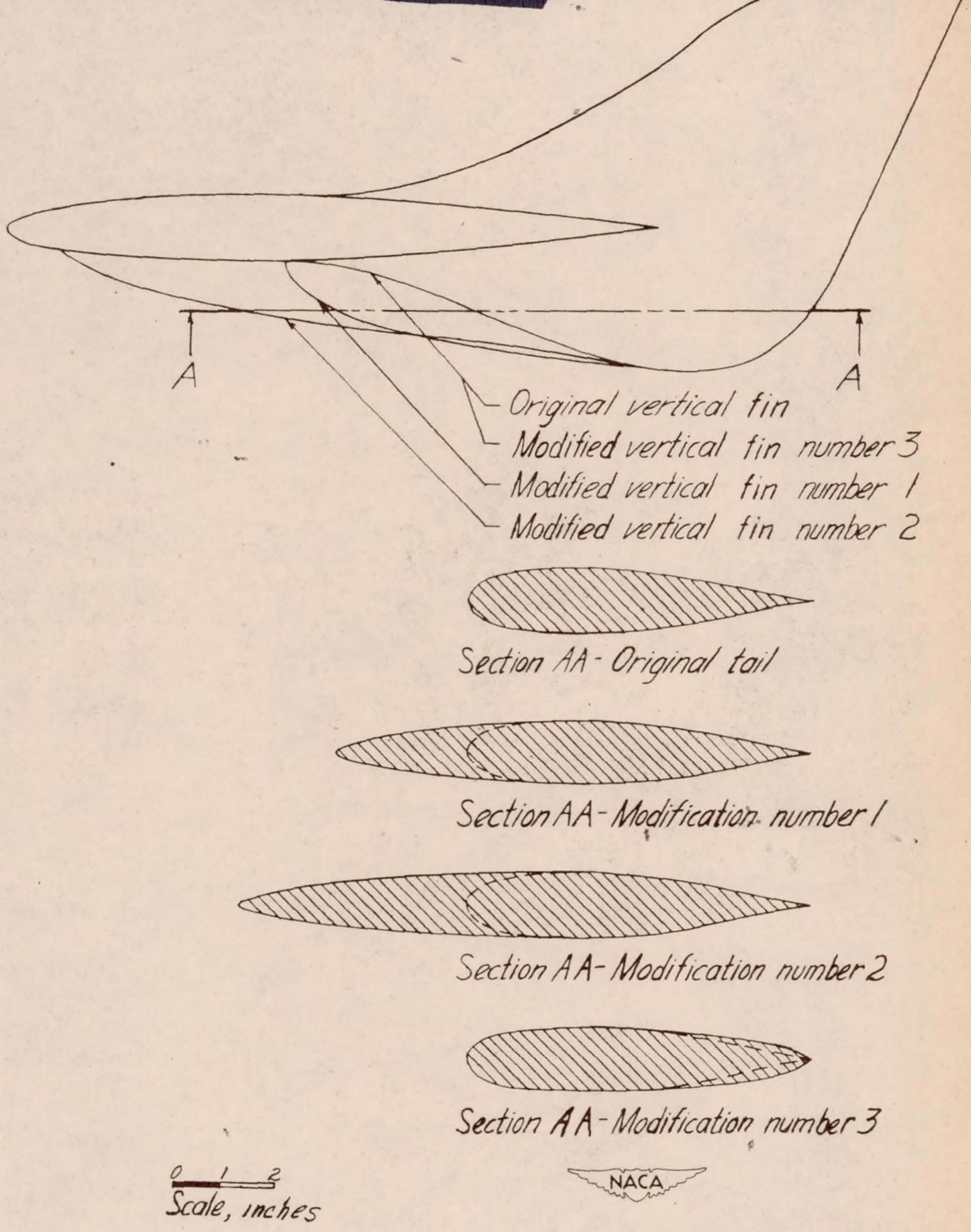

CONFIDENTIAL

Figure 22.- Various vertical fin modifications of the 0.08-scale model of the Chance Vought XF7U-1 airplane.